TNO Institute of Environmental and Energy Technology

Laan van Westenenk 501
P.O. Box 342
7300 AH Apeldoorn
The Netherlands

Telex 39395 tnoap nl
Phone +31 55 49 34 93
Fax +31 55 41 98 37

TNO-report

Full-scale measurements at the Dutch experimental wind farm at Sexbierum

draft final technical report

Reference number 93-174
File number 112324-22420
Date June 1993
NP

Authors
J.W. Cleijne
H.K. Hutting

ST-code
C 19.3

Key-words
- wind energy
- full-scale measurements
- wake effects

Contract
Full-scale measurements in wind turbine arrays, JOUR-0064-NL

Intended for
National Power PLC,
attn. Dr. G.J. Taylor
Research and Technology
Bilton Centre Cleeve Road
Leatherhead Surrey KT22 7SE
United Kingdom

This draft report contains the interim results of the study on 'Full-scale measurements at the Dutch experimental wind farm at Sexbierum'. Because it is a provisional version of the report and thus gives preliminary results, this draft report is intended for internal use only. The results may not be presented publicly as being the results of a TNO study. The final results will be presented in a final report in accordance with authorised procedures.

Summary

Between 1991 and 1993 detailed measuring campaigns have been carried out in the Dutch Experimental Wind Farm in order to collect experimental data on the power output, the wind and turbulence structure in the wind farm and the dynamic loads experienced by a wind turbine inside the wind farm.

To this end the following quantities have been monitored
- fast rate wind speed data in wakes;
- wind turbine power;
- fatigue loads in various components, such as blades, hub and shaft.

The lay-out of the Dutch Experimental Wind Farm is described. Instrumentation and measuring campaigns are described in detail.
Measurement of the wind farm power output shows that the wake losses in the wind farm are approximately 4%. Apparently the losses are limited due to the orientation of the wind farm with respect to the prevailing wind. The measurements indicate that the power output of the individual wind turbines drops off sharply in the second and third row and gradually increase again going to the turbines further downstream.

Two campaigns are described covering measurements of the wake properties behind a single turbine and behind turbines in line. The single wake campaign contains measurements at 2.5, 5.5 and 8 rotor diameters downstream. The double wake campaign (with the turbines at 5 rotor diameters inter-distance) describes measurements at 4 rotor diameters downstream the second turbine. The analyses described comprise the u-, v-, and w-components of the wind speed, of the turbulence intensity and of the shear stresses in the wake.

Power Spectral Densities of the wind have been determined in free-wind conditions and in the wake of a single wind turbine at 4 rotor diameters and at 7 rotor diameters downstream. The measured spectra can be described well by an ESDU-spectrum, using a modified length scale. In the wake the length scale is decreased by a factor of 4 approximately, compared to the free-stream situation. Analysis shows that at 7 rotor diameters the influence of the upstream wind turbine has largely disappeared.

Table of contents

List of symbols

a_{hub}	Weibull scale factor at hub height
c_P	Power coefficient
D	Rotor diameter
H	Hub height
I	Turbulence intensity (e.g. u'/U)
k	turbulent kinetic energy per unit mass $^1/_2(u'^2+v'^2+w'^2)$
k_{hub}	Weibull shape factor
M_{mn}	Meteo mast #m, height #n
P	Turbine Power
T_{nn}	Turbine nn
U	wind speed component along the undisturbed wind
u'	rms value of turbulent velocity fluctuations in U-directions
u'v'	U-V component of turbulent shear stress
u'w'	U-W component of turbulent shear stress
U_0	undisturbed wind speed
$u_{0'}$	undisturbed U-component of turbulent velocity fluctuations
V	wind speed component perpendicular to the undisturbed wind direction
v'	rms value of turbulent velocity fluctuations in V-directions
v'w'	V-W component of turbulent shear stress
W	vertical wind speed component
w'	rms value of turbulent velocity fluctuations in W-directions
z	height
z_0	roughness height
δ	wind direction
κ	Von Kármán constant
λ	tip speed ratio
ρ	air density

Suffix

max	maximum value
min	minimum value
0	undisturbed conditions

1 Introduction

Between 1991 and 1993 detailed measuring campaigns were carried out in the Dutch Experimental Wind Farm in order to collect experimental data on the Power output, the wind and turbulence structure in the wind farm and the dynamic loads experienced by a wind turbine inside the wind farm.

The measuring campaigns were part of the CEC-project 'Full-Scale measurements in Wind Turbine Arrays' (JOUR0064) and funded by the CEC and by the Dutch Utilities 'Sep'. The project aimed at collecting full-scale data for the purpose of
- validation of wake and wind farm models;
- providing input data for load calculations.

To this end long term measurements and short term campaigns have been carried out in various wind farms within the CEC.

This final report gives the main results of the measurements and subsequent analysis of the wake effects in the Dutch Experimental Wind Farm. It gives a detailed description of the measuring conditions and the geometry of the wind farm. It summarizes the contributions of Kema and TNO in the project.
The information is also passed to the participants in the project Wake and Wind Farm Modelling (JOUR0087), who will use it for the development and validation of wake models.

In the Sexbierum wind farm the following quantities have been monitored
- fast rate wind speed data in wakes;
- wind turbine power;
- fatigue loads in various components, such as blades, hub and shaft.

In The Netherlands KEMA and TNO jointly have carried out the measurements and the analysis of the experimental data. KEMA has been responsible for the measurements and pre-processing of the data and the analysis of the wind farm power data; TNO has carried out the analysis of the wind measurements in the wake and has prepared the final report.

The report discusses the following items. Chapter 2 describes the lay-out of the Sexbierum Wind Farm, the instrumentation and the data-acquisition system.
Chapter 3 discusses the variation of the power output of the wind farm with the wind direction and the power output of the individual turbines. These data are also compared with calculation results from FARMS.
In chapter 4 two measuring campaigns on the wind turbine wake are described. These campaigns were carried out in order to get insight in the wind velocities in a wind turbine's wake, the turbulence levels and the level of shear in a wind turbine wake. One campaign has been performed in the wake of a single turbine, in the second campaign various quantities were measured in the wake of two turbines in line. These campaigns have been reported more extensively in [Cleijne, 1992; Cleijne, 1993]

Chapter 5 describes the measurement of Power Spectral Densities of the turbulent wind in the wake of a single turbine. Measurements have been made in undisturbed conditions, at a distance of 4 rotor diameters and at a distance of 7 rotor diameters. Further the turbulent length-scales are derived for these cases. The measured spectra are compared with known empirical correlations. These results have been taken from [Verheij, 1993].

2 The experimental wind farm

2.1 Site details

The Dutch Experimental Wind Farm at Sexbierum is located in the Northern part of The Netherlands at approximately 4 km distance of the seashore and is surrounded by flat homogeneous terrain, mainly grassland used by farmers for the grazing of cows. In the direct vicinity of the wind farm only a few scattered farms are found. The surface roughness z_0 is about 0.05 m.

The wind farm has a total of 5.4 MW installed capacity, consisting of 18 turbines of 310 kW rated power each. The wind turbines are placed in a rectangular grid of 3×6 rows at inter distances of 5 or 10 rotor diameters along the major grid line and at an inter- distance of 8 diameters perpendicular to this grid (see figure 2.1). The direction of this line is at 353° with the North. The prevailing wind direction in the wind farm is South West. The wind climate at hub height is given by Weibull frequency distribution with scale factor a_{hub}= 8.6 m/s and shape factor k_{hub}= 2.1. The average wind speed is 7.6 m/s.

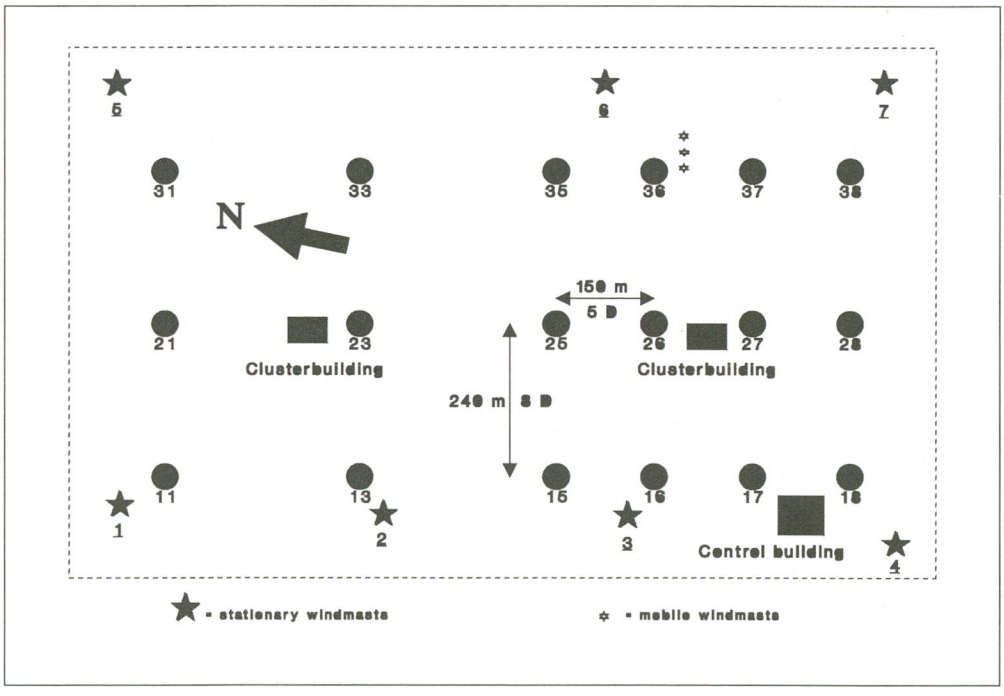

Figure 2.1 Lay-out of the wind farm

2.2 Wind turbine details

2.2.1 General

The main properties of the Holec WPS-30 turbines are listed in table 2.1. The electrical system of the wind farm consists of a synchronous generator and a rectifier for each turbine. Each turbine is part of a cluster of six turbines that are connected by a 1 kV DC link. Every cluster has its own grid driven invertor, which takes care of the required 50 Hz frequency. After transformation from 1 kV to 10 kV, the power is transported to the nearest substation, where it is delivered to the public grid at 110 kV.

Table 2.1 Main properties of Holec WPS-30 turbine

Type	Horizontal axis wind turbine
Rotor	Upwind
Rotor diameter	30.1 m
Number of blades	3
Blade material	Steel
Blade profiles	NACA 230XXX series
Tilt angle	5.5°
Cone angle	0°
Tower height	35 m
Rated power	310 kW
Rated rotor speed	44 rpm
Rated wind speed	14 m/s
Cut in wind speed	5 m/s
Cut out wind speed	20 m/s
Control	variable speed/ variable pitch
Tip speed ratio	7
Constant tip speed range	6-10 m/s
Yaw Control	Centralized through farm control

Further details are reported in [Bulder et al.,1991].

2.2.2 Power curve

Of all turbines the power output as a function of undisturbed wind speed has been determined in two different ways.

1. A power curve based on 'natural wind' was measured by using the IEA-recommendations as close as possible. The power output was averaged over 2-minute periods and bin-sorted according to the average wind speed of the closest anemometer at hub height. This power curve is to be used in power output predictions and wind farm calculations.
2. The second power curve was based on the measurement of the average power in short selected series of 20 seconds. The time series were selected on low turbulence level. In this way a power curve is obtained which more or less represents the behaviour of the machine in constant wind. This power curve may be used for the validation of performance calculations using rotor-aerodynamic codes.

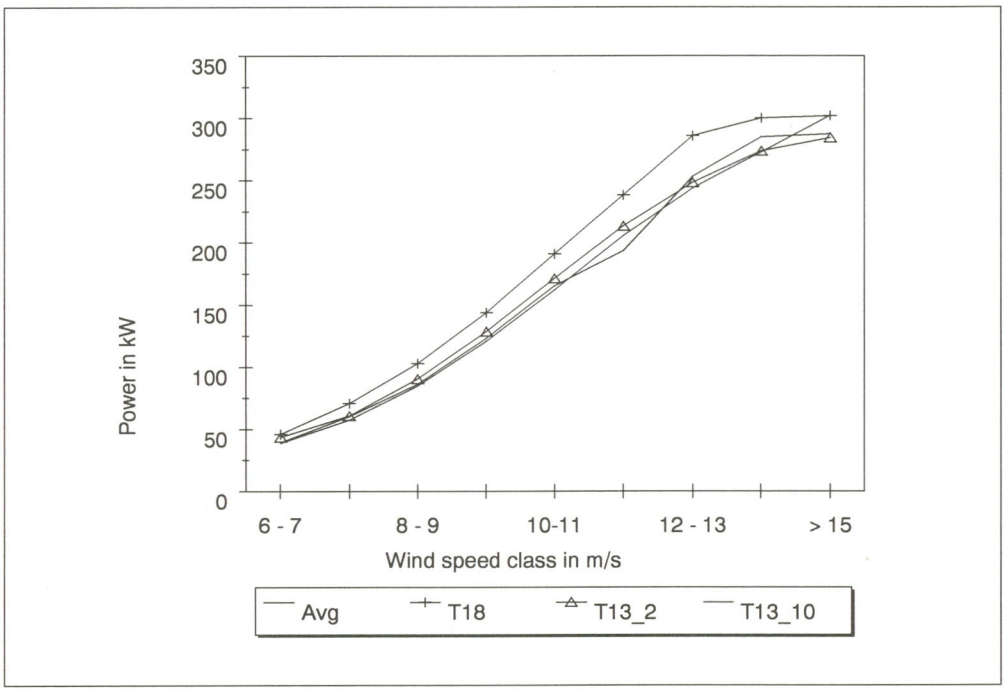

Figure 2.2 Power output of the turbines as a function of wind speed; comparison between 'natural wind' and 'constant wind'

Figure 2.2 displays the result of these measurements for the turbines T13 and T18 using these two methods. In the figure are also depicted the power curve obtained when applying an averaging period of 10 minutes and the power curve obtained from averaging the power curves of all turbines in the wind farm. The power curves obtained by using the first method agree very well. The power curve obtained in the second way is clearly different.

The standard deviation of the average power output values of all wind turbines is about 3%, which indicates, that the turbines are rather identical.

2.2.3 Pitch control

The HOLEC WPS turbines have a constant pitch angle below 10 m/s and are kept at constant tip speed ratio by load variation. Above 10 m/s the pitch angle is varied in such a way that the tip speed remains constant. Above 13 m/s (constant windspeed) the power is limited to 310 kW. Figure 2.3 shows the pitch angle of turbine T18 as a function of the undisturbed wind speed at 20 m height.

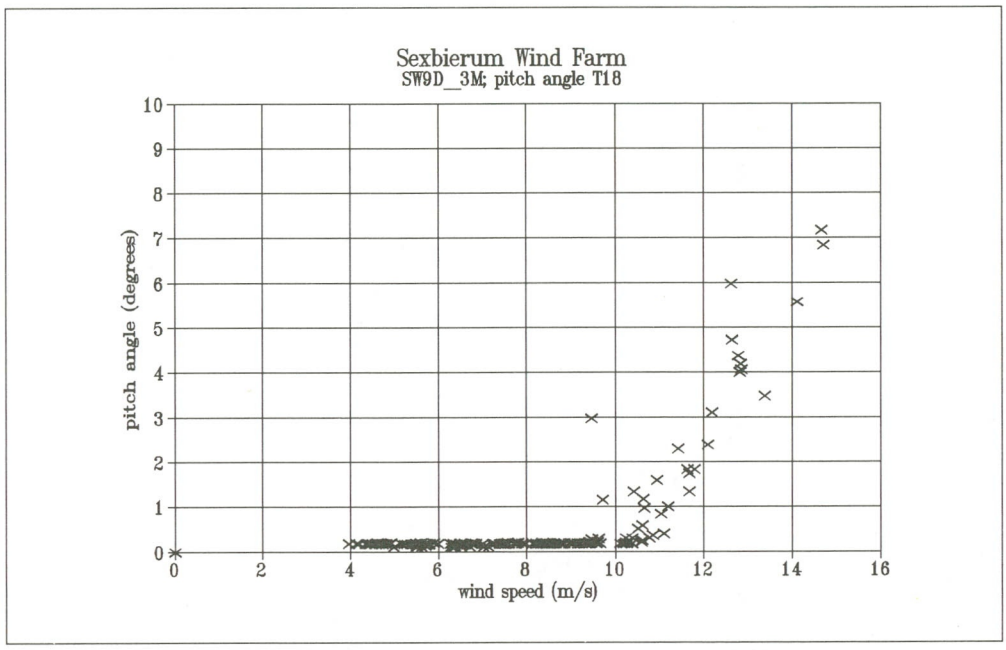

Figure 2.3 Pitch angle as a function of undisturbed wind speed at 23 m height

2.3 Instrumentation

The wind farm is surrounded by 7 fixed wind measurement masts. The locations of the masts are given in figure 2.1. Each mast has a wind anemometer and a wind vane at 35 m (hub height). The masts 4 and 6 have also wind sensors at 20 m and 50 m height. At mast 3 the temperature and air pressure at hub height are measured.
The standard instrumentation of all turbines comprises sensors for DC current and voltage, yaw and pitch angle, rotational speed and several control signals.

For wake measurements there are three mobile wind measuring masts. It is possible to install the masts anywhere inside the wind farm, enabling detailed wind measurements of the wake structure. One mast is equipped with 3-component propeller anemometers at 47 m, 35 m and 23 m respectively. At the height of 41 and 29 m two extra cup anemometers have been mounted. The other two masts contain 3-component propeller anemometers at 35 M. The signals from the mobile masts are sampled at a sampling rate of 4 Hz.

The 3-component propeller anemometer (see figure 2.4) consists of three lightweight carbon fibre propellers, which are mounted on a cone-shaped rig at angles of 30° relative to each other. Combination of the three anemometer signals gives the X, Y and Z components of the wind.

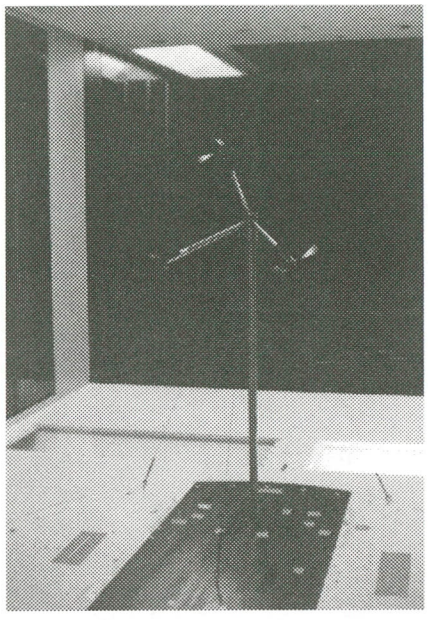

Figure 2.4 Propeller anemometer in wind tunnel for calibration

Turbine T36 (see figure 2.1) has been extra instrumented. It contains sensors for the measurements of mechanical loads in the blades, the hub, the tower and the drive train.

Sensors have been mounted for measurement of the pitch angle, blade position and nacelle direction. Further, various electrical signals are measured. The signals are sampled at a sampling rate of 32 Hz. A complete list of the measured signals is given in annex 1.

2.4 Data acquisition system

The data acquisition system of the wind farm serves the following purposes:
- monitoring of the wind farm;
- detailed measurements of the wake structure inside the farm;
- wake effects on the mechanical loads on the turbines;
- wake effects on the aggregate wind farm power;
- electrical behaviour of the wind farm.

For this purpose the wind farm has a central computer, which takes care of monitoring and control of the wind farm and a data-acquisition system consisting of measuring computers and data elaboration computers (see figure 2.5).

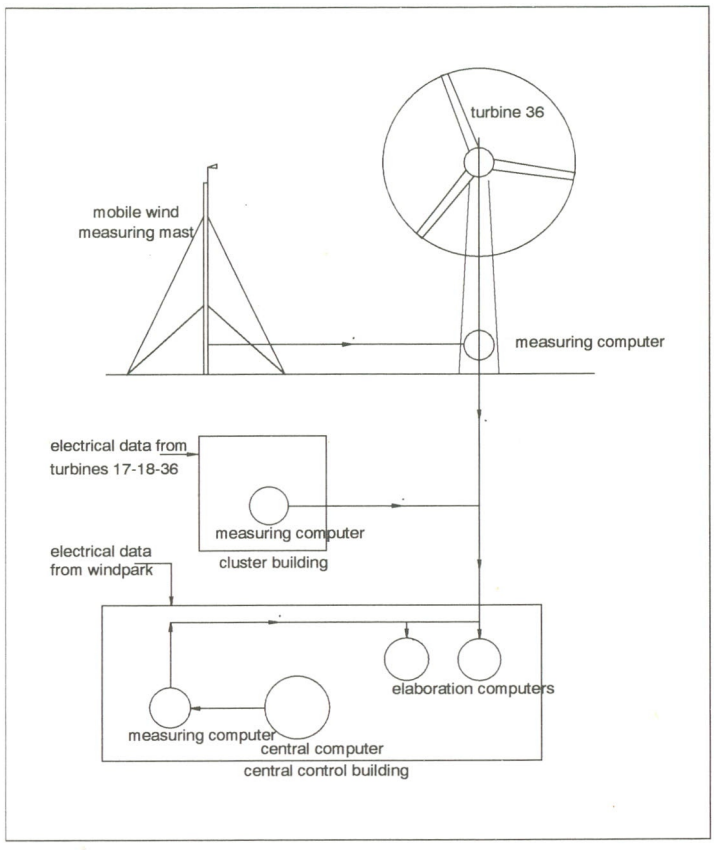

Figure 2.5 Data-acquisition system

The signals from the extra-instrumented turbine T36 are sampled at 32 Hz by a measuring computer inside the tower. The signals from the mobile measuring masts are also connected to this computer and sampled at 4 Hz. Signals with respect to the electrical behaviour of the wind farm are sampled at 32 Hz by a measuring computer in the central control building. This computer is connected to the central computer that supplies at 1 Hz the following data:
- undisturbed wind speed and wind direction from the stationary wind masts;
- air pressure and temperature;
- status of each wind turbine;
- power of each turbine;
- yaw and pitch angle of each turbine;
- rotational speed of each turbine.

The central computer also stores the 1-minute average values of these signals in a database. All acquired data are passed to the two central data elaboration computers in the central control building, which can calculate pseudo signals in real time. Pseudo-signals are signals, which can be made through any mathematical operation on one or several individual real signals.
The elaboration computers can process the data in the following ways:
- event recording;
- statistical recording.

Event recordings are time recordings of signals that are of interest during an event. Events can be described by a collection of conditions, with a maximum of six conditions, which are used to trigger the event recording. This has made it possible to collect the data selectively and to reduce the amount of data. If an event is triggered, the history of the past ten minutes, which is stored in the memory of the computer, can be recorded on tape. The recording proceeds until the user defined time is elapsed or until the conditions are no longer met.
Most of the data is processed statistically in real time. Before an operation is performed on a signal, the computer checks the signal quality automatically. The signal quality is checked by calculation of proceeding average, proceeding standard deviation and the difference between two successive signal samples. Signals, which are out of the range defined by the user, are cancelled automatically.
Statistical operations that can be performed are:
- one-dimensional bin-analyses;
- two-dimensional bin-analyses;
- one-dimensional probability density functions;
- two-dimensional probability density functions;
- rain flow counting.

The result of each operation can be stored in three-dimensional parameter classes. A class is defined by a range of the average of a parameter over a period, par example: the rain flow counts of each 10 minute period will be stored separately, depending on wind speed and wake situation classes. The wake classes are 5D, 8D, little and no wake. The wind speed classes are 0-8, 8-10, 10-12, 12-14, 14-16, and > 16 m/s with turbines in operation and 1 class with no operation of the turbine.

Further details are reported in [Kamphuis et al.].

3 Wake effects on wind farm power output

3.1 Introduction

This chapter describes the measurements on the power output of the wind farm. The objective of the power measurements was to determine the influence of wake effects on the power output of wind turbines within a farm, in such a way that developers of numerical wake models will get a reliable database to validate their calculations of the wake effect on the yearly output of a wind farm.

The measurements started in the beginning of 1991. The results presented in this report cover the period November 1991 up to the end of 1992. After the discovery that the pitch angle settings of the turbines were not the same for all turbines, the settings were corrected. Because of that, proper measurements could not start until November 1991.

During this period the availability of the turbines in the farm was 89%. Because the availability of the farm was mainly reduced through the failure of one turbine, most of the data processing was done on a part of the wind farm in order to get a proper amount of samples in each bin interval.

3.2 Data processing

3.2.1 Software

The data from the 1-minute time history database, has been processed by a special bin analysis programme. The features of this programme are:

- averaging data over a number of minutes after checking that all minutes contain proper data and taking into account signal transitions of the direction sensors around 0° and 360°. For this case we have chosen an averaging period of 2 minutes.
- Selecting an upstream anemometer out of the available anemometers to relate the power data to.
- Processing of a selected part of the farm or the whole farm after checking that all turbines of that part were in operation.
- Processing of all turbines separately after checking that all upstream machines were in operation. This way of checking improves the number of valid samples, significantly.
- The output of the programme gives in each bin the number of samples, the average, standard deviation, minimum and maximum values of the power and the average of the wind speed.
- The two dimensional bins are defined by 144 direction intervals of 2.5° and by 10 wind speed classes. The wind speed class intervals are 0-6, 6-7, 7-8, 8-9, 9-10, 10-11, 11-12, 12-13, 13-15 and >15 m/s.
- The output format is organised in a such way, that the data can be easily imported in spreadsheet programmes for making graphs.

The programme processes a time series of one month. Another programme is made to add results from the months. A special programme has been developed to convert the file format in the special file format used in the project for the transfer of data.

3.2.2 Procedure

Before the bin analyses were made, the wind speed time series were checked graphically and through feedback from the results. The results of the checks were, that the following anemometers were not usable under the conditions mentioned:
- anemometer 1 most of the time;
- anemometer 42 for about 20 days in the first and the last 3 months of 1992;
- anemometer 5 in February 1992;
- all anemometers at the top of the masts in the direction interval between 160° and 210°, due to the presence of a lightning rod;
- all anemometers at a lower level at the mast in the interval 100° to 160°, due to the wake of the mast.

When an anemometer signal was disturbed during a period, either another one was chosen to give the reference wind speed or the data was marked not valid. Spatial averaging, using more anemometers, was performed to get the reference wind speed in order to improve the correlation between power and wind speed.

The anemometer selection was:
- anemometer 5 for wind directions 0° to 30° and 330° to 360°;
- the average of anemometers 5 and 7 for wind directions 30° to 160°;
- anemometer 42 for wind directions 160° to 210°;
- the average of anemometers 2 and 3 for wind directions 210° to 330°.

The bin results of each month were checked graphically before they were added.

3.3 Analyses of the results

3.3.1 Total power output

The processing of the total power data was done on a part of the wind farm in order to get a proper amount of samples in each bin interval. This had to be done, because the availability of the farm was mainly reduced through the failure of turbine 11 for 7 months and of turbine 31 for 2 months. This part describes the power output of all turbines except T11, T21 and T31, see figure 2.3.1. These turbines have little influence on the wind farm efficiency, unless the wind is blowing from the north. So in the graphs the data around 0° and 360° are less reliable, but in all other directions the total number of bins is almost 5 times higher, so the confidence interval is improved with at least a factor of 2.

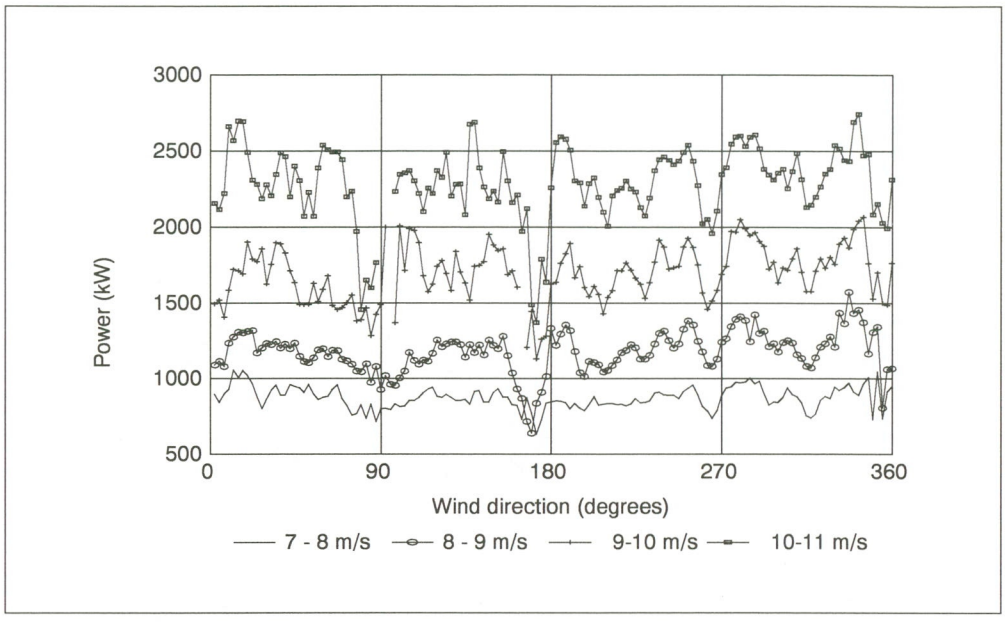

Figure 3.1 Power output as function of wind direction of 15 turbines

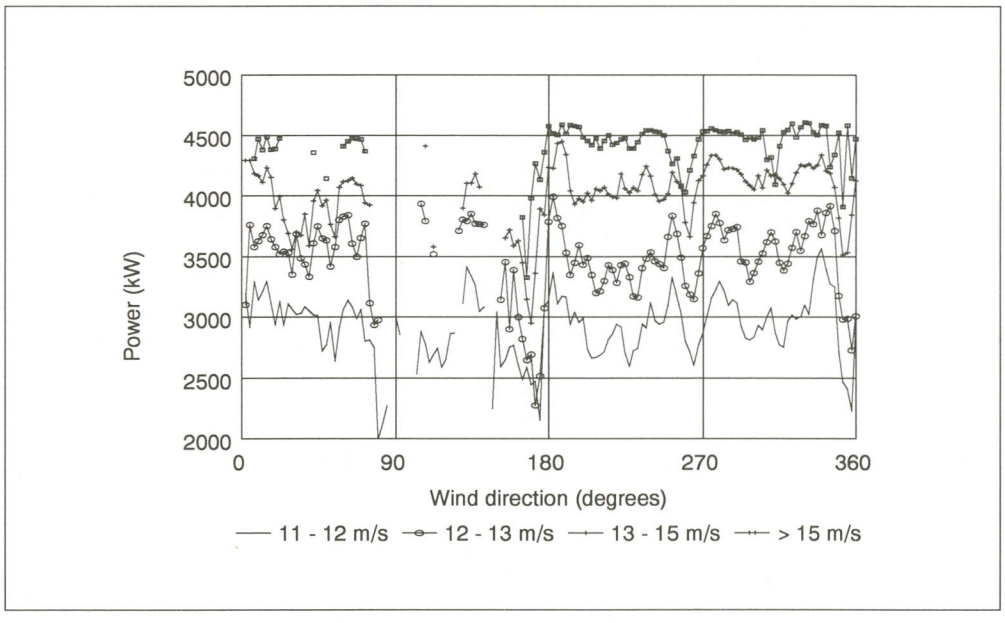

Figure 3.2 Power output as function of wind direction of 15 turbines

In figures 3.1 and 3.2, an overview is given of the power output of the selected group of turbines in the wind farm as a function of wind direction and wind speed. In the graphs the wake influence on the power output is clear, especially in the direction of the main axes of the farm at 82°, 172°, 262° and 352°. In the diagonal direction of the farm, the influence of the wake is also clear, but the dips in the power output are less pronounced.

In figures A.1 to A.8 the power output is given for different wind speed classes, including the limits of the 68% confidence interval and the extreme values. In figures 3.8 and 3.9, the number of samples in the bin intervals are given. The power figures show large confidence intervals in bins with a low number of samples, which is to be expected, and large maximum values, when the number of samples is large, because a large number of samples increase the possibility of large deviations from the mean. The graphs of the number of samples clearly show the large number of samples in the prevailing wind direction and the low number of samples in the direction of the main axis of the farm.

3.3.2 Turbine efficiency within the farm

The efficiency of the turbines in a row, when the wind is blowing along the row with speeds between 8 and 11 m/s, is presented in figures 3.3 and 3.4 for different rows. For 5 D inter-distances between the turbines, figure 3.3 shows that the minimum efficiency is 47% for the second and the third turbine in the row and that the wake recovers slightly when going downstream to the fourth turbine. Between the further downstream machines the space is 10 rotor diameters, which gives more distance for the wake to recover to about 70% efficiency.

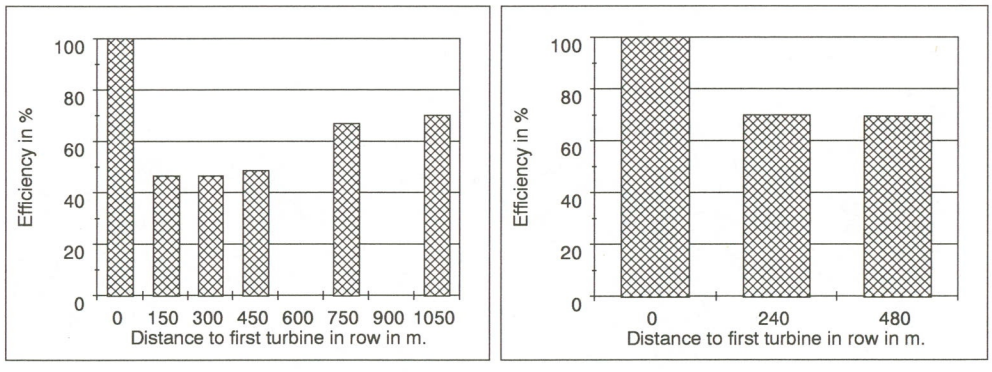

Figure 3.3 and 3.4 Efficiency of turbines in a row as function of distance

At distances of 8D the efficiency is reduced to 70% for the second and third turbines, see figure 3.4. There is not a fourth row to show the slight recovery of the wake as seen in figure 3.3, but it is likely since it has also been proven in other farms.

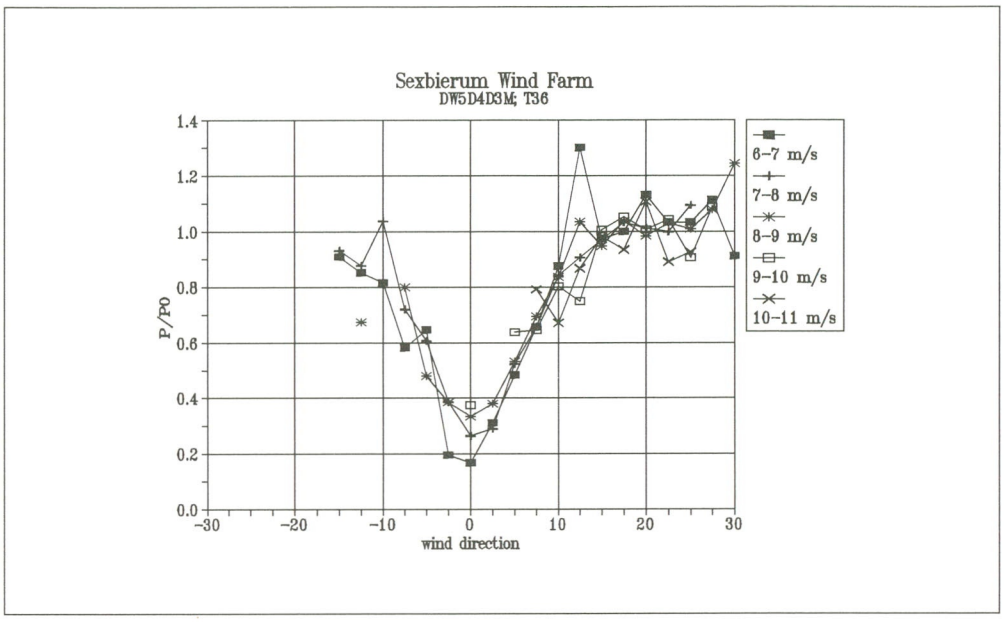

Figure 3.5 Power ratio of turbines T36 with respect to turbine T38

Figure 3.5 shows the power output of turbine T36 non-dimensionalized with the power output of T38. T36 operates in the wakes of both T38 and T37.

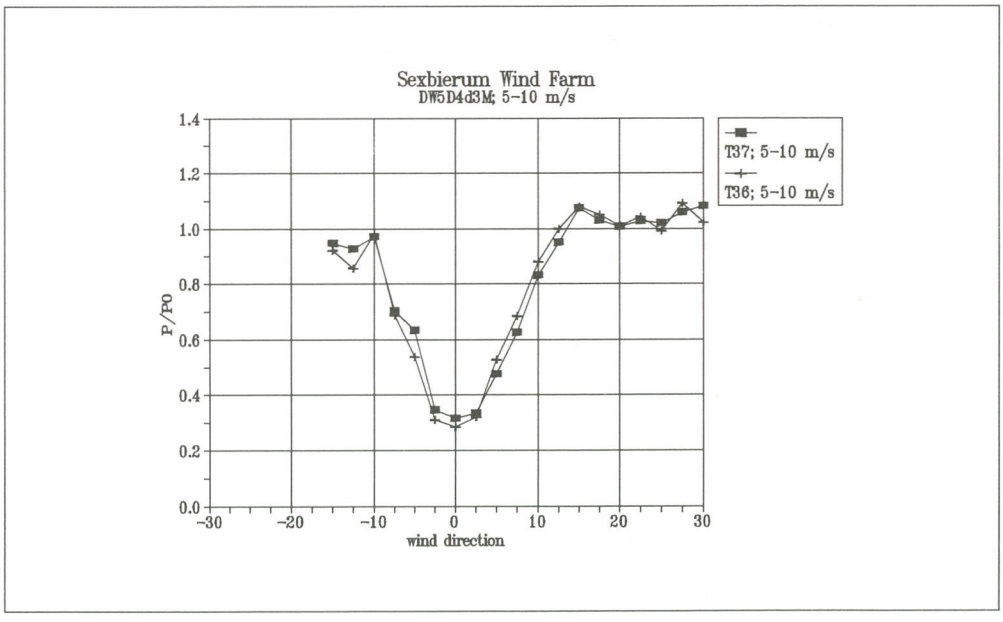

Figure 3.6 Aggregated power ratio of turbines T36 and T37 with respect to turbine T38

Figure 3.6 gives the results of the power loss due to wake effects averaged over the wind speed interval from 5-10 m/s. Remarkably, the power deficit curves of T38 and T37 almost coincide.

3.3.3 Comparison with model

During the measurement period the power output of the farm was reduced due to wake effects with 4%. The losses are that low, because of the lay-out of the wind farm, which has the main axis in the direction with the minimum frequency of occurrence, as indicated by the figures 3.8 and 3.9. The FARMS model of TNO (using a calculated thrust-curve) predicts a value of 4%, which compares well with the measured value.
A closer look at the prediction of the power output as a function of wind speed class and wind direction compared with the experimental results, presented in figure 3.7, shows that the dips in the power output are underpredicted.

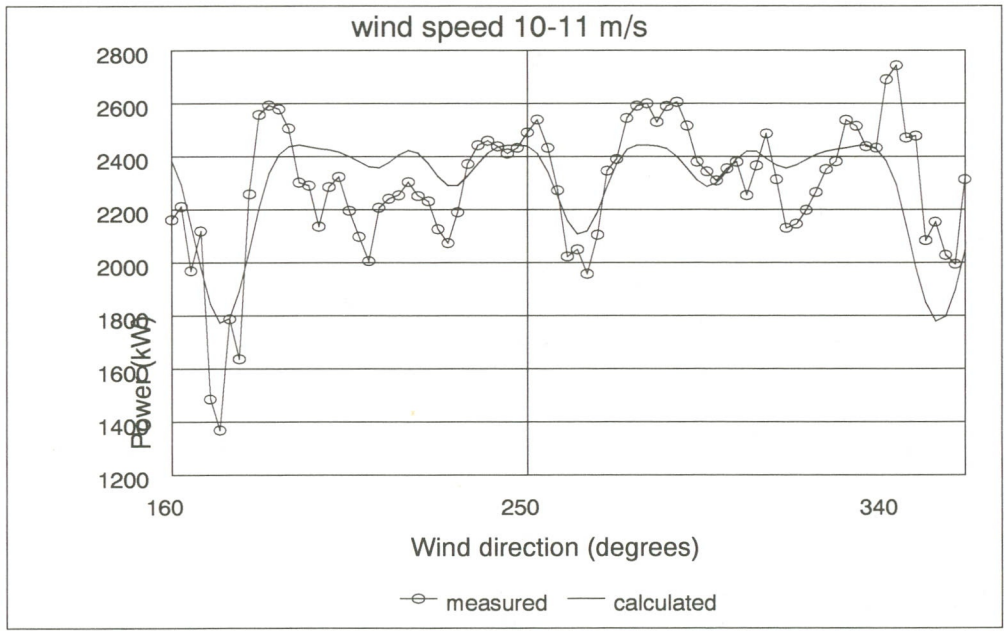

Figure 3.7 Comparison of measured and predicted power output of the wind farm as function of wind direction in the wind speed class 10 - 11 m/s

3.4 Accuracy analyses

3.4.1 Power measurement

The DC voltage and current sensors have an accuracy of 0.2%. The whole transmission line from sensor to computer has been calibrated to give an accuracy of 1% in each signal, which results in an accuracy of 2% in the product of the two, the

power. These errors are systematic. In judging the relative power loss due to wake effects, systematic errors are not relevant.

3.4.2 Wind direction measurement

The wind direction sensors have a resolution of 2.5°, which coincides with the binning interval. Averaging over one minute gives a small probability of putting the data into a bin next to the real bin. The sensor can have a systematic offset error of 5°. For the analyses the average of all (3 or 4) undisturbed upstream direction sensors are used. This will give a reduction on stochastic errors and will improve the correlation with the average wind direction within the farm.

3.4.3 Wind speed measurement

The cup anemometers have an accuracy of 1.5% at the moment of calibration for wind speeds between 5 and 20 m/s. The error in the speed can increase in time due to changes in the lubrication of the bearings. The anemometers have had maintenance and recalibration every two years. Due to overspeeding, the one-minute average of the wind speed is overestimated by about 1.5% in undisturbed flow at hub height, because according to [Bush et al., 1979] the overspeeding of a cup anemometer is about the square of the turbulence intensity. The measured turbulence intensity around the farm was about 8%, based on a one hour value of 13%, approximately.

3.4.4 Yaw error

The direction of the nacelle is controlled by the turbine by calculating the yaw angle from the nacelle direction and the wind direction signal it gets from the central computer. The central computer determines the direction from the average of 3 or 4 upstream wind direction sensors around the farm. The turbine controller keeps the yaw angle, averaged over 20 seconds, below 5°. The nacelle direction sensor can have an error of 2.5°.
The total systematic error, caused by nacelle and wind direction errors, is 5°, as well as the stochastic error due to the control.
The effect of a yaw error of a total of 10° on the power output is only 1.5%.

3.4.5 Estimation errors

A large error in the determination of the power versus wind speed curves is due to the lack in correlation between the upstream wind speed and the wind speeds at the turbines. This stochastic error will be reduced by averaging over many samples. Unfortunately the measurement period was not sufficient to fill all bins properly. The number of samples in the bins is given in figures 3.8 and 3.9. The influence of the

number of samples on the error becomes clear when the confidence intervals are determined.

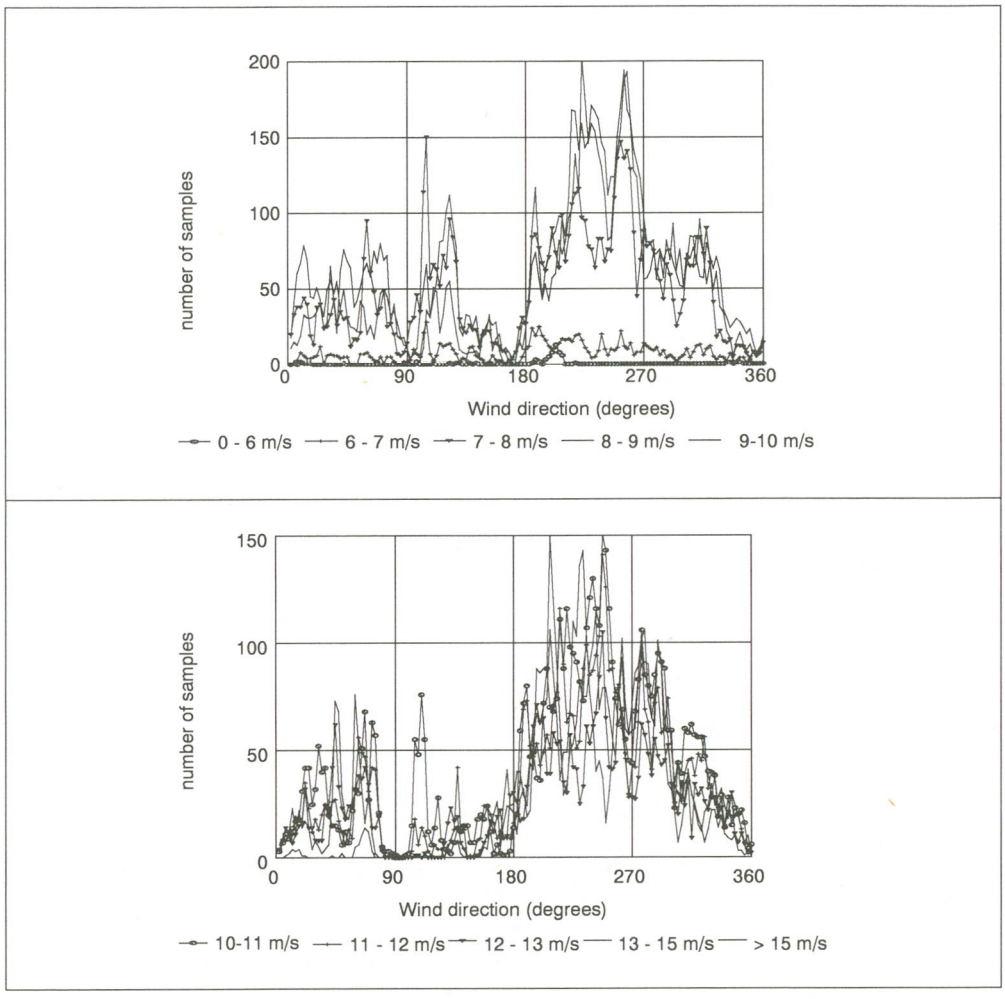

Figure 3.8 and 3.9 Number of samples in the bins for all wind speed bins

The 68% confidence interval for the mean μ is given by:

$$\bar{x} - k \leq \mu \leq \bar{x} + k$$

In case the standard deviation is not known a priori, according to [Kreyszig, 1988], k is given by:

$$k = {}^{sc}/_{\sqrt{n}}$$

where n denotes the number of samples in the record, s denotes the estimate for the standard deviation and c is a number found for the Student t-distribution, dependent on the confidence level and the number of samples.

In the figures A.1 to A.8, the limits of 68% confidence interval in the mean value are presented. These stochastic errors range from 15%, when there are only 2 samples, to 0.6% when more then 200 samples have been counted in a bin.

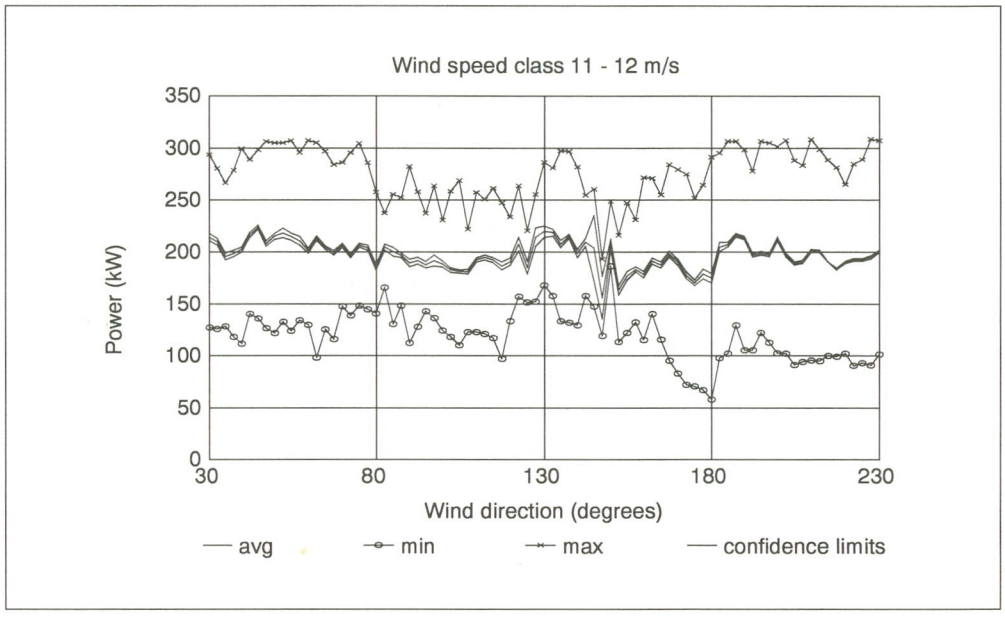

Figure 3.10 Power output of turbine 38 as a function of wind direction in the wind speed class 11-12 m/s

Another important source of uncertainty in the power output is the influence of atmospheric conditions. The effect of atmospheric stability on wind shear can change the actual wind power, which passes a rotor plane, with about 5%. Further, differences in turbulence intensities change the mixing in the wake and hence the power produced by the wind farm. Unfortunately these atmospheric influences are not evenly distributed over all wind directions. The influence of the unevenly distributed atmospheric conditions on the power output of a single turbine without wake effects is shown in figure 3.10. It presents the power of turbine 38 as a function of wind direction in the wind speed class 11-12 m/s. The power output should be independent of the wind direction, but the figure clearly shows the deviations. The standard deviation of the mean values of all undisturbed directions is 6%. This standard deviation gives an impression of the error level, but not more than that, because the distribution of the atmospheric conditions is not known. The graph also shows, that the variation due to atmospheric conditions is larger than the stochastic errors.
This influence of the atmospheric conditions was known before the beginning of the measurements, but provisions were not made, because the results of the measurements are intended to be used as validation for models, which predict the yearly output of a farm of which only the wind distribution is known.

3.5 Conclusions

The measurements have provided model developers with a good data base of full-scale power and wind data. The following conclusions can be drawn from the previous discussed results:

- The overall power loss in this wind farm is about 4% only.
- The minimum efficiency of turbines in a row is already reached at the second and third turbine in that row.
- The existing Farms model of TNO predicts an overall power loss of 4%.

To improve the accuracy of the data, collected in this project, it is recommended to continue to collect the power and wind data.

4 Measured properties of wind turbine wakes

4.1 Introduction

During 1992, detailed measuring campaigns were carried out in the Sexbierum Wind Farm in order to collect experimental data on the wind speed, turbulence intensity and shear stresses in the wake of a wind turbine. One campaign concerned measurement of these properties in a double wake, i.e. the wake of two turbines in line. A second campaign concerned measurements in a single wake, behind a single turbine. These campaigns have been reported in detail in [Cleijne, 1992] and [Cleijne, 1993].

This chapter summarizes the main results of the two measuring campaigns. Section 4.2 describes the applied analysis procedures in both cases. In section 4.3 the results of the double wake measurement are presented. Section 4.4 describes the results of the single wake campaigns. First both sections describe the measuring campaign. Then, the results are given concerning the undisturbed wind during the measurements, followed by the power output of the turbines concerned. Finally, the measured properties of the wind in the wake are discussed.

4.2 Analysis of measuring results

4.2.1 Pre-processing and resulting database

A first data-reduction and quality control of the measured data was done during pre-processing of the data. The 1 Hz and 4 Hz time series of the measured quantities were manipulated in order to obtain time series of 1-minute averages of various quantities such as the wind speed, the turbulent velocities and the shear stress. Table 4.1 gives an overview of the time series contained in the data base. The 1-minute data have served as the working data base. The chosen format makes it possible to combine the 1-minute averages into samples with multiple-minute averages. [Cleijne, 1992] describes the statistical operations used for the data manipulation.

4.2.2 Time averaging

Before the data base was further analysed, the samples were combined to obtain 3-minute averaged quantities. Considerations for selecting a period of 3 minutes were the following:

- **Stationarity of the data.**
  It is common practice to assume a spectral gap for wind velocity data between 10 minutes and 1 hour. Shorter averaging periods will result in non-stationary records due to turbulence;

- **Coherence between undisturbed wind signal and wake signal.**
  Meteorological mast 7 and the mobile masts are 350 m apart. assuming a wind speed of 8 m/s, this corresponds to a delay of 45 seconds, approximately. In order to obtain a reasonable coherence between the wake wind data and the undisturbed wind data it is necessary to use an averaging period of more than this period.

- **Effect of slow wind direction variations.**
  If the averaging period is chosen too long, slow variations in the wind direction will blur the details of the wake.

- **Number of available records.**
  Longer averaging periods result in less samples. A 3-minute averaging period resulted in a database with 873 samples for the single wake campaign and 573 samples for the double wake campaign.

- **Effect on wind turbines.**
  Power curves for wind turbines are most often determined using averaging periods of 10 minutes; Wind fluctuations shorter than 1 minute are most important for the determination of wind turbine loads. Slower fluctuations are absorbed by the control system.

The wake deficit profiles are hardly affected by the averaging period. However, non-linear signals, such as turbulent velocities and shear stresses are indeed affected by the changing averaging period. Longer averaging periods result in higher turbulent velocities, for instance. Nevertheless, it is not easy to select an optimum averaging period. Taking into account the arguments listed above, it was decided to analyse the data on the basis of 3-minutes averaged samples.

4.2.3 Frame of reference

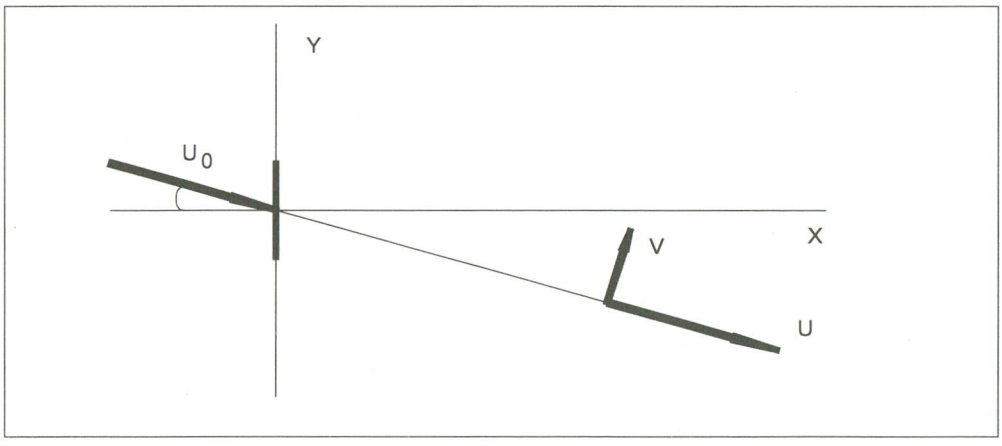

Figure 4.1 Definition of the frame of reference

Besides scalar quantities, such as the wind turbine power, the total turbulent kinetic energy k, also vector quantities (wind vector) and tensor quantities (turbulent co-variance matrix) had to be analysed. Therefore it was necessary to define a proper frame of reference for the presentation of the data. It was decided to couple the frame of reference of the wake data to the co-ordinate system of the undisturbed wind. The definition of the frame of reference is given in figure 4.1. The undisturbed wind direction is given with respect to the line connecting the turbines T18 and T27 in the single wake case and the line connecting T38 and T36 in the double wake case. These wind directions are defined as 0 degrees. The u-component is parallel to the undisturbed wind, the v-component is perpendicular to the undisturbed wind in the horizontal plane. The w-component is in the vertical direction. u'v and w define a right-handed co-ordinate system. This conforms to the normal meteorological definitions. Before the 3-minute samples were bin-sorted, they were converted first to the above given co-ordinate system, using the co-ordinate transformation formulas given in [Cleijne,1992].

4.2.4 Bin-sorting

The 3-minute samples were sorted into different bands of undisturbed wind speed and wind direction. Between 5 m/s and 12 m/s a bin width of 1 m/s was used; above 12 m/s the bin width was taken equal to 2 m/s. The selected wind direction bin width was 2.5°.

For each bin the mean value, variance, minimum and maximum values of the measured quantities were determined and saved in separate files. Together with these quantities the number of samples in the bin, the average undisturbed wind speed and the average wind direction were saved.

Since the wind turbines operate at constant tip speed ratio in the interval 6-10 m/s, it was expected that the wake effects would not vary much over this speed range. A selected number of bin analyses has been made using a single wind speed bin of 5-10 m/s.

4.2.5 Dimensionless quantities

The results of the measurements are presented in non-dimensional form. First, the measured quantities have been non-dimensionalized with the undisturbed wind speed:
- U/U_0, V/U_0, W/U_0;
- u'/U0, v'/U0, w'/U0, k/U_0, u'/u'_0;
- $u'v'/U_0^2$, $u'w'/U_0^2$, $v'w'/U_0^2$.

Second the quantities have been non-dimensionalized using local parameters:
- V/U, W/U;
- u'/U, v'/U, w'/U, k/U;
- u'v'/k, u'w'/k, v'w'/k.

4.3 Measurements in the wake of two turbines in line

4.3.1 The measuring campaign

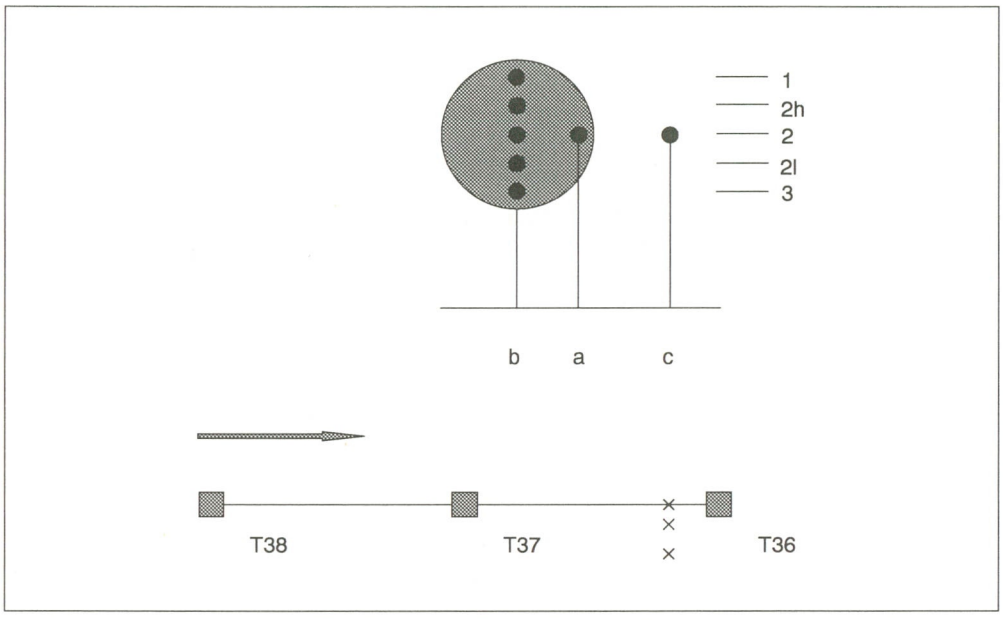

Figure 4.2 Experimental set-up during the measuring campaign

Between March and May 1992 measurements have been made in the double wake of T38 and T37, just ahead of T36 (see figure 4.2). In the indicated direction the distance between the turbines is 150 m, i.e. 5 rotor diameters.

The 3 mobile masts were installed at a distance of 120 m (4 D) behind T37. Mast **b**, which is in line with the turbines, contained the 3-component propeller anemometers at 47 m, 35 m and 23 m, denoted **b1**, **b2**, and **b3** respectively. The middle anemometer was thus mounted at hub height, the top and bottom anemometers at 0.4 rotor diameters above an below hub height. At the two intermediate heights, i.e. 41 m and 29 m, cup anemometers were mounted, denoted b2h and b2l. Next to the centre-line mast **b**, masts **a** and **c** were erected at distances of 12 m and 30 m, respectively. Both masts contained a 3-component propeller anemometer at 35 m height. The undisturbed wind conditions were measured with cup anemometer and a wind vane at 35 m height in mast M7. Simultaneous with the wind measurements the power of T36, T37 and T38 was measured. Table 4.1 gives an overview of the stored data.

Table 4.1 Overview of the measured and stored data

Sensor	Signal
a2..c2	U, u', U_{max}, U_{min}, V_{max}, V_{min}, W_{max}, W_{min}, U'^2 V'^2, W'^2, u'v', u'w', v'w'
b2l, b2h	
P36..P38	P, σ_P, P_{max}, P_{min}
wvel72	U_0, u'_0, U_{0max}, U_{0min}
wdir72	δ_0, σ_{d0}, δ_{0max}, δ_{0min}

The measured data were stored on hard disk and every day a back-up was made on magnetic tape. Later, the tapes were pre-processed off-line into 1-minute averaged samples.

4.3.2 Observations

During the campaign no serious problems arose. There was a problem with sensor b2, caused by hum in the measurement amplifier of the upper leg of the sensor which resulted in, among others, in an apparent average vertical wind speed. The signals have been corrected by setting the vertical component of the wind speed to zero. As a result no vertical turbulent velocities are available for this sensor.

During maintenance after the measurement campaign had finished it was noticed that sensor c2 showed an angle off-set with the main axes of 11 degrees. This has been corrected during pre-processing of the data. The results of this sensor for large angles of attack may therefore be unreliable.

During the analysis of the data it showed that the sensor used to measure the undisturbed wind direction had a misalignment of 5°. Prior to the analysis, the undisturbed wind direction and the other measured quantities have been corrected for this misalignment.

For negative wind directions the undisturbed wind measurements U72 are probably disturbed by the lightning rod which is mounted on top of the measuring mast.

4.3.3 Undisturbed wind conditions

This section describes the undisturbed wind conditions at the Sexbierum wind farm during the described measuring campaign. Further a description of the undisturbed turbulence intensity is given and the roughness length of the upwind terrain is derived.

Wind speed distribution

Figure 4.3 gives the wind speed distribution during the measuring period. It shows that the majority of the data has been found between 7 and 9 m/s. The figure also shows that the wind direction distribution is non-symmetrical about the axis.

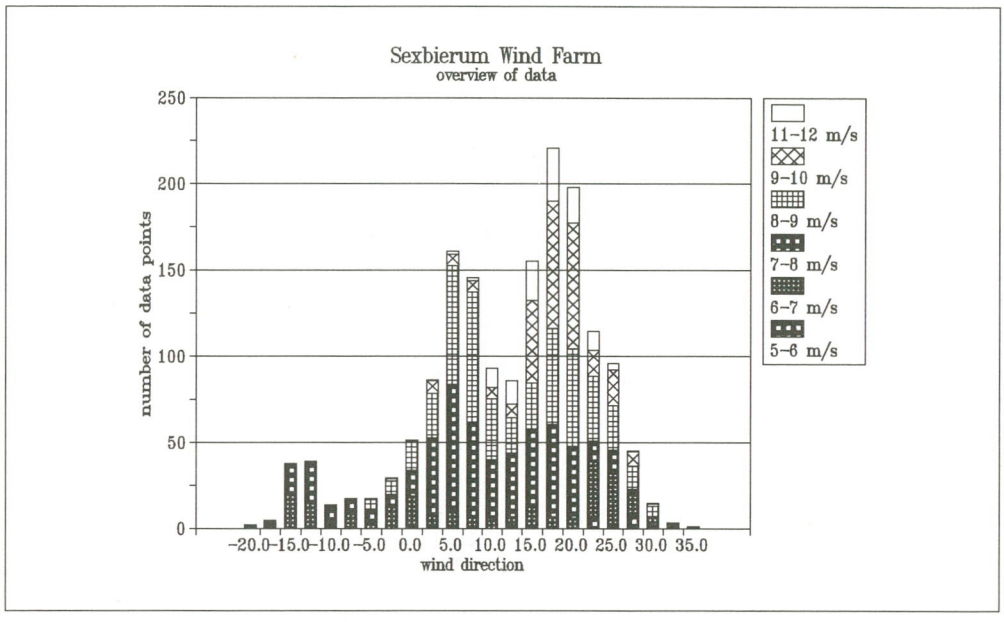

Figure 4.3 Overview of available data

Table 4.2 Turbulence intensity of undisturbed flow as a function of averaging time

Averaging time (min.)	Turbulence intensity	Corrected intensity	z_0	Number of samples
1	0.086	0.169		1726
3	0.095	0.136	0.046	573
10	0.107	0.132	0.038	137
60	0.131	0.138	0.051	10

The turbulence intensity has been determined by applying linear regression on pairs of undisturbed wind speed U_0 and turbulent velocity u'_0. The measured turbulent intensity is a function of the averaging time. This is shown in table 4.2.

[Panofsky and Dutton 1984] give a relation between the turbulence intensity, using an averaging period of one hour, and the upstream terrain roughness. The relation is given by:

$$I = \frac{\alpha.k}{\ln(z/z_o)}$$

Panofsky finds values for the constant $\alpha=2.39\pm0.03$. Holtslag has analysed turbulence data in the Dutch situation and finds the value $\alpha=2.2$.

The turbulence intensity corresponding to an averaging period of 1 hour was determined in two distinct ways:

1. the data was processed using an averaging time of 60 minutes. Using this method the value $I=0.131$ was found. Although this is the most straightforward way, it has the disadvantage that only a few 60-minutes samples were available, since the database contains only very few continuous time series of 60 minutes length;
2. [ESDU] gives expressions for the transformation of turbulence intensities obtained using shorter averaging periods into turbulence intensities based on 1-hour averaging period. This results in the corrected turbulence intensities given in table 4.2.

Discarding the value for the 1-minute averaging period and using the corrected turbulence intensities for the roughness length upstream of the farm a value of $z_0=0.045\pm0.007$ m is found.

4.3.4 Wake deficit

Wake deficit per bin

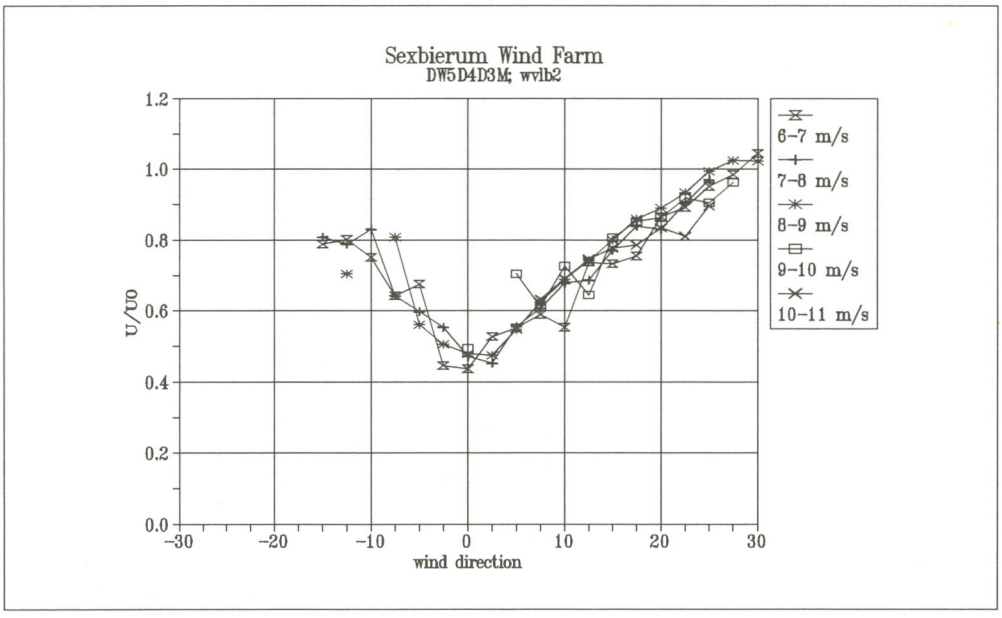

Figure 4.4 Wind speed ratio U/U_0 at sensor b2 as a function of the undisturbed wind direction

Figure 4.4 shows the wind speed ratio U/U_0 at sensor b2 as a function of the undisturbed wind direction for the wind speed classes between 6 m/s and 11 m/s.

The figure shows that the wind speed ratio U/U_0 is almost equal for the depicted wind speed classes, which can be explained by the fact that the wind turbines operate at

constant tip speed ratio between 6 and 10 m/s. In this range the thrust or axial force is therefore almost constant.
At the wake centre-line U/U_0 reaches a minimum of 0.45, approximately. At an undisturbed wind direction of 30 degrees the edge of the wake is observed and U/U_0 is equal to unity. This means that the double wake is approximately 2 diameters wide. Overspeeding ($U/U_0>1$) which is sometimes seen at the wake edge, can not be observed in this case. If it would occur, it would be at an angles larger than 30 degrees. The figure does not show the complete wake profile. Negative wind directions were only scarcely available in the data base. The shape of the wake profile is not completely symmetrical about the origin, positive wind direction show a somewhat smaller value of U/U_0 than negative wind directions.

Aggregated results

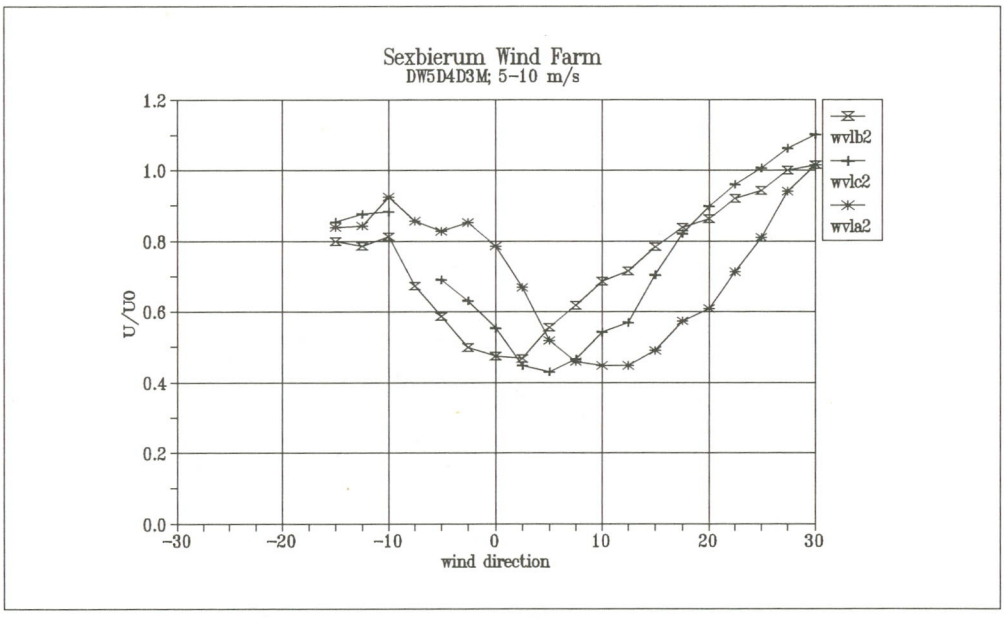

Figure 4.5 Wind speed ratio U/U_0 as a function of wind direction for sensors b2, c2 and a2

Figure 4.5 shows the aggregated results in the wind speed range of 5-10 m/s for the three sensors b2, c2, a2 in the horizontal plane at hub height. The sensors are all on one side of the line connecting turbines T38-T37-T36. b2, a2 and c2 are at a distance of 0 m, 12 m and 30 m from this line, respectively.
As is expected the minimum values of U/U_0 are shifted with respect to the 0 degree undisturbed wind direction, as is expected from the geometry of the sensor positions. Sensor c2 is at the wake centre of turbine T37 at a wind direction of 5 degrees, and sensor a2 at 14 degrees. The figure shows that the minimum of c2 is indeed found at the given value, but that the minimum of a2 is found at a smaller angle. This is due to the fact that the minimum is not found at the wake centre of T37, but is determined by the superposition of the wakes of T37 and T38. The wake centre of turbine T38 is found at 6 degrees. Further it can be noticed that the minimum ratio U/U_0 is nearly equal for the three sensors (0.45).

With the undisturbed wind direction changing, the wake configuration changes. At 0 degrees the wakes are fully immersed, but for larger angles the wakes only partially overlap. However, at one particular wind direction the three sensors give the wind speed at different positions in the wake, but for identical wake configurations.

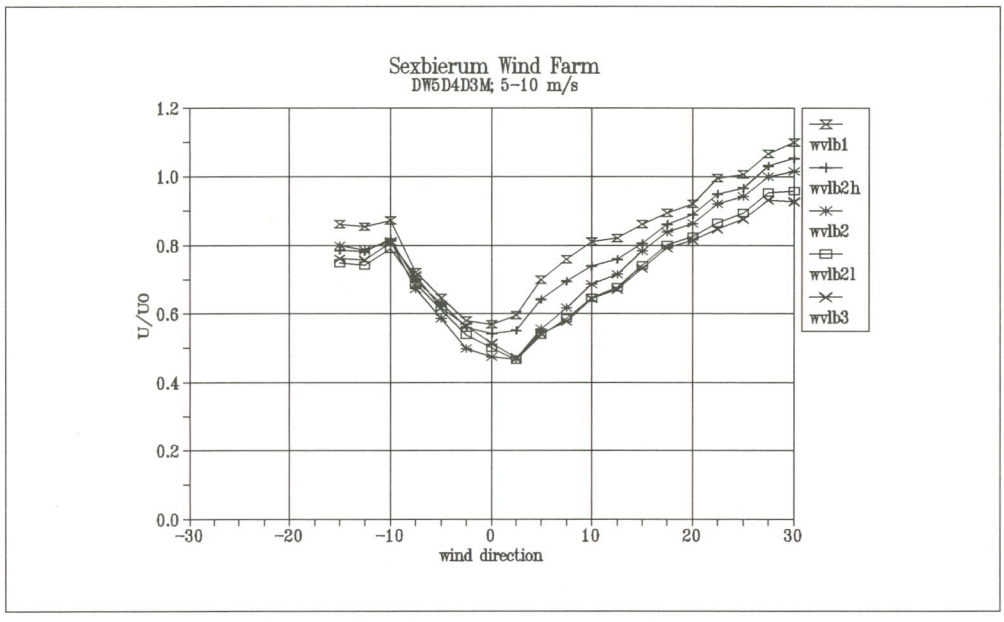

Figure 4.6 Wind speed ratio U/U_0 as a function of wind direction for sensors b1, b2h, b2, b2l and b3

Figure 4.6 gives the ratio U/U_0 at the 5 sensors mounted at different heights on mast b. The figure clearly reveals that the wake profiles are almost identical at the given heights, with the lowest values of U/U_0 at hub height. However, the figure also shows that the profiles are asymmetrical. For negative wind directions the measured profiles coincide, while for positive wind directions they are clearly different in magnitude. This effect is caused by systematic errors in the undisturbed wind measurement.

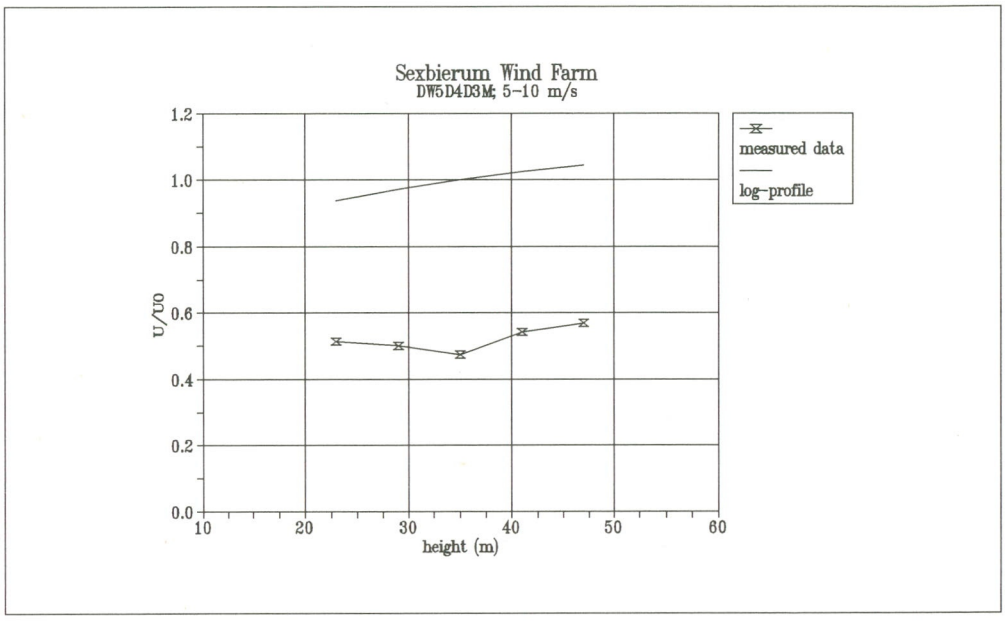

Figure 4.7 Vertical wake profile at the wake centre-line

In figure 4.7 the vertical profile of U/U_0 is given, together with the calculated undisturbed wind profile using z_0=0.045 m.

4.3.5 Turbulence intensity

Turbulence intensity data per bin

In this section we show the results of the analysis on the measured turbulence in non-dimensional form.

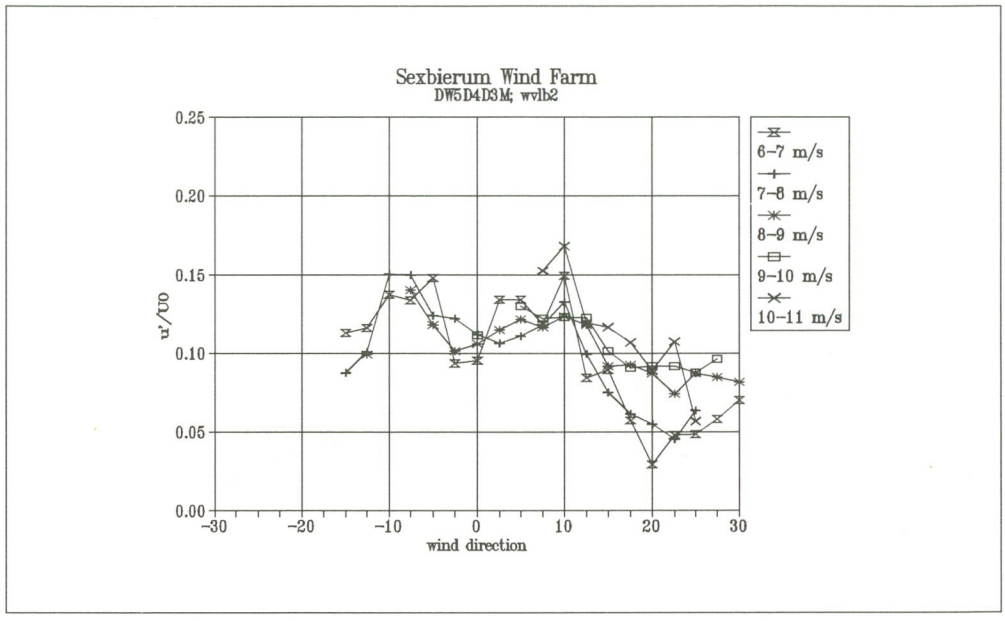

Figure 4.8 Turbulence intensity u'/U_0 as a function of wind direction at sensor b2

Figure 4.8 shows the turbulence intensity (non-dimensionalized with U_0) of the horizontal wind component for sensor b2 as a function of the wind direction. Figures 4.9 and 4.10 show the lateral and vertical turbulence intensity. The figures show that the turbulence intensity increases towards the centre of the wake. Unlike the lateral and the vertical turbulence intensity, the u-component shows peaks at a wind direction of approximately 10 degrees, which corresponds with the locus of the maximum wind speed gradient (see figure 4.20), which corresponds with maximum turbulence production. k and u' are more or less symmetrical about the zero wind direction, but v' and w' are higher for the negative wind direction than for the positive ones.

Although the figures show some scatter, it seems that the turbulence intensity scales with U_0 for wind directions between -10 an 10 degrees. For larger angles two branches can be observed, one for wind speeds below 8 m/s and one for the higher wind speeds.

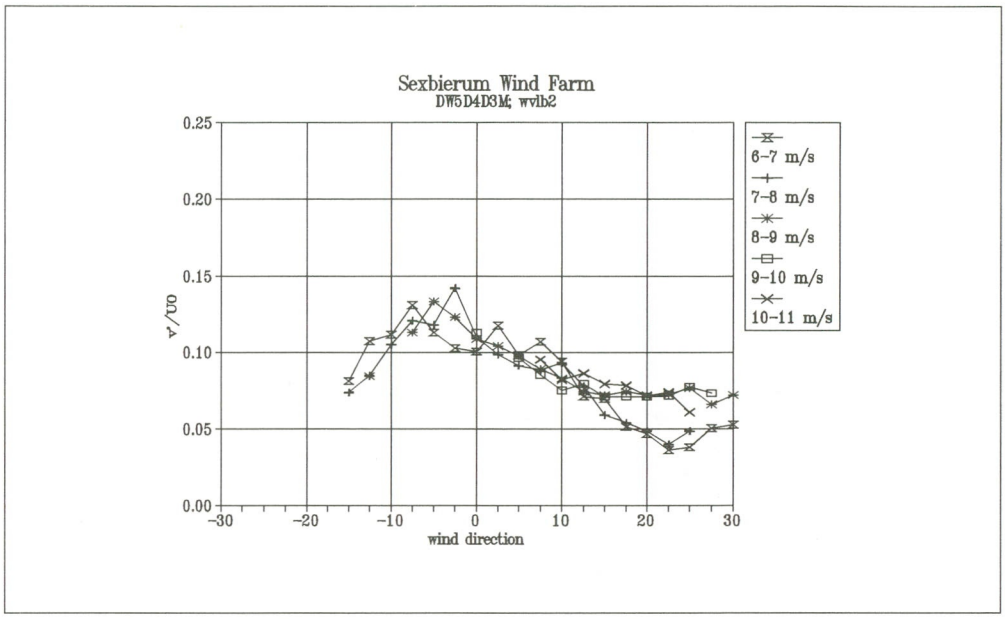

Figure 4.9 Lateral turbulence intensity v'/U_0 as a function of wind direction at sensor b2

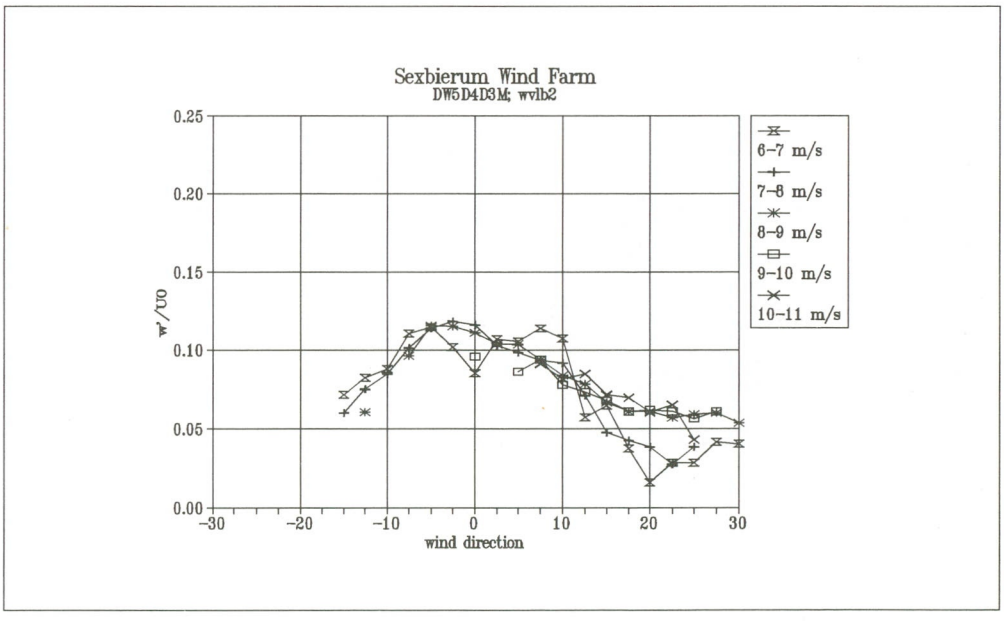

Figure 4.10 Vertical turbulence intensity w'/U_0 as a function of wind direction at sensor b2

Figure 4.11 shows the turbulent kinetic energy k (non-dimensionalized with U_0) as a function of the wind direction. The behaviour of k is roughly the same as that of the components of the turbulence. Non-dimensionalized with the local wind speed k varies much more smoothly with the wind direction.

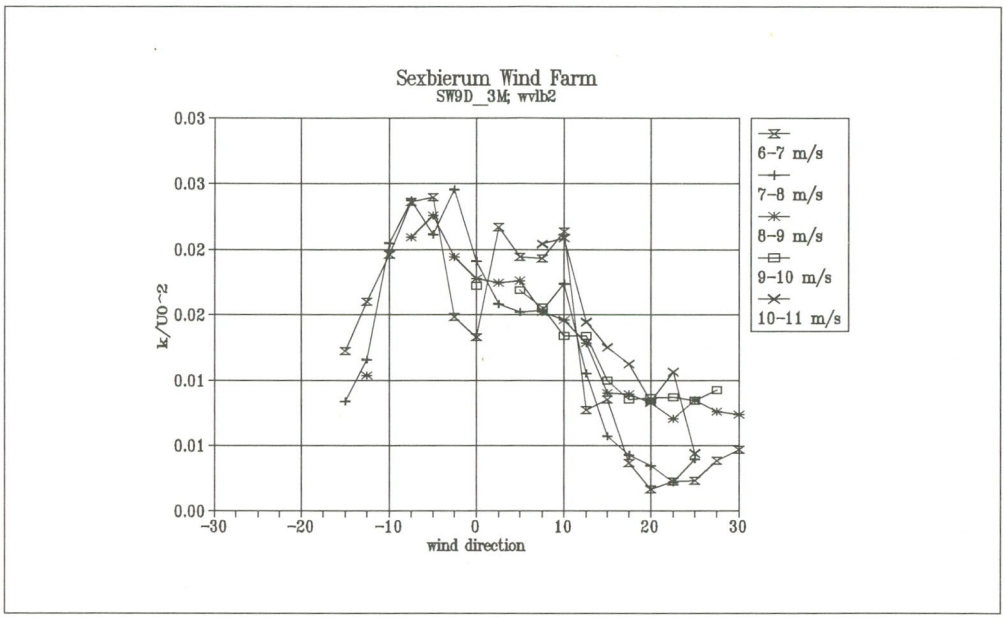

Figure 4.11 Turbulent kinetic energy k/U_0 as a function of wind direction at sensor b2

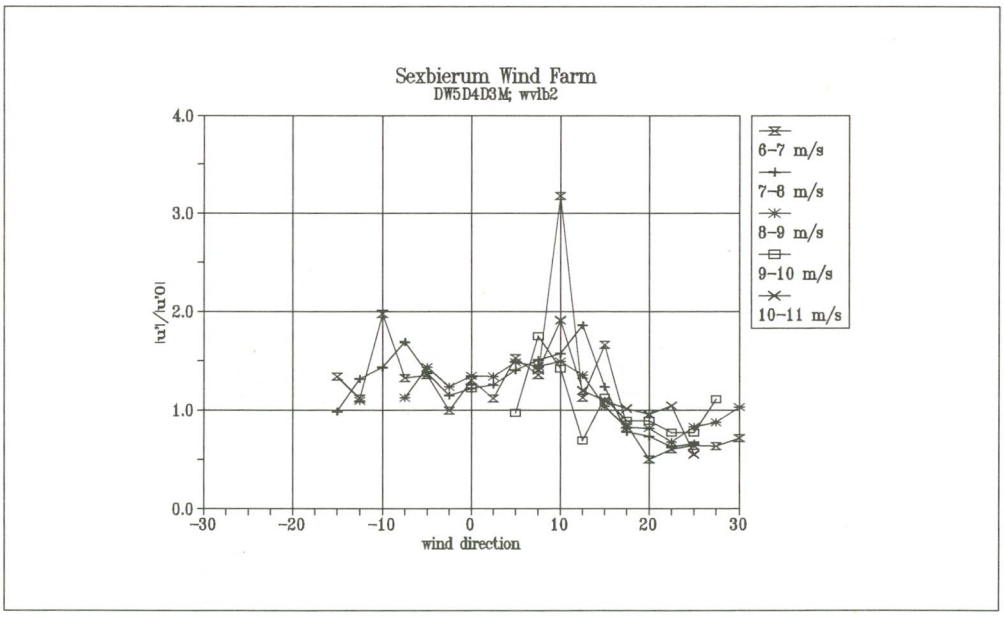

Figure 4.12 Ratio of wake turbulence and undisturbed turbulence u'/u_0' as a function of wind direction at sensor b2

In figure 4.12 the ratio u'/u'_0 is given as a function of the wind direction. The figure shows that inside the wake the turbulent velocities are higher than at the edge of the wake. Although this general behaviour is correct, it seems that there is something peculiar about these data. At the wake edge the ratio u'/u'_0 remains below unity. It is expected, however, that this ratio returns to unity at the wake edge, as for these angles

the undisturbed wind conditions should be restored. It might be argued that different sensors are used for the measurement of the undisturbed wind conditions and for the wind conditions in the wake with for instance different sample rates. Nonetheless, comparison of the data of sensors b2h and b2l, which are identical to that at mast M72, shows the same results. The cause for these peculiarities are as yet unclear.

Aggregated results

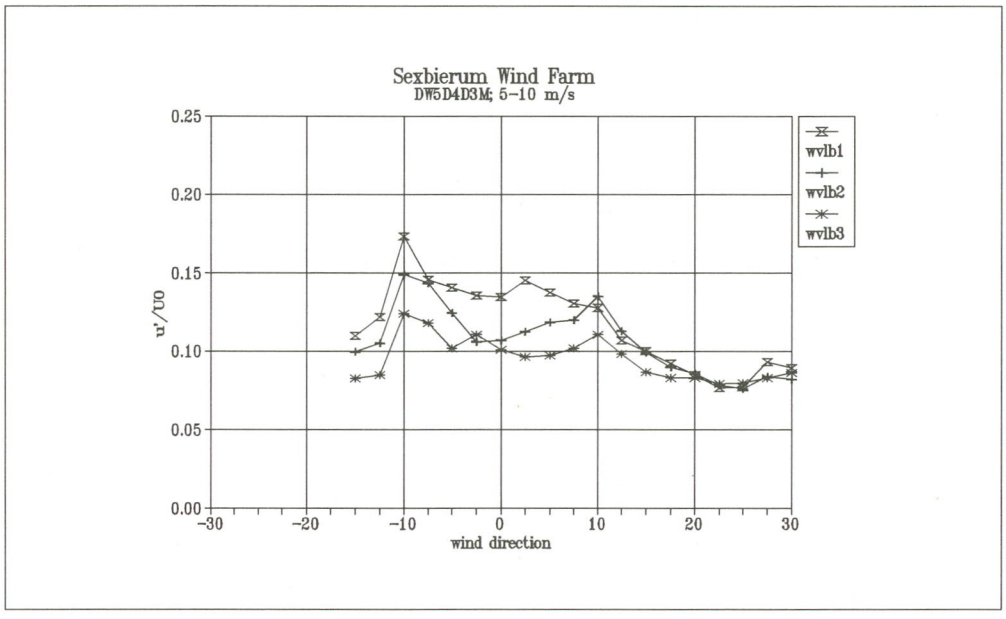

Figure 4.13 Aggregated turbulence intensity u'/U_0 as a function of wind direction at mast b

Figure 4.13 depicts the turbulence intensity u'/U_0 at mast b for the positions 1, 2 and 3. The figure shows again that there is some asymmetry in the course of the turbulence over the wind direction. Clearly, the turbulence intensity is the highest at the top-most sensor ($k/U_0^2 = 0.027$) and lowest at the bottom-most sensor ($k/U_0^2 = 0.016$). This corresponds well to what is expected. As production of turbulence is related to the wind velocity gradient, the highest turbulence is expected where the gradients are at maximum. At the highest sensor position the boundary layer wind velocity gradient is increased by the presence of the wake, while the wake decreases the gradient at the lowest sensor position (see figure 4.20).

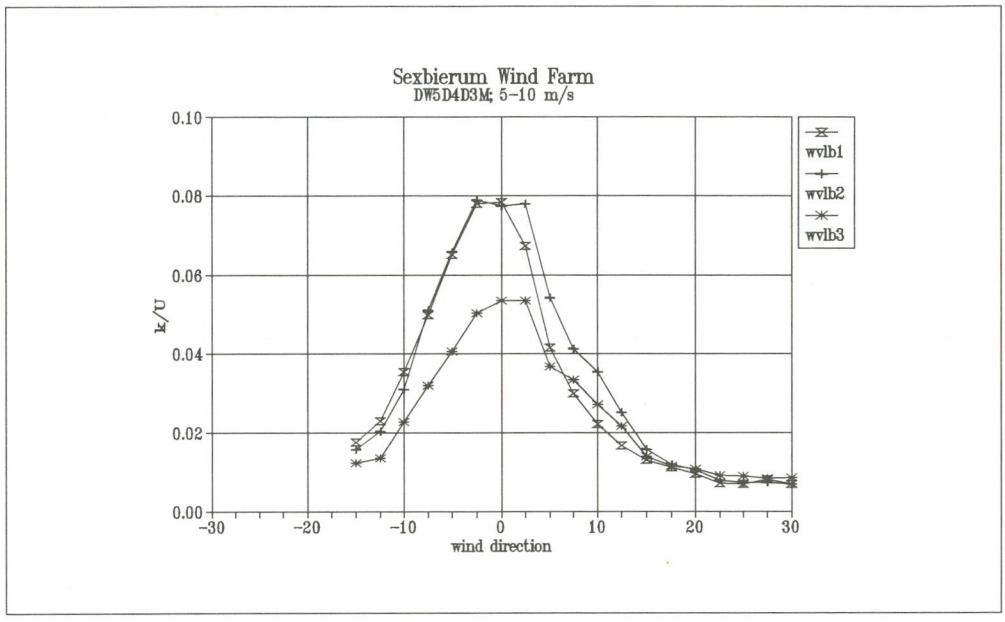

Figure 4.14 Turbulent kinetic energy non-dimensionalized with local velocity as a function of wind direction

Figure 4.14 depicts the turbulent kinetic energy non-dimensionalized with the local wind speed. Again most of the asymmetry has disappeared and the curves have a more or less Gaussian shape.

4.3.6 Shear stress

Shear stress per bin

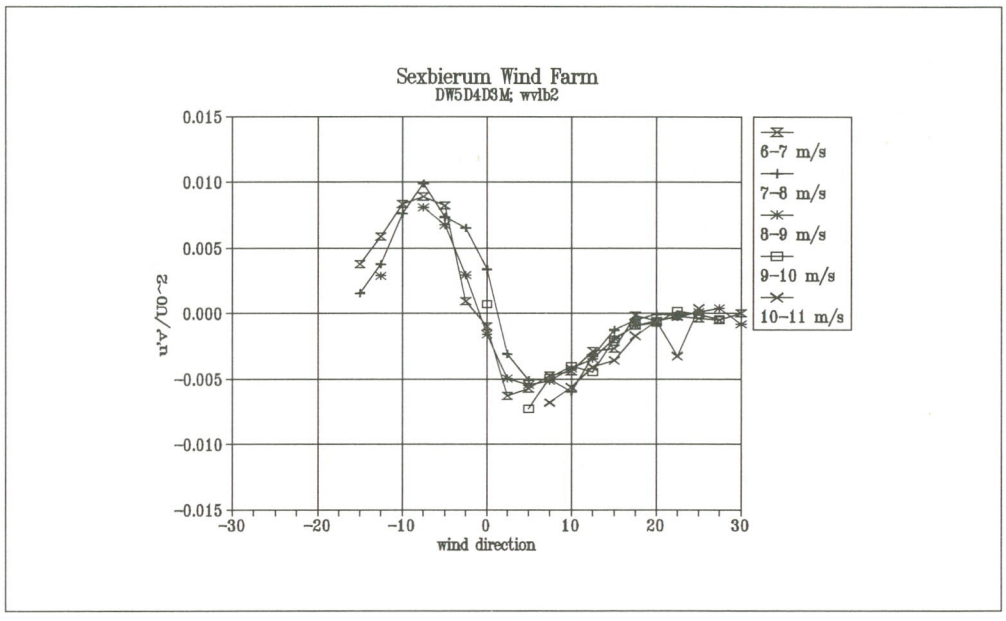

Figure 4.15 Shear stress $u'v'/U_0^2$ as a function of wind direction at sensor b2

The Reynolds-stress u'v' is the turbulent shear stress which is the driving force for the recovery of the wake deficit in horizontal direction. Figure 4.15 shows the shear stress u'v' non-dimensionalized with the undisturbed wind speed U_0 against the undisturbed wind. Starting from the right side of the figure (positive wind directions) and going to the negative wind directions it shows that at the edge of the wake $u'v'/U_0^2$ is equal to zero and then shows a minimum of -0.005. At 0° wind direction it goes through zero, shows a maximum of 0.01 before it relaxes again to 0 at the left edge of the wake. Generally speaking this is expected, since it is assumed that the shear stress is proportional to the local wind shear, i.e. the horizontal wind gradient. The fact that the curves return to zero at the edge of the wake, and that they cross the x-axis at 0° wind directions gives confidence in the quality of the data. Scaling of the data with U_0 seems to be successful.

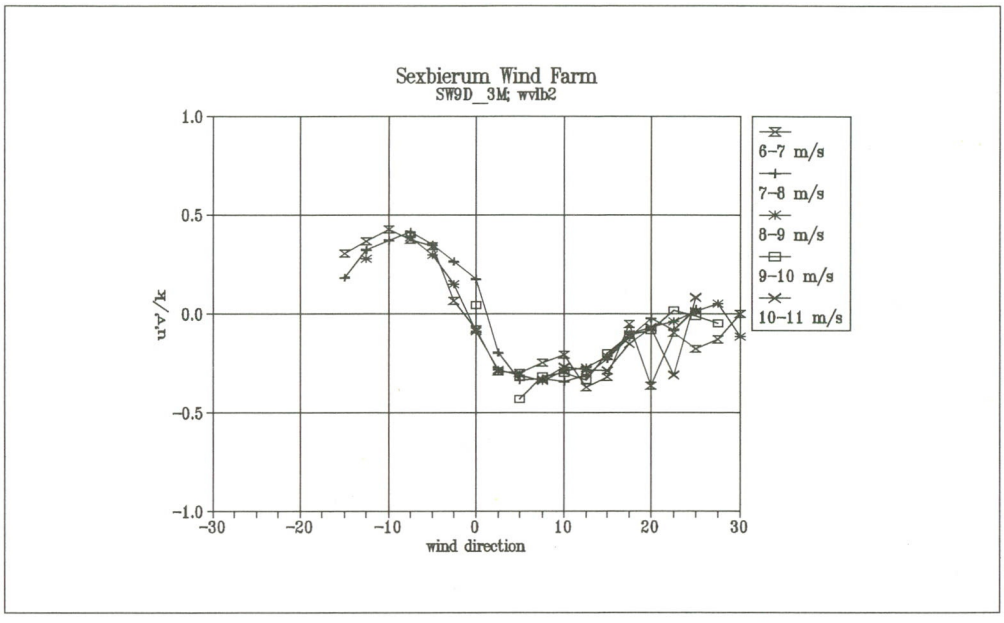

Figure 4.16 Shear stress u'v' non-dimensionalized with the local turbulent kinetic energy as a function of wind direction at sensor b2

The profile for u'v' shows to be asymmetrical. This is consistent with the measurements of the turbulence intensity and the horizontal wind profile. Figure 4.16 shows that if the shear stress is not non-dimensionalized by the undisturbed wind speed, but by a local quantity such as k, the asymmetry partly disappears.

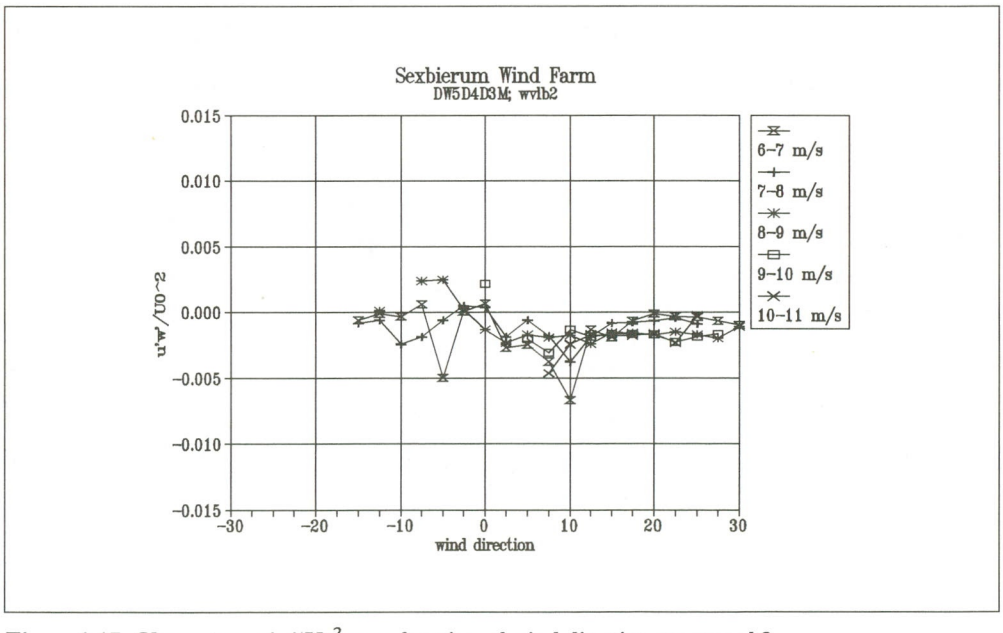

Figure 4.17 Shear stress $u'w'/U_0^2$ as a function of wind direction at sensor b2

The u'w'-component is given in figure 4.17. Apparently there is hardly a u'w'-component at sensor b2. This can be explained by the fact that sensor is at the symmetry plane of the wake. Indeed the sensors at different positions show a significant u'w'-component variation over the wind directions. This will be discussed in the next section.

The v'w'-component of the shear stress turns out to be very small at each of the sensor positions. This shear stress component is proportional to the spatial derivatives of V and W, which are both very small throughout the wake. Hence the shear stresses are also small.

Aggregated results

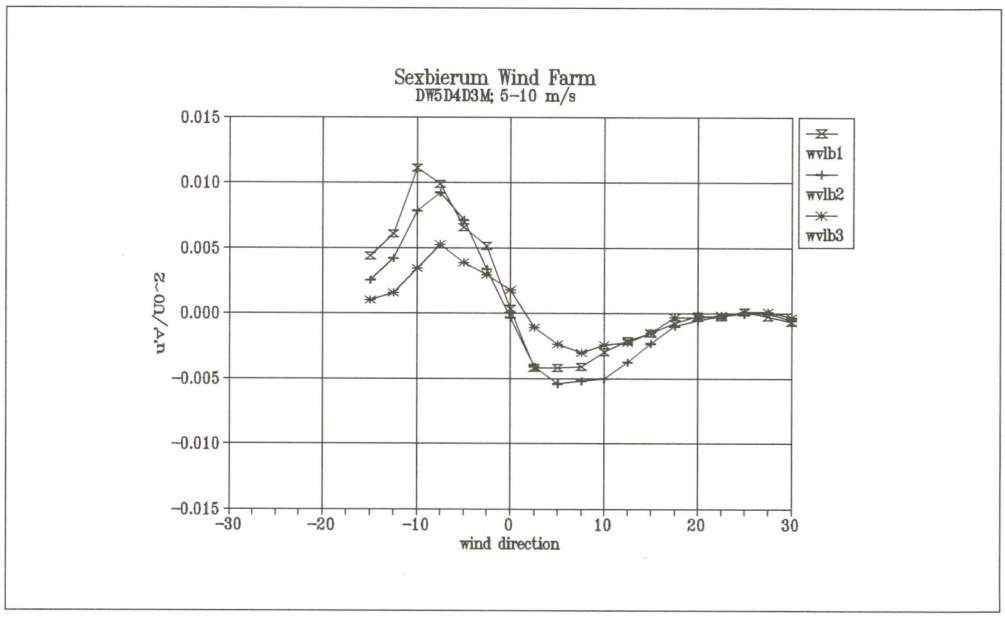

Figure 4.18 Shear stress $u'v'/U_0^2$ as a function of wind direction for sensors b1, b2 and b3

Figure 4.18 shows the non-dimensional shear-stress $u'v'/U_0^2$ for the three sensors at mast b as a function of the undisturbed wind direction. The shape of the three curves is again very similar except horizontal shift. Eddy-viscosity theory for turbulence assumes that the turbulent shear stress is proportional to the local shear. This is clearly reflected in the curves of figure 4.18. Outside the wake no horizontal wake effect is present and hence the horizontal wind gradient is zero. At the maximum gradient dU/dy shear stress reaches a maximum, after which it decreases zero, where the wind speed shows a minimum. For larger wind directions the shear shows a similar behaviour but of an opposite sign.

The shape and the magnitude of the shear stress curves compares well with results of wind tunnel tests [Smith].

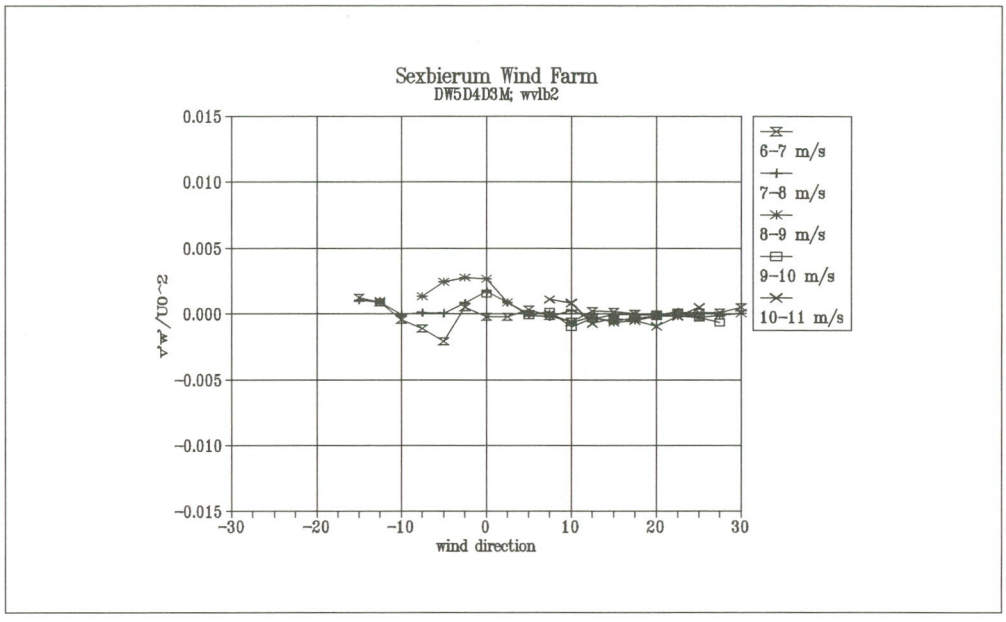

Figure 4.19 Shear stress u'w'/U_0^2 as a function of wind direction for sensors b1, b2 and b3

Figure 4.19 shows the non-dimensional turbulent shear stress u'w'/U_0^2 as a function of the wind direction at the three sensor positions b1, b2, b3. The graphs show quite a distinct behaviour from the horizontal shear.
The shear stress u'w' is proportional to the vertical wind speed gradient dU/dz. Outside the wake the u'w' is negative corresponding the shear stress in the atmospheric boundary layer. Traversing through the wake at the top position b1, the vertical gradient increases with the increasing wake effect and so u'w' becomes more negative (figure 4.20). At the bottom sensor b3 the situation is different. When the wind direction changes the wake effect becomes stronger; the wind gradient and hence u'w' changes sign.

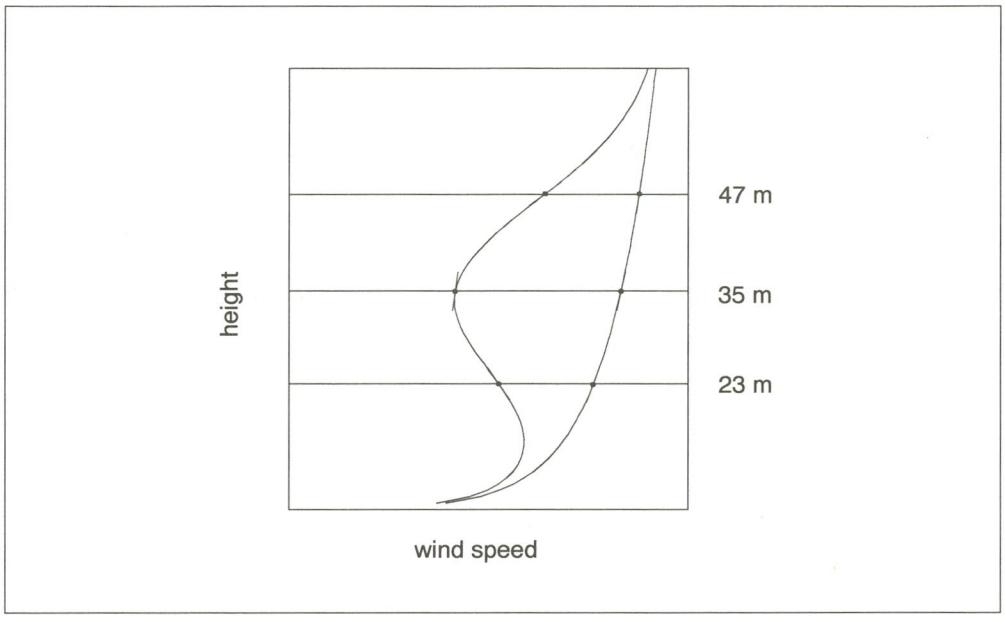

Figure 4.20 Change of the vertical wind gradient under influence of the wake deficit

4.4 Measurements in the wake of a single machine

4.4.1 The measuring campaign

Between July and November 1992 measurements have been made in the wake of T18, ahead of T27 (see figure 4.21). In the indicated direction the distance between the turbines is 285 m, i.e. 9.4.

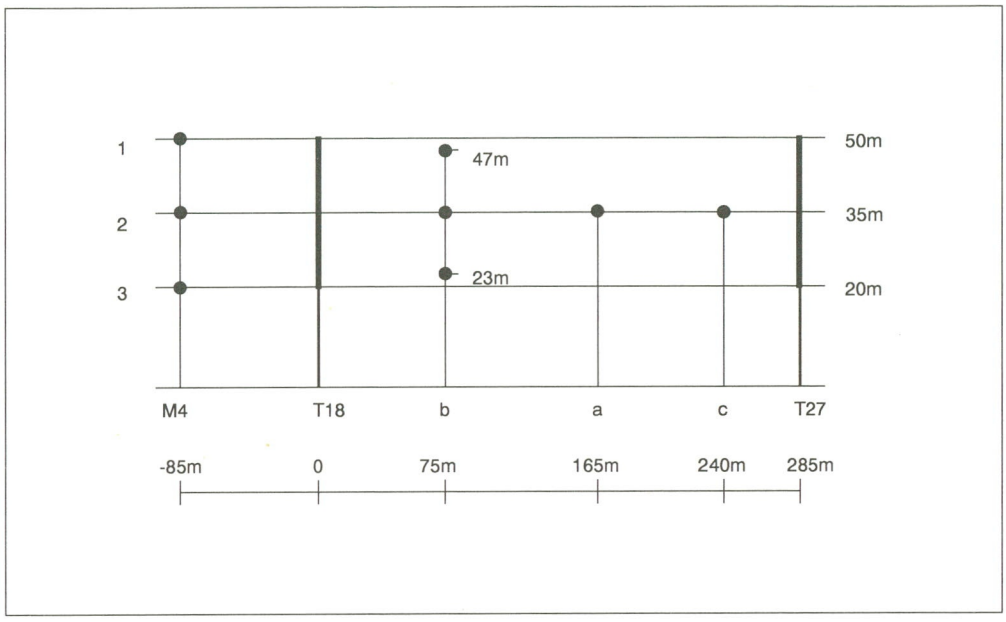

Figure 4.21 Experimental set-up during the measuring campaign

Mast b, installed 75 m (2.5 D) behind T18, contained the 3-component propeller anemometers at 47 m, 35 m and 23 m, denoted b1, b2 and b3. The middle anemometer was thus mounted at hub height, the top and bottom anemometers at 0.4 rotor diameters above and below hub height. Mast a was erected 165 m (5.5 D) behind T18 and contained a 3-component propeller anemometer at hub height, denoted a2. Mast c was installed at 240 m (8 D) behind T18 and contained a 3-component propeller anemometer at hub height, denoted c2. The undisturbed wind conditions were measured with cup anemometers at wind vanes at mast 4 at 3 levels (20 m, 35 m and 50 m). Simultaneously with the wind measurements the power of T18 was measured. Table 4.3 gives an overview of the stored data.

Table 4.3 Overview of the measured and stored data

Sensor	Signal
a2..c2	U, V, W, U_{max}, U_{min}, V_{max}, V_{min}, W_{max}, W_{min}, u'^2, v'^2, w'^2, u'v', u'w', v'w'
b2l, b2h	U, u', U_{max}, U_{min}
P18	P, σP, P_{max}, P_{min}
wvel41, 42, 43	U_0, u'_0, U_{0max}, U_{0min}
wdir41, 42, 43	δ_0, σ_{d0}, δ_{0max}, δ_{0min}
sblh18	pitch angle T18, σ_{pitch}, $pitch_{max}$, $pitch_{min}$

4.4.2 Observations

During the measuring campaign no serious problems arose and a body of approximately 2700 1-minute samples were recorded successfully.
The following problems were observed:

- sensor wvlc2 (X/D=8) had no signal for about one third of the samples;
- the wind direction sensors at the undisturbed wind measuring mast had a misalignment of +5°, +5° and -10° for height 1, 2 and 3, respectively. The measurements have been corrected for this;
- the topmost sensor wvel41 showed a dip in the wind speed measurements due to shading of a lightning rod for wind directions between 170° and 210°;
- sensor wvel42 showed malfunctioning at the end of the measuring period, indicating too low wind speeds. During a first analysis this resulted in 'skew' profiles of (for instance) U/U_0 combined with considerable scatter. In the final analysis use was made of sensor wvel43, which resulted in 'flat' profiles with reduced scatter.

4.4.3 Undisturbed wind conditions

This section describes the undisturbed wind conditions at the Sexbierum wind farm during the single wake measuring period. Further a description of the undisturbed turbulence intensity is given and the roughness length of the upwind terrain is estimated.

Wind speed distribution

Figure 4.22 gives the wind speed distribution during the measuring period. It shows that the majority of the data has been found between 7 and 9 m/s. The average wind speed in the measuring period was 8.4 m/s. Negative wind directions clearly prevail. Figure 4.23 shows the frequency distribution during the measuring campaign.

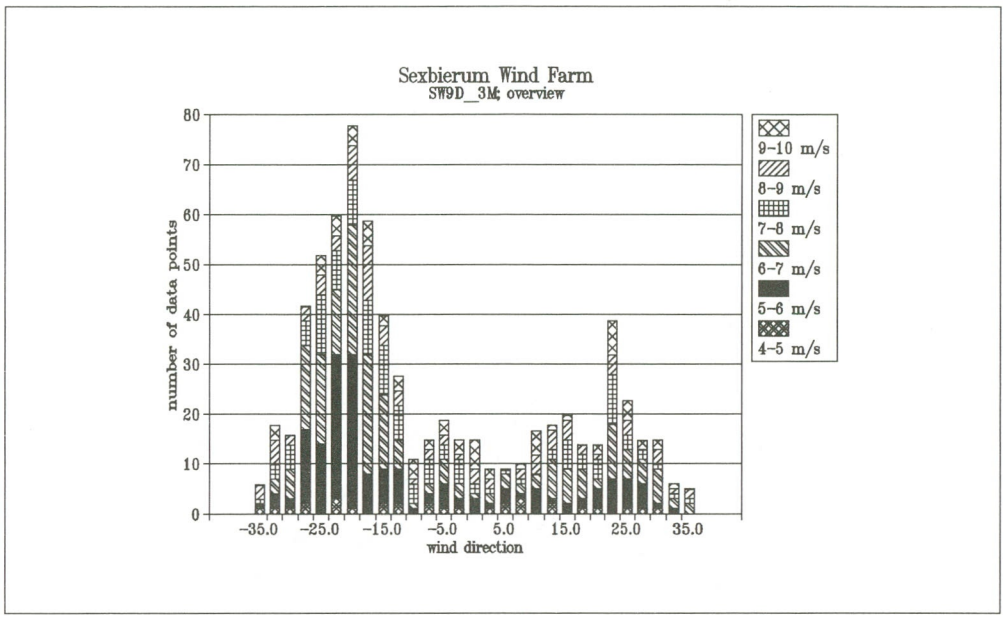

Figure 4.22 Overview of available data

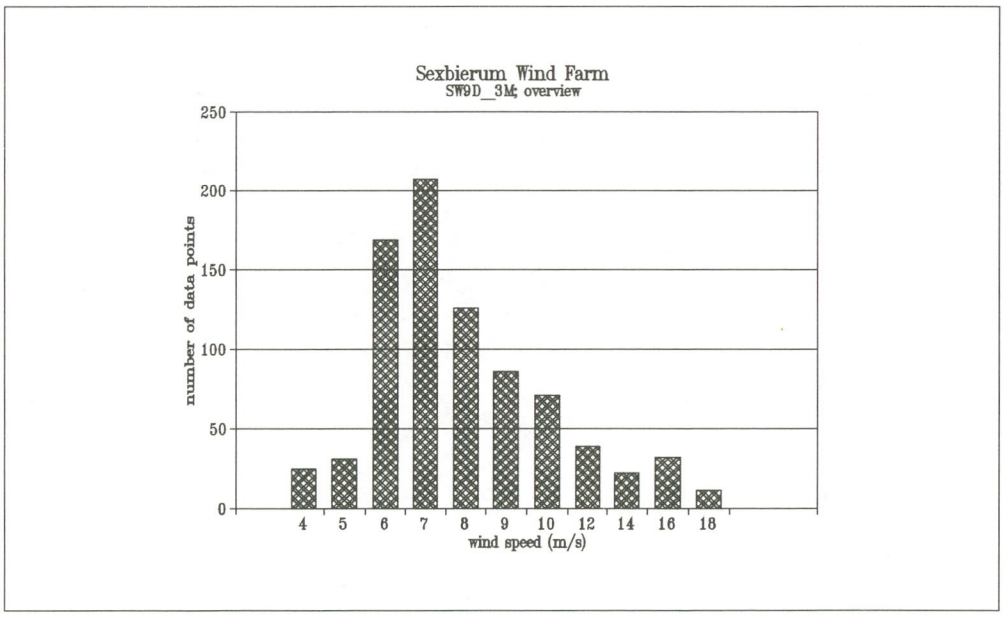

Figure 4.23 Frequency distribution of the wind speed during the measuring campaign

The average wind speed during the measuring campaign was 8.4 m/s

Undisturbed wind profile

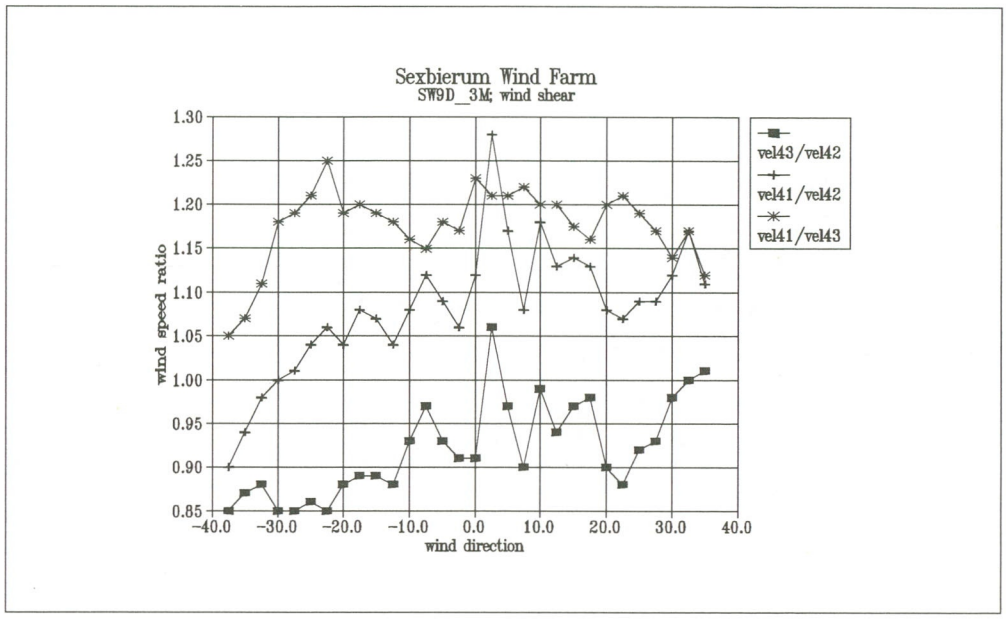

Figure 4.24 Ratio of the undisturbed wind speeds at three heights

Figure 4.24 gives the ratio of the wind speed for the combinations wvel41/wvel42, wvel43/wvel41 and wvel41/wvel43 in the wind sector under consideration. The following remarks can be made:

- for wind directions from -40 to -20 degrees wvel41/wvel43 and wvel41/wvel42 show a dip. This is caused by the wake of a lightning rod which is mounted on top of meteorological mast 4. The other anemometers are not affected by this effect because they are connected to the mast by means of a boom;
- Except for the velocity dip due to the lightning rod the ratio wvel41/ wvel43 is constant. The ratio wvel42/wvel43 and wvel41/wvel42 shows a steady increase with increasing values of the wind direction. During initial analysis of the single wake data, making use of wvel42 for binning the data, this resulted in skew wind profiles. Reviewing of the wvel42 records showed that this anemometer showed irregular malfunctioning during the last period of the measuring campaign. Therefore it was decided to use the undisturbed anemometer wvel43 for the analysis of the wake data.

Due to the above-mentioned effects it is hard to determine a reliable estimate of the roughness length z_0. Yet, using the data resulted in a roughness length of $z_0 = 0.13$ m. In the next section the roughness length is also estimated from the measured turbulence intensity.

Turbulence intensity

Table 4.4 Turbulence intensity at 3 measuring heights

Measuring height	Turbulence intensity	Corrected intensity	z_0
20 m	0.100	0.145	0.046
35 m	0.095	0.138	0.058
50 m	0.086	0.125	0.044

The turbulence intensity has been determined by applying linear regression on pairs of undisturbed wind speed U_0 and turbulent velocity u'_0 for an averaging time of 3 minutes. In order to estimate the turbulence intensity for a 1-hour average the correction was applied as described in [Cleijne, 1992]. The result is shown in table 4.4 for the three measuring heights.
Using the expressions given in [Panofsky and Dutton,1984] the roughness length has been estimated. This results in a roughness length of $z_0 = 0.047$ m, which seems to agree well with the results from the double wake campaign. It should be noted that this estimate is insensitive to calibration errors in the sensors. Finally, it is possible to estimate z_0 from the turbulence intensity profile I (z) using regression. This method resulted in the estimate $z_0 = 0.049$ m.
Taking into account the uncertainties in the measurement of the wind profile, the roughness length estimate from the turbulence intensity is preferred to the one from the wind profile.

4.4.4 Wake deficit

Wake deficit per bin

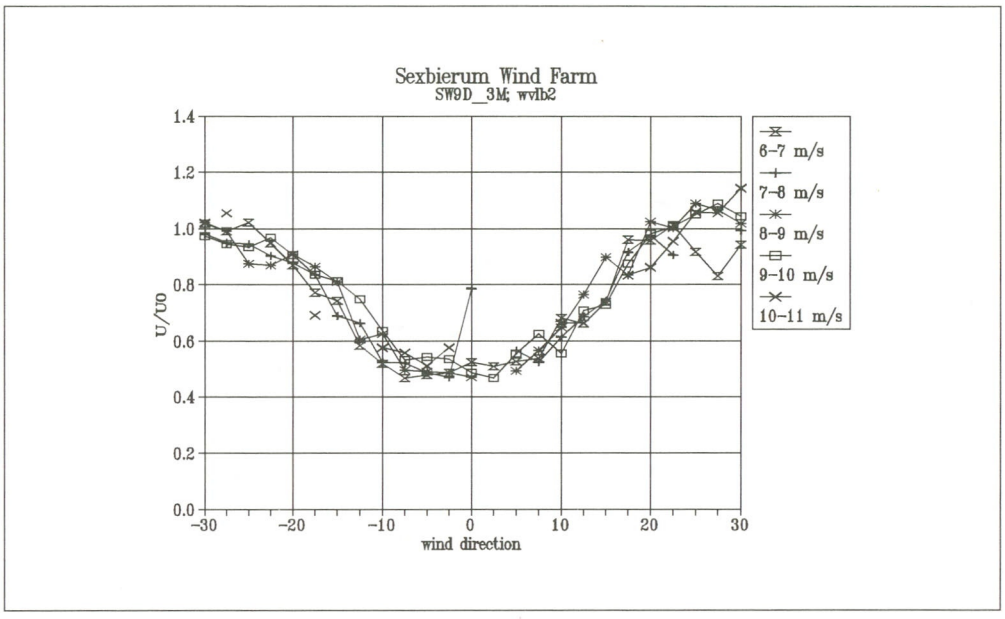

Figure 4.25 Wind speed ratio U/U_0 at sensor b2 as a function of the undisturbed wind direction

Figure 4.25 shows the wind speed ratio U/U_0 at sensor b2 as a function of the undisturbed wind direction for the wind speed classes between 6 m/s and 11 m/s. Sensor b2 was located at hub height 2.5 D behind T18. As in the case of the double wake measurements the wind speed ratio U/U_0 is almost equal for the depicted wind speed classes, which can be explained by the fact that the wind turbines operate at constant tip speed ratio between 6 and 10 m/s.
At the wake centre-line U/U_0 reaches a minimum of 0.50, approximately. At an undisturbed wind direction of 20 degrees the edge of the wake is observed and U/U_0 is equal to unity. The shape of the wake profile is not completely Gaussian, but more flattened. This is probably due to the fact that mast b is at a distance of 2.5 D only.

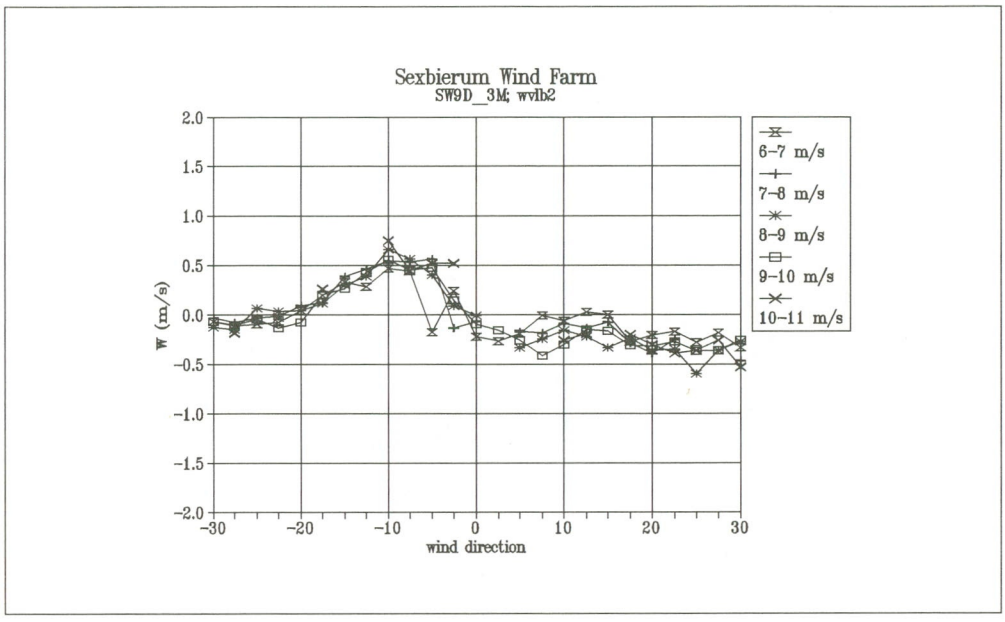

Figure 4.26 Vertical wind speed W as a function of wind direction at sensor b2

The values of the lateral wind speed V are small compared to those of the longitudinal component and have not been depicted.
Figure 4.26 shows the vertical velocity W. The figure shows that W/U_0 is positive for negative wind directions and W is negative for positive wind directions. This agrees with the fact that the rotor rotates clock-wise, when looking down-wind. The velocities are small, however.

Aggregated results

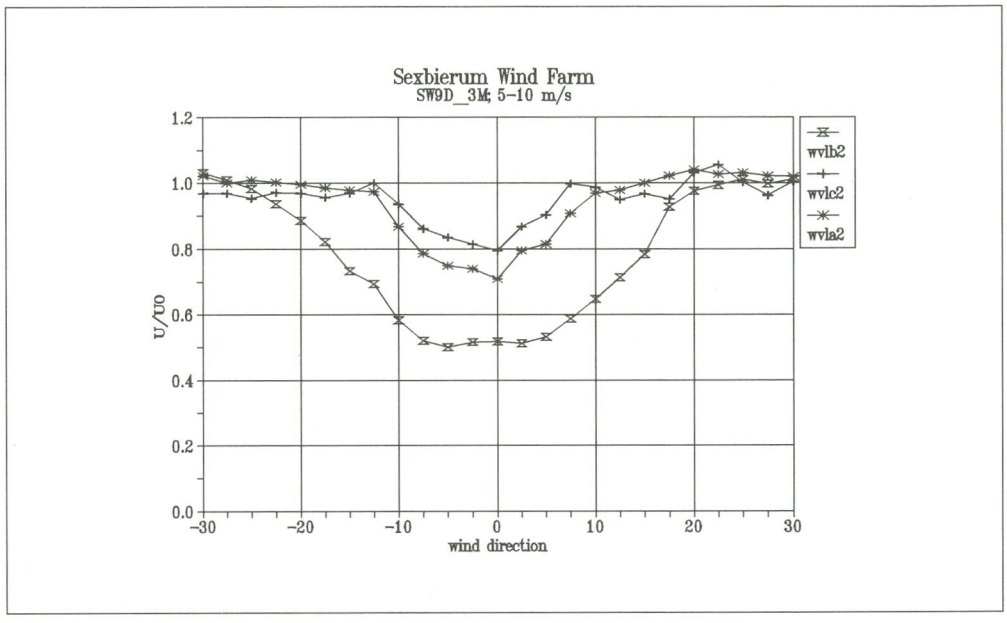

Figure 4.27 Wind speed ratio U/U_0 as a function of wind direction for sensors b2, a2 and c2

Figure 4.27 shows the aggregated results in the wind speed range of 5-10 m/s for the three sensors b2, a2, c2 at hub height. Sensor b2 is at 2.5 D behind the rotor; a2 at 5.5 D and c2 at 8 D.
At x = 2.5 D the wind speed ratio is 0.5; at x = 5.5 D a value of $U/U_0 = 0.7$ is found and at x = 8 D the wind speed ratio is 0.8.
Clearly, the flattened profile at x = 2.5 D develops in a more pronounced profile.

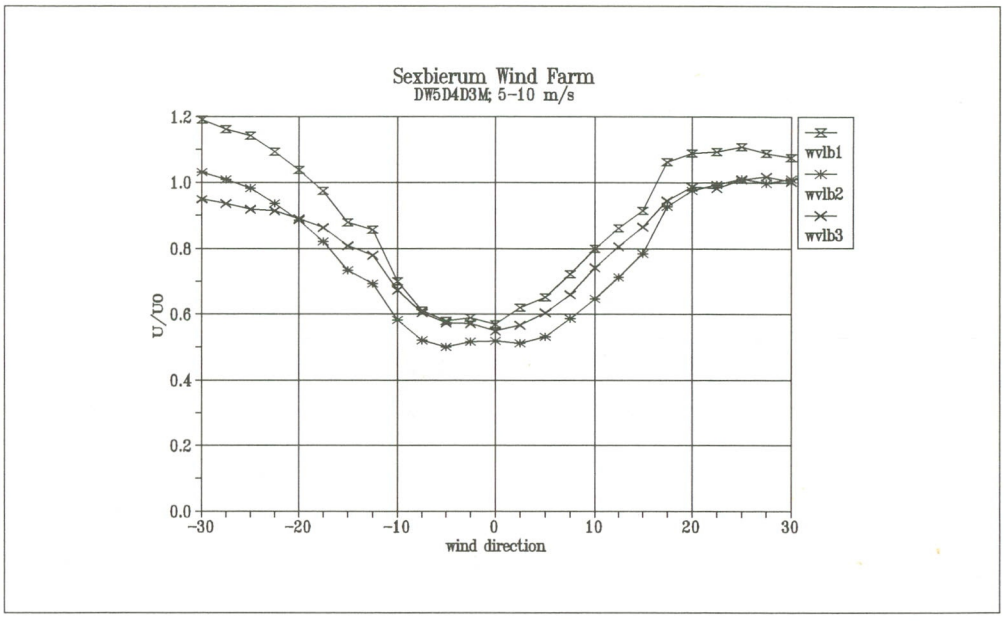

Figure 4.28 Wind speed ratio U/U_0 as a function of wind direction for sensors b1, b2 and b3

Figure 4.28 gives the ratio U/U_0 at the 3 sensors mounted at different heights on mast b, which is at 2.5 D behind turbine T18. The figure clearly reveals that the wake profiles are almost identical in shape at the given heights, with the lowest values of U/U_0 at hub height. Outside the wake (see negative wind direction), the wind speeds increase from the lowest sensor b3 to the highest sensor b1, which agrees with a normal boundary layer flow.

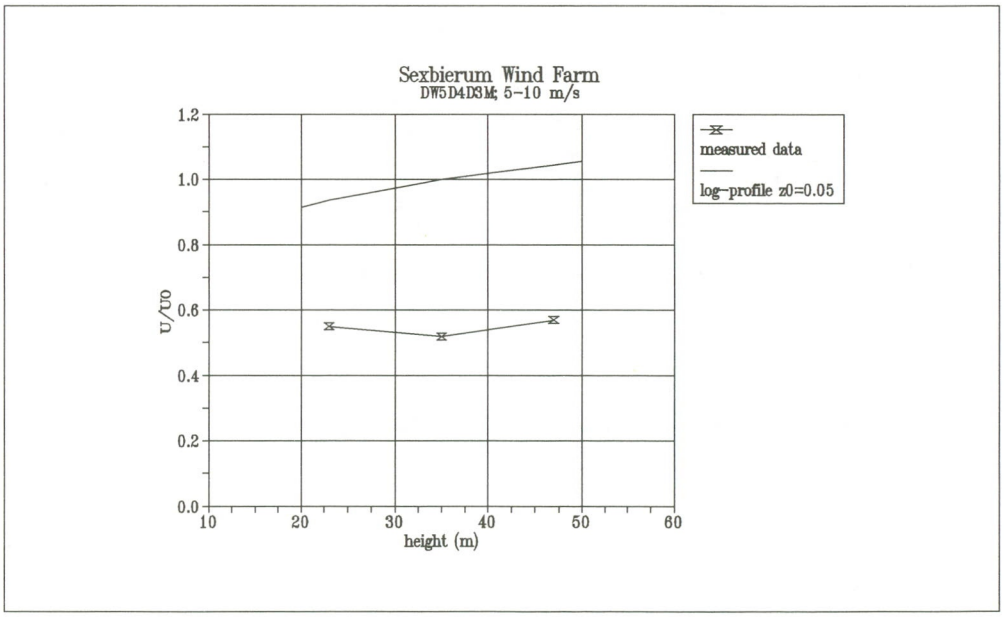

Figure 4.29 Vertical wake profile at the wake centre-line

In figure 4.29 the vertical profile of U/U_0 is given, together with the calculated undisturbed wind profile using z_0= 0.045 m.

4.4.5 Turbulence intensity

Turbulence intensity data per bin

In this section we show the results of the analysis on the measured turbulence in non-dimensional form.

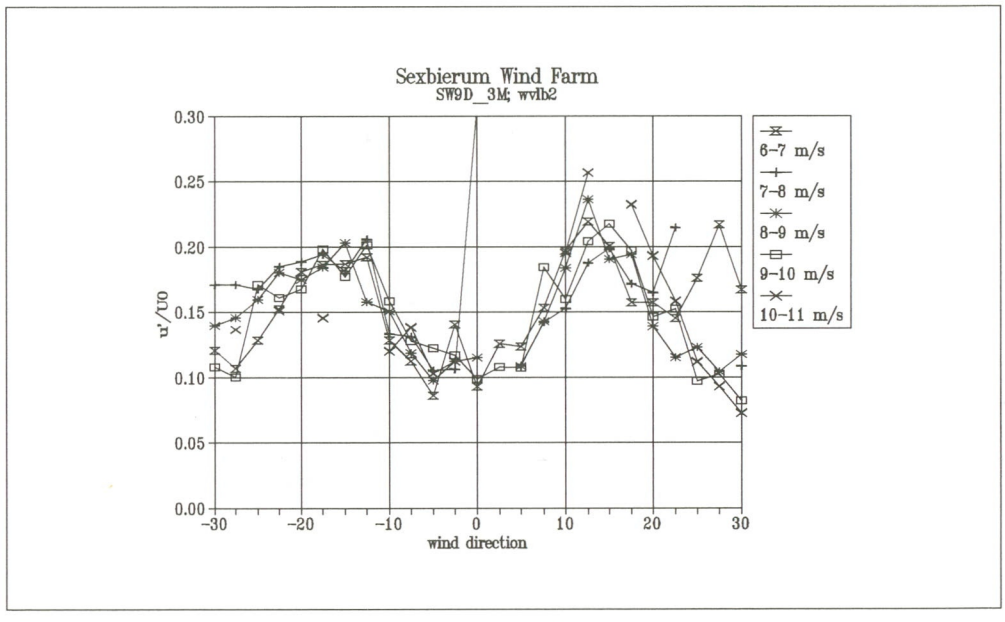

Figure 4.30 Turbulence intensity u'/U_0 as a function of wind direction at sensor b2

Figure 4.30 shows the turbulence intensity (non-dimensionalized with U_0) of the horizontal wind component for sensor b2 as a function of the wind direction. Figures 4.31 and 4.32 show the lateral and vertical turbulence intensity. The figures show that the turbulence intensity increases towards the centre of the wake. u'/U_0 is strongly peaked for wind directions of -15 and +15 degrees, which corresponds to the locus of the maximum wind speed gradient (see figure 4.20). There the turbulence production is at a maximum: $u'/U_0 \approx 0.2$, compared with an undisturbed value of $u'/U_0 \approx 0.1$
The peaks in the lateral and vertical turbulence intensity are less pronounced (see figure 4.31 and 4.32).

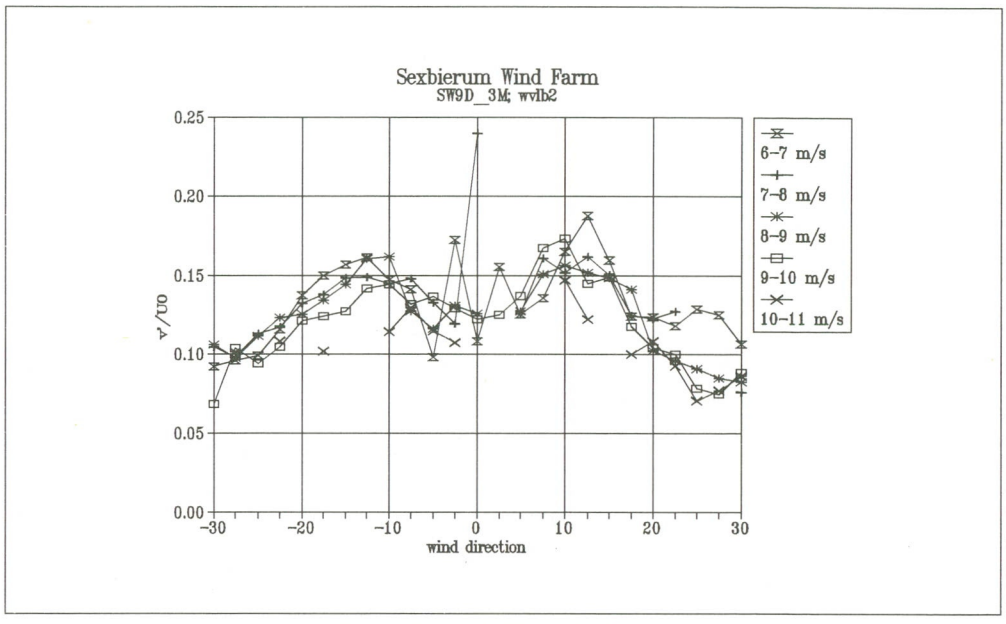

Figure 4.31 Lateral turbulence intensity v'/U_0 as a function of wind direction at sensor b2

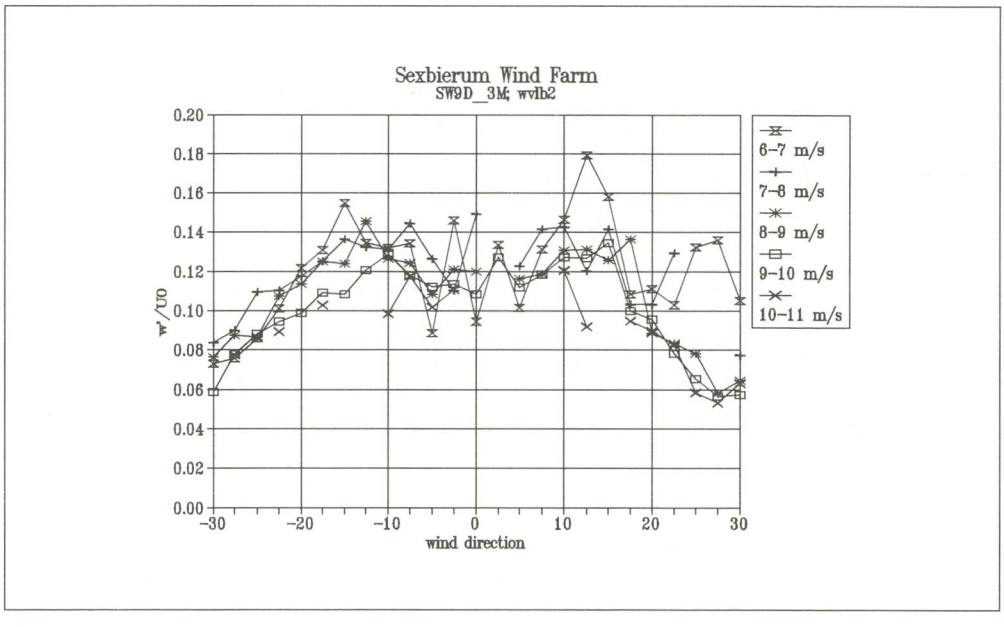

Figure 4.32 Vertical turbulence intensity w'/U_0 as a function of wind direction at sensor b2

Figure 4.33 shows the turbulent kinetic energy k (non-dimensionalized with U_0) as a function of the wind direction. The behaviour of k is roughly the same as that of the components of the turbulence.

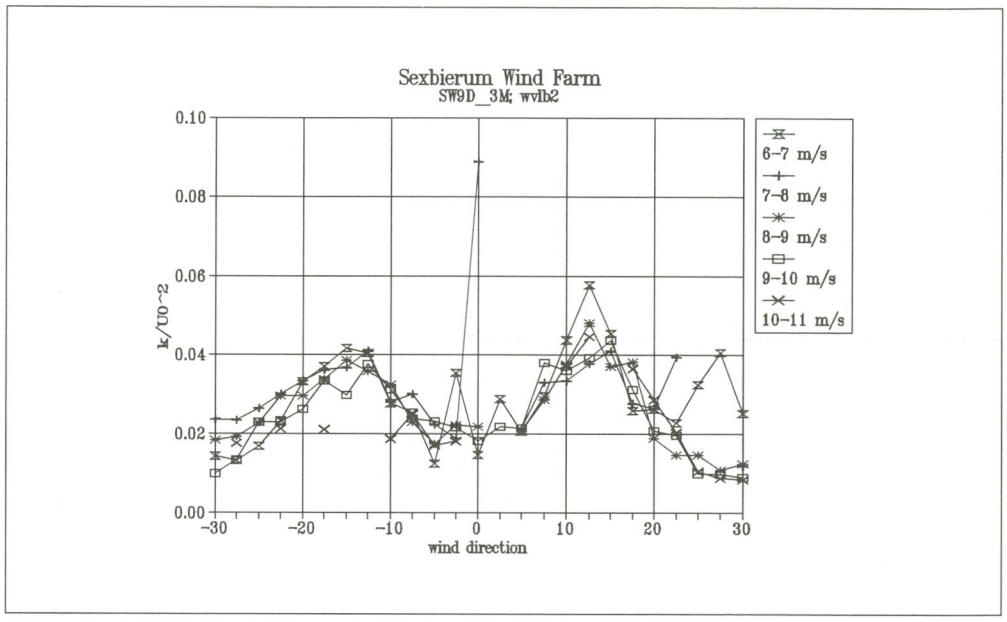

Figure 4.33 Turbulent kinetic energy k/U_0^2 as a function of wind direction at sensor b2

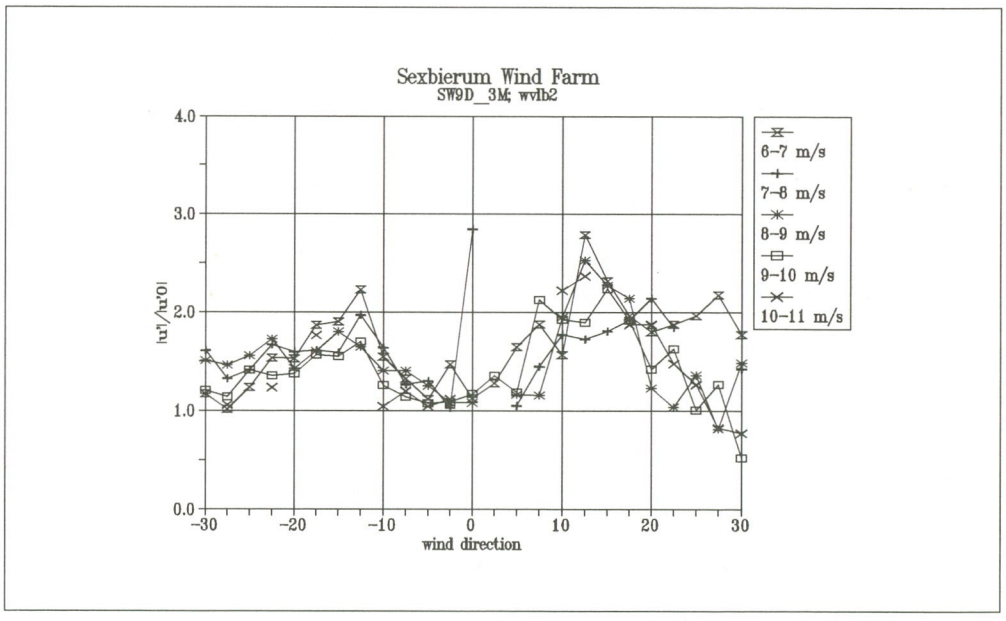

Figure 4.34 Ratio of wake turbulence and undisturbed turbulence u'/u_0' as a function of wind direction at sensor b2

In figure 4.34 the ratio u'/u'_0 is given as a function of the wind direction. The figure shows again that the turbulence level is increased in distinct peaks at this distance (x = 2.5 D). The turbulence levels are increased by a factor of 2 in the peaks, approximately.

Aggregated results

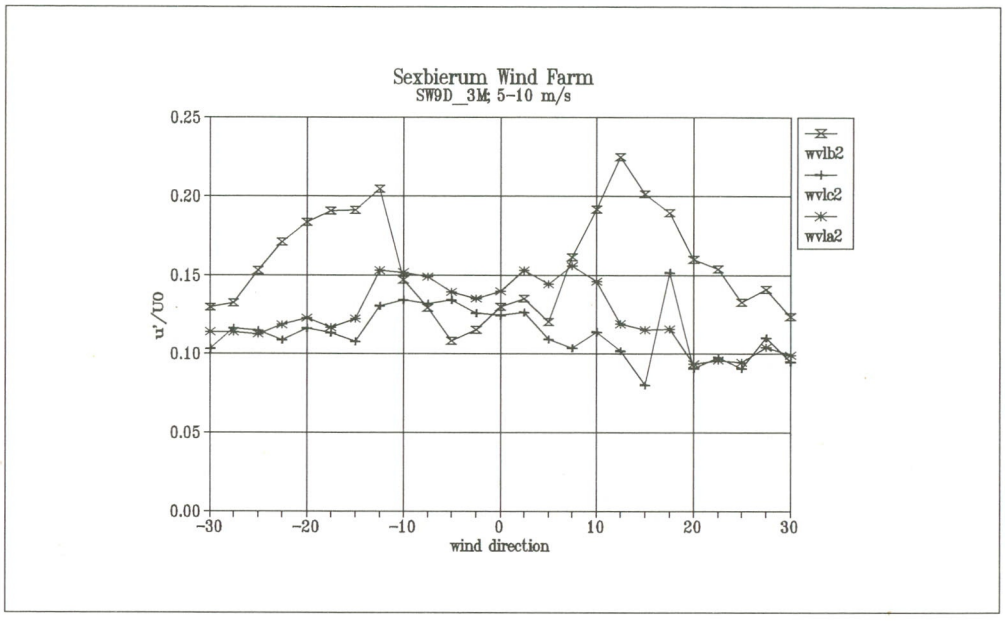

Figure 4.35 Aggregated turbulence intensity u'/U_0 at different distances behind the rotor (wvlb2: x = 2.5 D, wvla2 x =5.5 D; wvlc2: x = 8 D)

Figure 4.35 shows the development of the turbulence intensity profile as a function of the distance behind the wind turbine. Clearly, at a distance of x = 5.5 D the peaks have diffused into a plateau, with a level about 1.5 times higher than the undisturbed turbulence intensity.

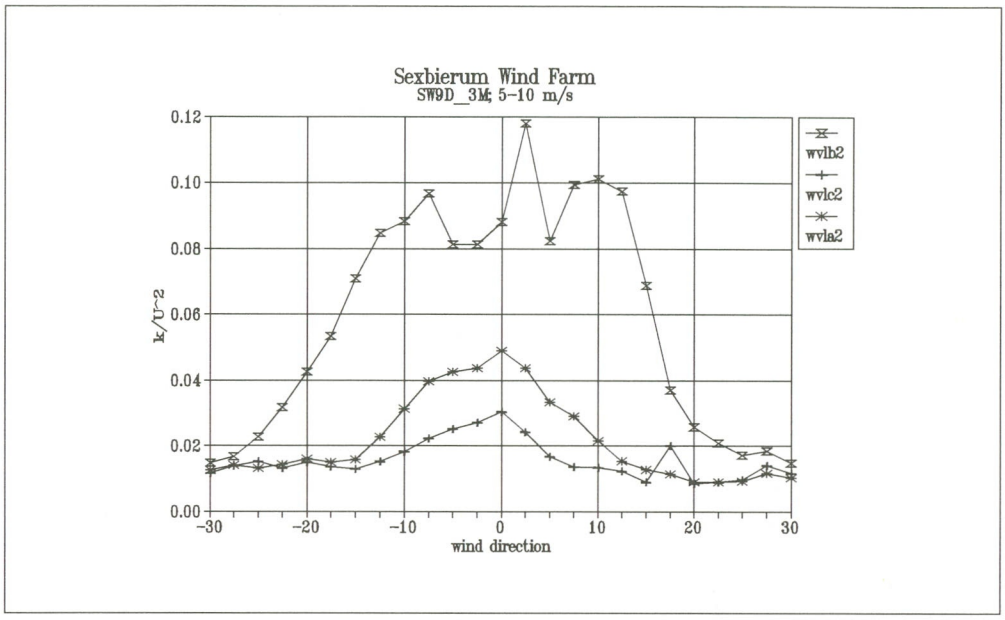

Figure 4.36 Aggregated turbulent kinetic energy k non-dimensionalized with the local wind speed U at x = 2.5 D (wvlb2); k = 5.5 D(wvla2) x = 8 D (wvlc2)

Figure 4.36 shows the development of the turbulent kinetic energy non-dimensionalized with the local wind speed U at the three measuring positions x = 2.5 D, x = 5.5 D and x = 8 D.
At x = 2.5 D $k/U^2 \approx 0.10$; at x = 5.5 D $k/U^2 \approx 0.05$ and at x = 8 D $k/u^2 \approx 0.03$.

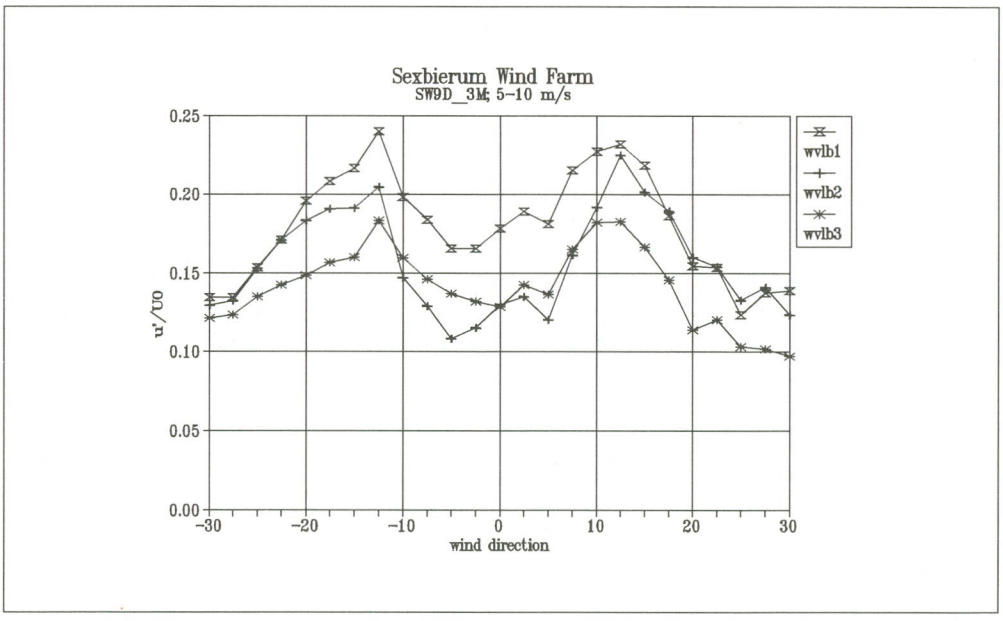

Figure 4.37 Aggregated turbulence intensity u'/U_0 as a function of wind direction at mast b

Figure 4.37 depicts the turbulence intensity u'/U_0 at mast b for the positions 1, 2 and 3. Peaks are found at wind directions of -12.5 and +12.5 degrees. Clearly, the turbulence intensity is the highest at the top-most sensor ($k/U_0^2 = 0.24$) and lowest at the bottom-most sensor ($k/U_0^2 = 0.18$). This corresponds well to what is expected. As production of turbulence is related to the wind velocity gradient, the highest turbulence is expected where the gradients are at maximum (see figure 4.20).

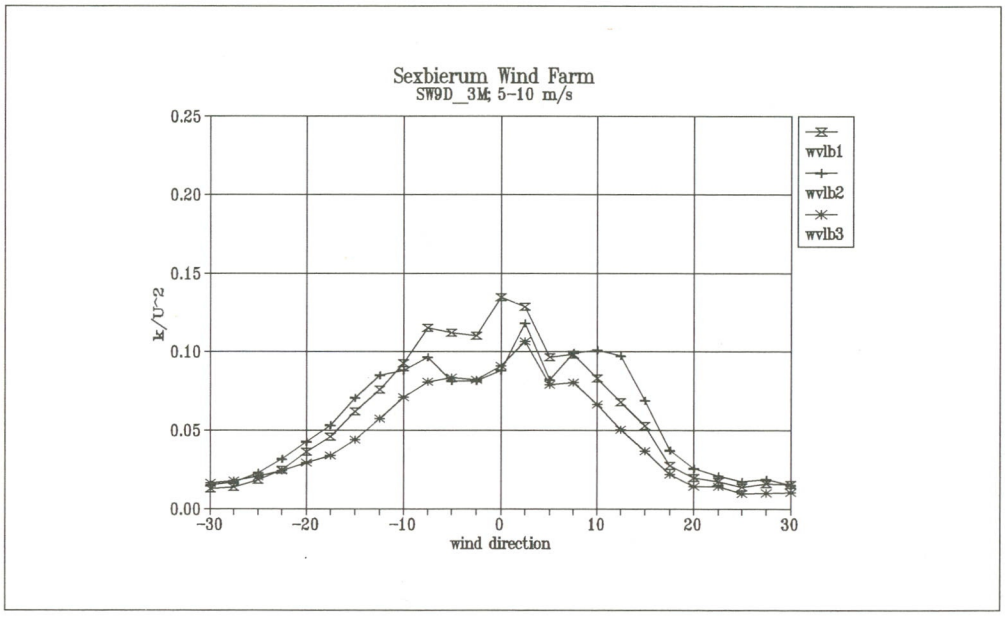

Figure 4.38 Turbulent kinetic energy non-dimensionalized with local velocity as a function of wind direction

Figure 4.38 depicts the turbulent kinetic energy non-dimensionalized with the local wind speed.

4.4.6 Shear stress

Shear stress per bin

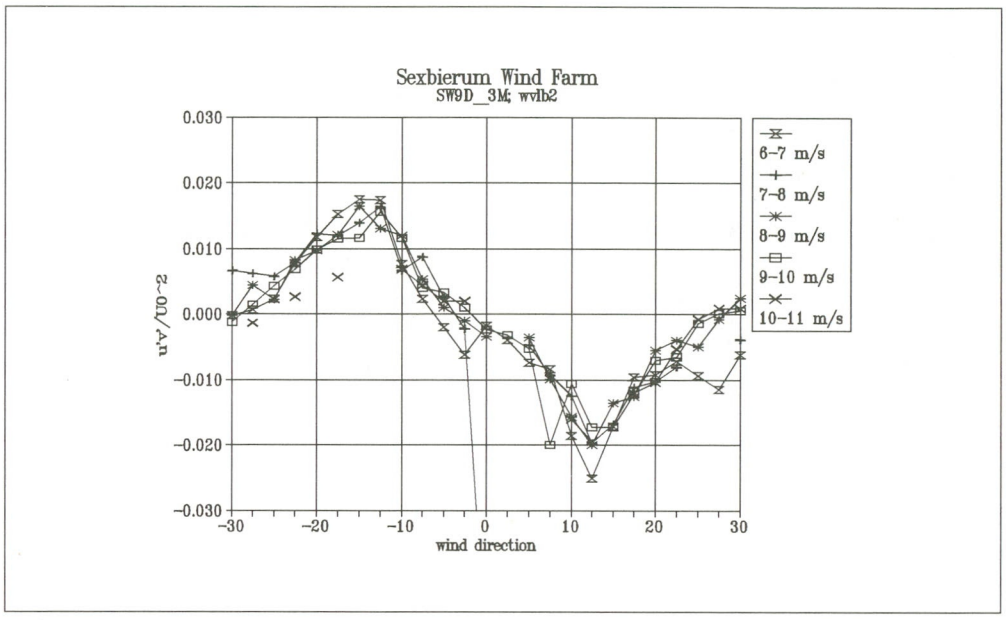

Figure 4.39 Shear stress $u'v'/U_0 2$ as a function of wind direction at sensor b2

The Reynolds-stress u'v' is the turbulent shear stress which is the driving force for the recovery of the wake deficit in horizontal direction. Figure 4.39 shows the shear stress u'v' non-dimensionalized with the undisturbed wind speed U_0 against the undisturbed wind. Starting from the right side of the figure (positive wind directions) and going to the negative wind directions it shows that at the edge of the wake $u'v'/U_0^2$ is equal to zero and then shows a minimum of -0.020. At 0° wind direction it goes through zero, it then shows a maximum of 0.015 before it relaxes again to 0 at the left edge of the wake. Generally speaking this is expected, since it is assumed that the shear stress is proportional to the local wind shear, i.e. the horizontal wind gradient. The fact that the curves return to zero at the edge of the wake, and that they cross the x-axis at 0° wind directions gives confidence in the quality of the data.

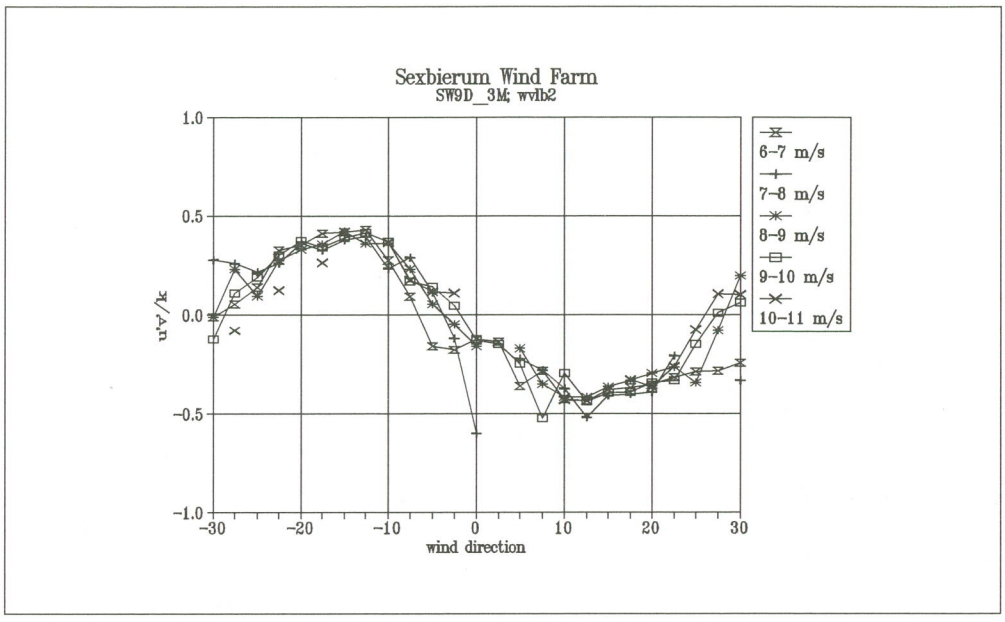

Figure 4.40 Shear stress u'v' non-dimensionalized with the local turbulent kinetic energy as a function of wind direction at sensor b2

Aggregated results

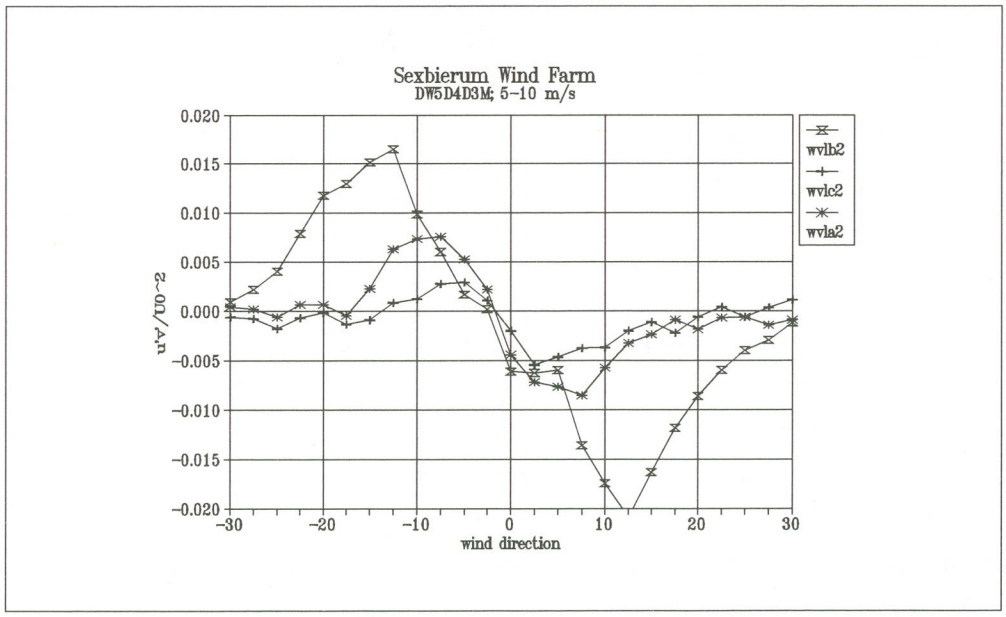

Figure 4.41 Non-dimensionalized shear stresses u'v'/$U_0$2 as a function of wind direction in wind speed bin 5-10 m/s
Distance x = 2.5 D: wvlb2x = 5.5 D: wvla2x = 8 D: wvlc2

Figure 4.41 shows the horizontal shear stress $u'v'/U_0^2$ as a function of wind direction at 3 different axial position x = 2.5 D, x = 5.5 D and x = 8 D. With the relaxation of the wake the maximum values of $u'v'/U_02$ decrease with increasing distance.

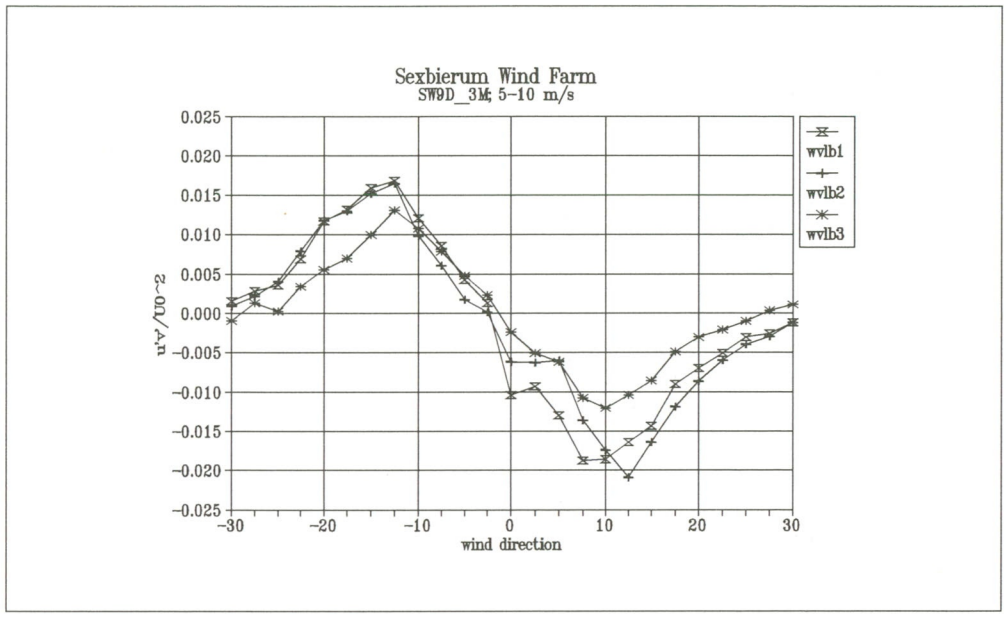

Figure 4.42 Shear stress $u'v'/U_0^2$ as a function of wind direction for sensors b1, b2 and b3

Figure 4.42 shows the non-dimensional shear-stress $u'v'/U_0^2$ for the three sensors at mast b as a function of the undisturbed wind direction. The shape of the three curves is again very similar. Eddy-viscosity theory for turbulence assumes that the turbulent shear stress is proportional to the local shear. This is clearly reflected in the curves of figure 4.42. Outside the wake no horizontal wake effect is present and hence the horizontal wind gradient is zero. At the maximum gradient dU/dy shear stress reaches a maximum, after which it decreases zero, where the wind speed shows a minimum. For larger wind directions the shear shows a similar behaviour but of an opposite sign.

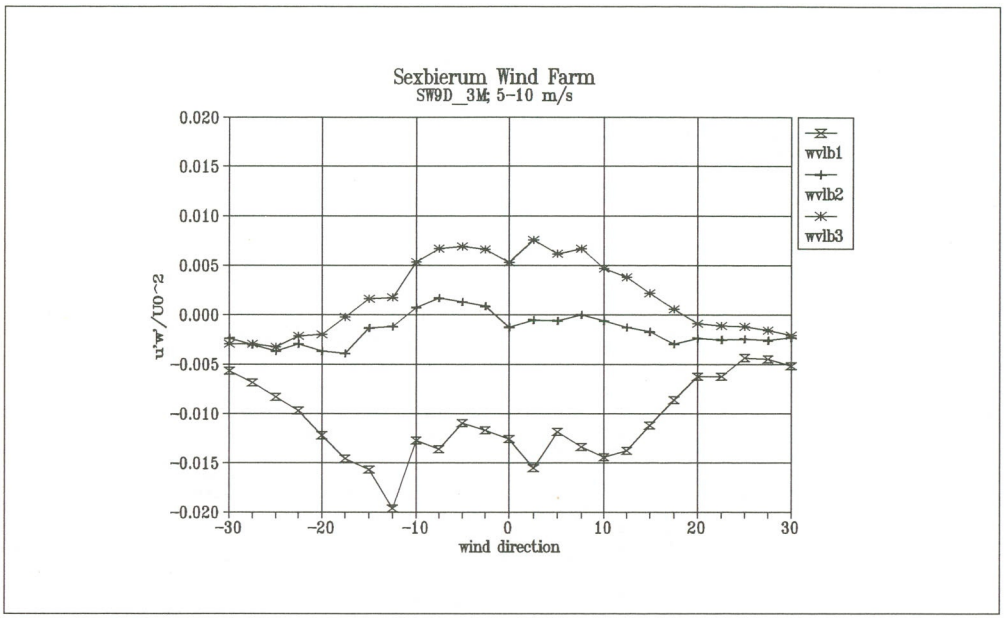

Figure 4.43 Shear stress u'w'/$U_0$2 as a function of wind direction for sensors b1, b2 and b3

Figure 4.43 shows the non-dimensional turbulent shear stress u'w'/U_0^2 as a function of the wind direction at the three sensor positions b1, b2, b3. The graphs show quite a distinct behaviour from the horizontal shear.
The shear stress u'w' is proportional to the vertical wind speed gradient dU/dz. Outside the wake the u'w' is negative corresponding to the shear stress in the atmospheric boundary layer. Traversing through the wake at the top position b1, the vertical gradient increases with the increasing wake effect and so u'w' becomes more negative (figure 4.20). At the bottom sensor b3 the situation is different. When the wind direction changes the wake effect becomes stronger; the wind gradient and hence u'w' changes sign.

4.4.7 Wake decay

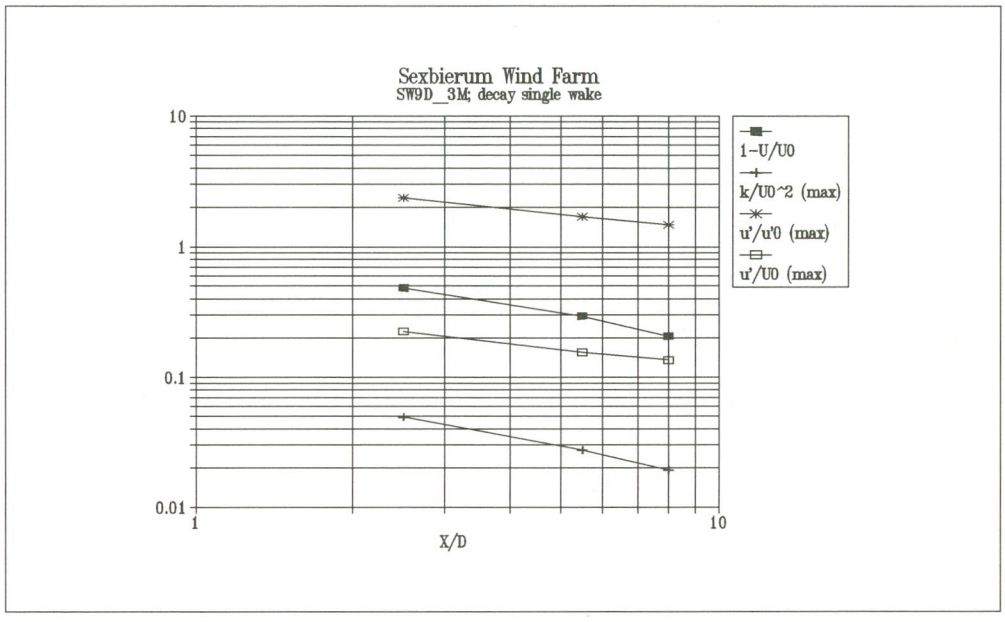

Figure 4.44 Wake decay for quantities 1-U/U_0, u'/U_0, u'/u_0' and k/$U_0$2 as a function of the longitudinal distance X/D

Figure 4.44 shows the decay of various quantities as a function of the non-dimensional distance behind turbine T18. U/U_0 gives the centre-line deficit as a function of the distance. k/$U_0$2, u'/u_0, u'/u'$_0$ give the maximum value (taken across the wake) of these quantities at the given position X/D.

4.5 Conclusions

The measurement campaigns have resulted in a useful data base for the validation of wake and wind farm models and for input to wind turbine load calculation programs. It contains data on undisturbed wind conditions, wind turbine power, wind speed components, turbulence and shear stress data.

The data base has been analysed with respect to the undisturbed wind conditions, i.e. with respect to wind speed and wind direction outside the wind farm. The upstream roughness length was derived from the turbulence intensity.

4.5.1 Double wake measurements

The double wake data base is built up of 1726 1-minute samples.

The wake deficit at the various measuring positions has been determined. The measurements do not show the shapes of the individual overlapping wakes clearly, but give the picture of one merged wake. For the centre-line measuring mast b, the measured wake turns out to be asymmetrical. This is caused by systematic errors due to the presence of lightning rod on top of mast 7. A similar asymmetry is found in the data of the turbulence intensities and the shear stresses. Only if the quantities are non-dimensionalized with local quantities, such as the wind speed or turbulent kinetic energy, the asymmetry seems to disappear.

The u-component of the turbulence intensity shows peaks at the maximum wind speed gradient. The other components lack such a peaked shape and have a much more smooth course. This also holds for the turbulent kinetic energy.

The shear stresses have been measured successfully. The course of the individual shear stresses can be explained qualitatively by making some simple assumptions about the wind speed gradient in the wake. Further the shape is very similar to the one measured previously in the wind tunnel.

4.5.2 Single wake measurements

The data base is built up of 873 3-minute samples.

During the measurements no serious problems arose. However, a number of systematic errors in the measurement of the undisturbed wind measurement was detected, for which the data had to be corrected. Because the undisturbed wind speed sensor at hub height was malfunctioning for part of the measuring campaign, the wind sensor at 20 m height has been used for the analysis.

The wake deficit at the various measuring positions has been determined. At X = 2.5 D the wake profile deviates markedly from a Gaussian shape, at larger distances this deviation disappears.

At X = 2.5 D turbulence intensity shows peaks at the maximum wind speed gradient. These peaks disappear for positions further downstream the turbine (X = 5.5 D and X = 8 D).
The shear stresses have been measured successfully. The course of the individual shear stresses can be explained qualitatively by making some simple assumptions about the wind speed gradient in the wake.

5 Power spectral density in the wake of a wind turbine

5.1 Introduction

Turbulent spectra have been gathered during two measuring campaigns in the wake of a single wind turbine at X/D = 4 and X/D = 7, respectively. These spectra have been compared with empirical correlations from literature [ESDU, 1985] and with the measured spectra from the undisturbed wind.

For the 7D measuring campaign the mobile masts were positioned 1 rotor diameter upstream of turbine T36 on the line T16-T36. During the campaign turbine T16 was switched off. The undisturbed conditions were measured with meteorological mast M32, which has a single cup anemometer at hub height. Mast b containing the three propeller anemometers was positioned on the centre-line; masts a and c were positioned on either side of mast b at a distance of 0.4 rotor diameters.

The 4D measuring campaign was carried out with the mobile mast positions 1 rotor diameter upstream of turbine T36 on the line connecting T38-T36. During the campaign turbine T38 was switched off. Again mast b was positioned on the centre-line and masts a and c were at 0.4 D on either side of the centre-line. During the campaign two cup anemometers, b2h and b2l, were mounted on mast b at 41 m and 23 m height, respectively. Propeller b2 was not operating during this campaign. The undisturbed wind conditions were measured at masts M72.

For reasons of comparison three short time series were analysed with both the upstream turbines out (series 13, 14, and 23). Since series 13 contained the largest number of blocks, the analysis has focused on this series.

5.2 Analysis of turbulent spectra

5.2.1 Analysis

The measured wind speed time series have been delivered by KEMA in files of several minutes to about 3 hours length, dependant on the stationarity of the upstream wind condition and the operational condition of the concerned wind turbines. The data have been processed to Power Spectral Density Functions (PSD) by TNO.

The data were sampled at 4 Hz with the 3D-propeller anemometers of the mobile meteorological masts and at 1 Hz with the cup anemometers at the stationary meteorological masts and the additional cups at the mobile masts.

To arrive at the PSD's the time series were split up into 256 s blocks; the trend was removed by means of linear regression. Using FFT the spectra were calculated, and binned according to the undisturbed wind speed and wind direction. The wind speed

bins used are 2 m/s, the direction bins 2.5°. Within the wind speed and wind direction bins the spectra were ensemble-averaged [Verheij, 1993].

The Power Spectral Density functions have been non-dimensionalized with the local variance in the wake. The frequency have been non-dimensionalized with the product of local wind speed in the wake and an integral length-scale defined in the next section.

5.2.2 Empirical correlations

The measured PSD's have been compared with the theory. To this end the ESDU spectrum, based on the von Kármán spectral equations (ESDU '85), have been used. In neutral atmospheric wind conditions, which appears among others during periods of wind speeds higher than about 6 to 8 m/s, PSD's can be described with one single expression for each wind speed component:

$$n\,S_u(n)/\sigma_u^2 = 4\,n'/(1+70.8\,n'^2)^{5/6}$$

$$n\,S_v(n)/\sigma_v^2 = 4\,n'\,(1+755.2\,n'^2)/(1+283.2\,n'^2)^{11/6}$$

in which $n' = n\,x_{Li}/U$, n being the frequency, U the mean wind speed and x_{Li} the integral turbulence length scale in x-direction for i=u and i=v respectively.

According to ESDU '75 the integral turbulence length scale for the U- and the V-component are:

$$x_{Lu} = 25\,z^{0.35}/z_0^{0.063}$$

$$x_{Lv} = 5.1\,z^{0.48}/z_0^{0.086}$$

For z = 35 m (hub height) and z_0 = 0.05 m the results are 105 and 36 m respectively. For z = 20 and z = 50 m the results are 86 and 119 m for the U-component and 28 and 43 m for the V-component.

The length scales have been calculated by fitting the measured PSD's to the theoretical PSD given by ESDU, between the frequency where the maximum value of the PSD is found and the frequency where the inertia of the anemometer becomes noticeable. Due to the small number of blocks (in most bins) and the relatively short length of the blocks it is difficult to detect the maximum value of the measured PSD. Apart from the reliability of the method and the number of data a deviation of 10 to 20% in the individual results are possible.

5.3 Results

5.3.1 Undisturbed flow

The measured spectra correspond well to the ESDU-correlation for the lower frequencies. However, in the higher frequency range the measured spectra fall off much faster than the theoretical ones due to the inertia of the anemometers. The propeller anemometers start to fall off at 0.5 Hz, approximately, the response of the cup anemometers starts to deteriorate at 0.1 Hz. An example is shown in figure 5.1.

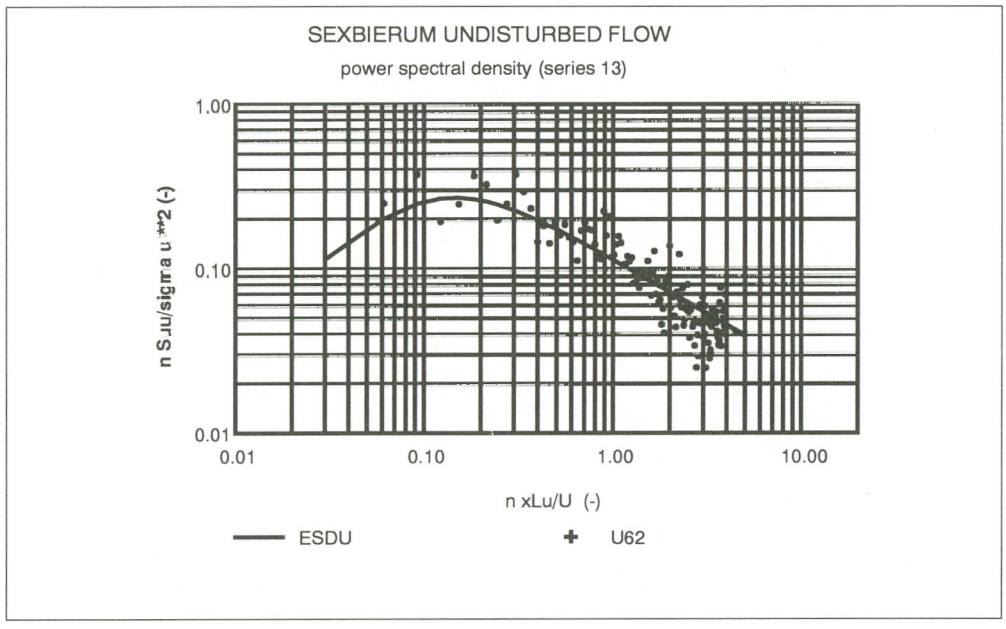

Figure 5.1 Power Spectral Density of the undisturbed wind

The results of the length scales (see table 5.1) of series 13 and 14 are rather close to the ones listed in section 5.2. The length scales of series 23 were extremely low, probably due to the small number of blocks contained in the series.

Table 5.1 Length-scales of the undisturbed wind

The values for the integral turbulence length scales, averaged over the blocks in series 13, 14 and 23. The (lateral) distance between masts A and B and between masts B and C is in both cases 12 m. Masts 6 and 7 are fixed masts, the masts A, B and C are mobile masts.

Series 13	U61	U62	U63
xLu (m)	110	110	90

Series 14	U61	U62	U63
xLu (m)	100	120	80

Series 23	A1	B1	B3	C2	U72
xLu (m)	20	15	20	15	15

5.3.2 7D single wake

In case of the 7D campaign no wake profile was found for the U/U_0 or the turbulence intensity in the wake. Over the whole range of wind directions the wind speed ratio was approximately $U/U_0=0.85$. The variance in the wake equalled the variance in the undisturbed flow. Also, the spectra showed no variation over the wind directions. In order to improve the statistic the PSD's were ensemble-averaged over the wind directions from 255 and 270 degrees. The final results have been compared with theory.

Except for the frequencies above 0.5 Hz (see 'undisturbed flow') the shape of the measured PSD's (symbols in the figures) compared well with ESDU (solid line in the figures 5.2, 5.3 and 5.4.

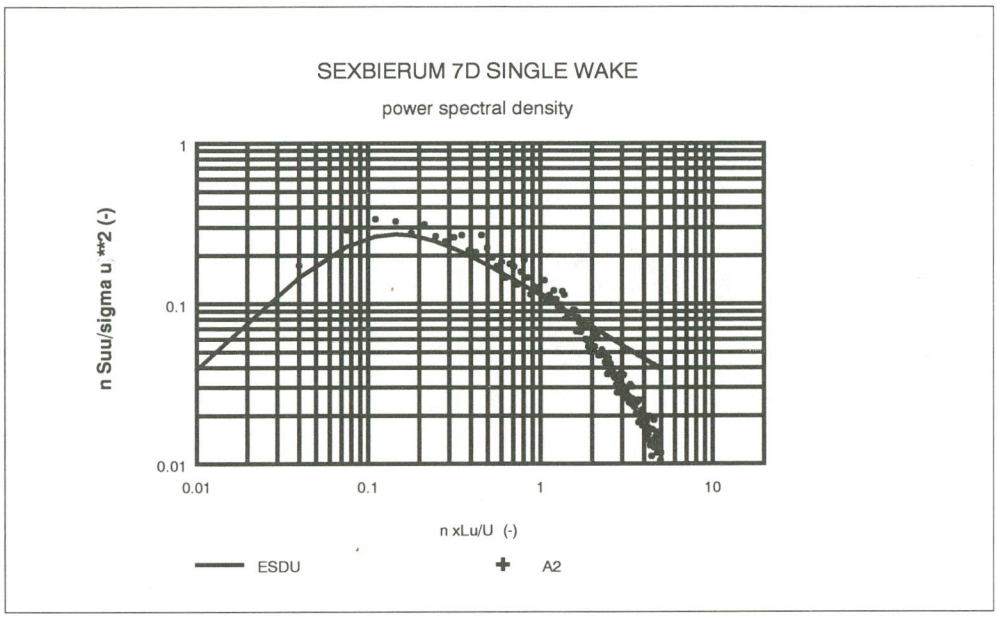

Figure 5.2 Power Spectral Density measured with sensor A2 at X/D=7

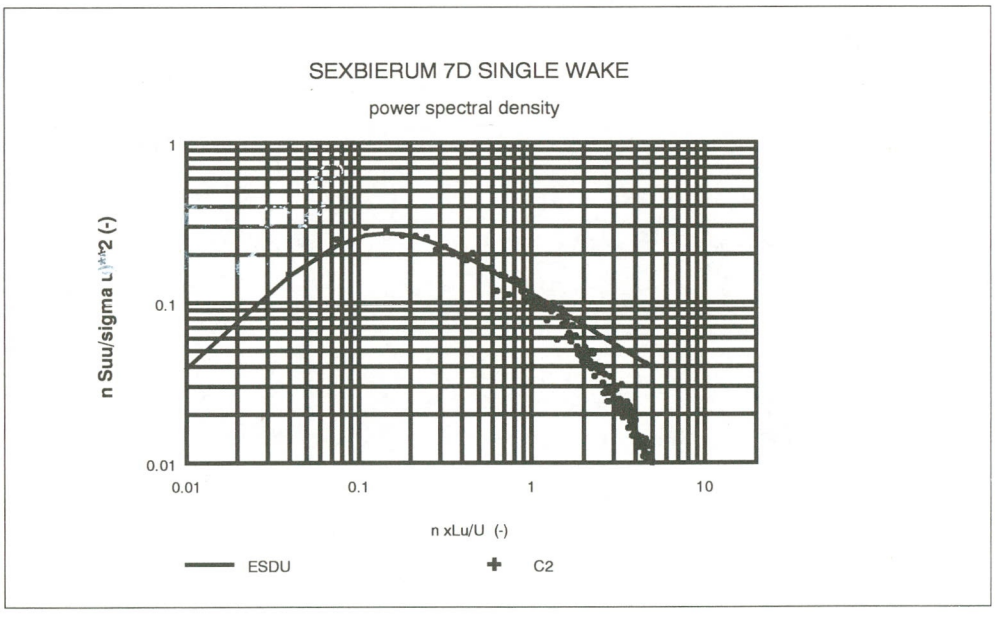

Figure 5.3 Power Spectral Density measured with sensor C2 at X/D=7

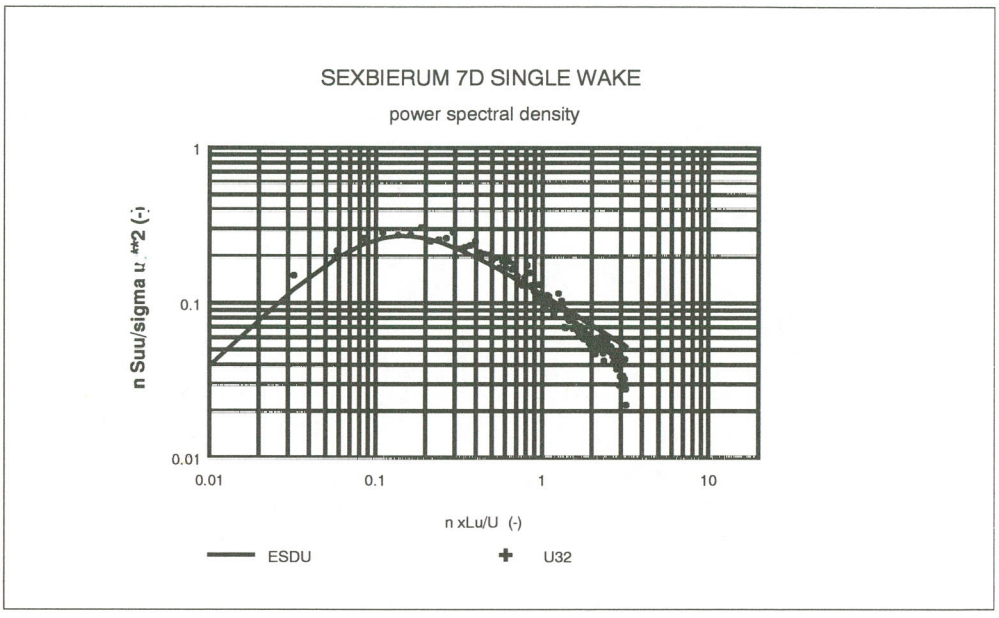

Figure 5.4 Power Spectral Density measured with sensor U32 (undisturbed) at X/D=7

The length scale (see table 5.2) of the undisturbed wind (signal U32) is about 0.60 times the one calculated by theory. The length scales of the 7D single wake data are about 0.75 times the length scale of U32. This value is close to the average wind speed ratio.

Table 5.2 Length-scales in the wind turbine wake at X/D=7

The values for the integral turbulence length scales, averaged over all blocks. The (lateral) distance between masts A and B and between masts B and C is in both cases 12 m.
The results for the undisturbed wind speed condition is given in column U32.

A2	B1	B2	B3	C2	U32
50	55	50	45	50	65

5.3.3 4D single wake

Compared to the 7D single wake data both mean wind speed and the turbulence intensity vary strongly over the various wind direction bins. Adding the PSD's in order to gain statistical reliability was not possible in this case.

Some examples of the PSD's are given in figures 5.5, 5.6 and 5.7 (line = ESDU, symbols = measured).

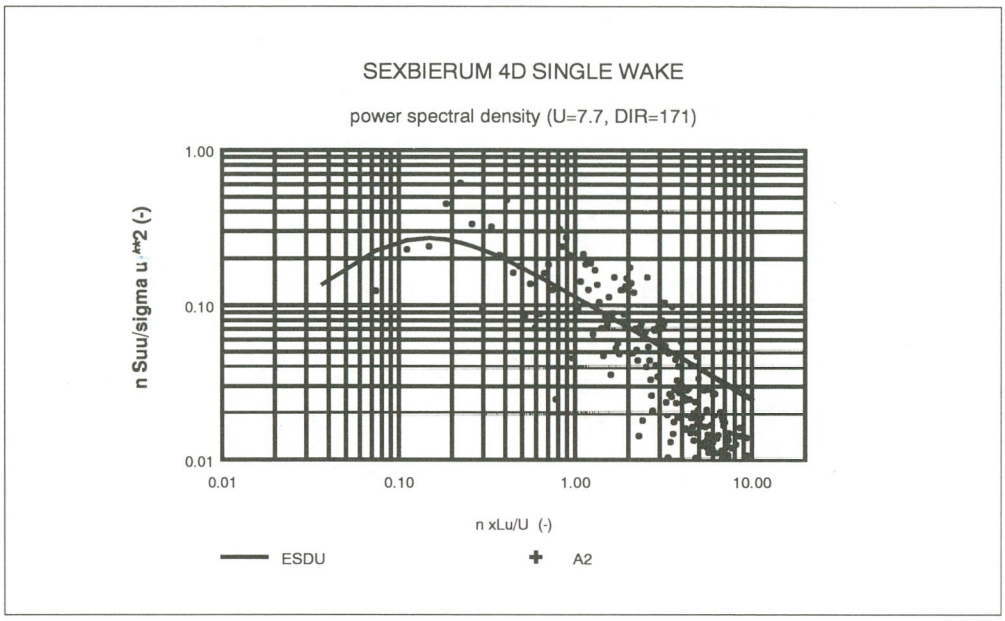

Figure 5.5 Power Spectral Density measured with sensor A2 at X/D=4

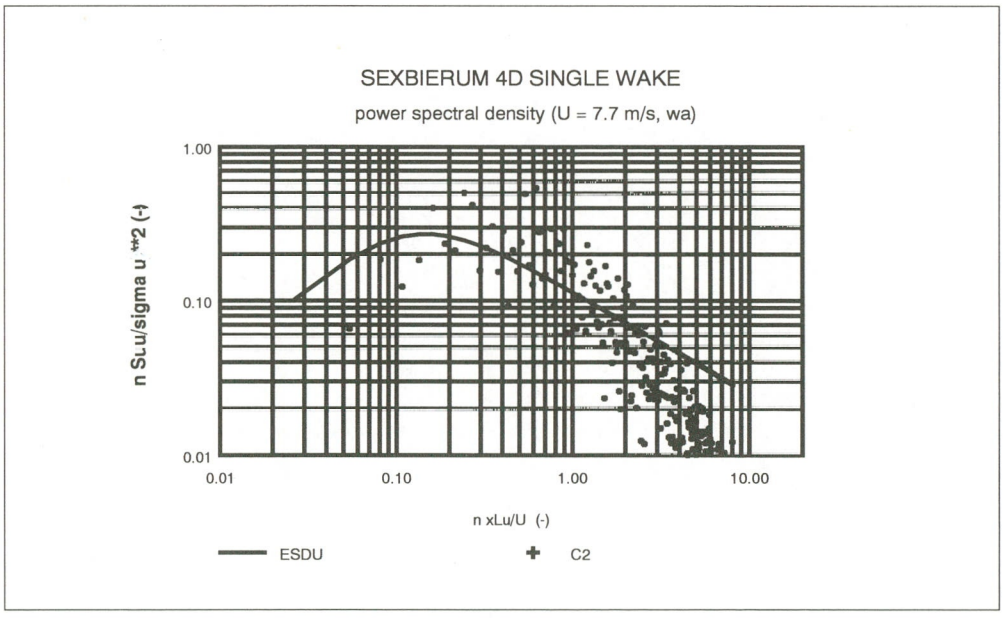

Figure 5.6 Power Spectral Density measured with sensor C2 at X/D=4

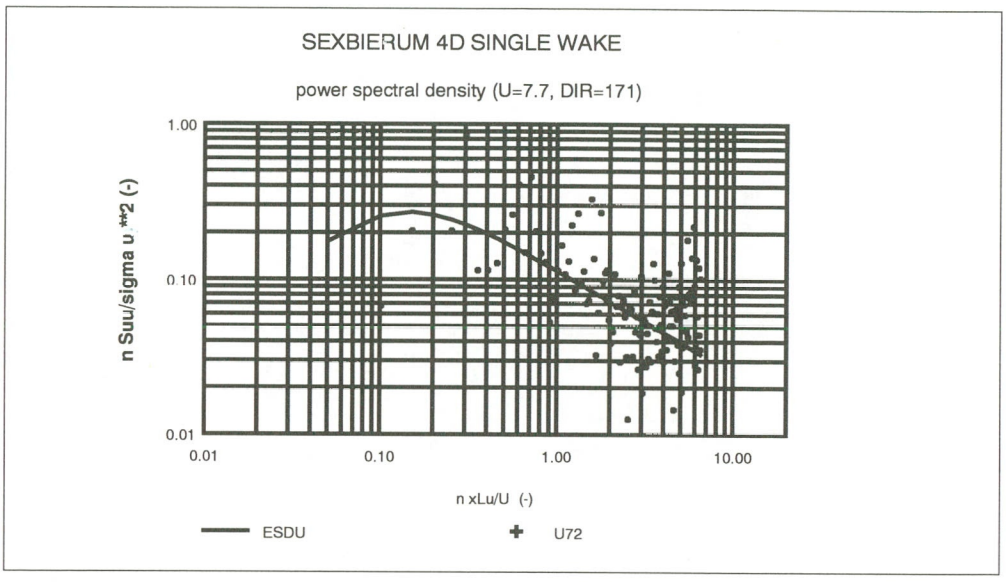

Figure 5.7 Power Spectral Density measured with sensor U72 (undisturbed) at X/D=7

The determination of the length scales has only been carried out in case the number of blocks in a bin is at least 2. For the undisturbed wind (signal U72) we found values ranging from 50 to 140 m.

When the length scales of the 4D single wake data are divided by the corresponding length scales of U72, there is a clear relation with the position in the wake. This length scale ratio is shown in figure 5.8 as a function of the wind direction. At the centre-line this ratio is about 0.25.

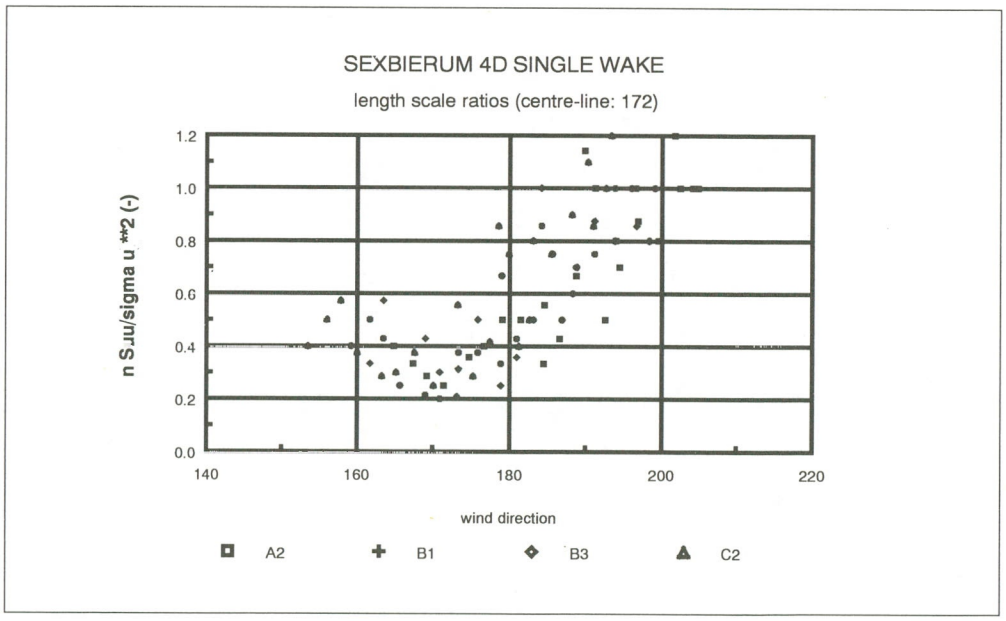

Figure 5.8 Length-scale ratio at X/D=4

Table 5.3 Length-scales in the wind turbine wake at X/D=7

No	A2	B1	B3	C2	U72	D72
2	40	40	40	40	100	159
2	20	30	20	30	60	162
1					162	
1					163	
3	20	30	40	40	70	164
2	20	20	20	30	80	166
4	25	15	30	20	70	169
5	40	20	30	30	100	171
5	40	30	25	30	80	173
1					174	
8	40	30	40	20	80	176
1					177	
11	40	40	30	25	120	179
3	50	60	60	50	90	179
5	60	60	50	40	140	181
1					180	
4	80	60	70	60	70	184
3	80	60	60	50	120	183
6	80	60	60	60	80	186
7	50	50	50	40	100	187
2	70	70	70	80	100	189
4	80	60	60	50	100	188
7	70	60	70	60	80	191
1					191	
3	80	100	80	90	100	194
2	80	80	80	90	50	194
7	120	100	100	110	100	196
3	70	70	60	60	70	197
9	50	40	40	50	50	198
2	50	50	50	60	50	199
1					199	

The values for the integral turbulence length scales x_{Lu}, averaged over the number of blocks (column No) per bin. The (lateral) distance between masts A and B and between masts B and C is in both cases 12 m.
The results of the undisturbed wind condition is given in column U72. In the last column (D72) the mean value for the undisturbed wind direction is given.
In case the number of blocks equals 1, the length scale has not been determined.

5.4 Conclusions

5.4.1 Undisturbed flow

The number of data is small. The analysis has been concentrated on series 13. The integral length scales of the turbulence and the shape of the PSD's show good agreement with the theoretical ones.

5.4.2 7D single wake

No wake profile can be distinguished for the wind speed ratio, turbulence intensity or the spectra. The wind speed ratio (wake/undisturbed) is about 0.85 over a wide range of wind directions. On the average the variance measured with the mobile masts is about equal to the one measured with the fixed mast.

The shape of the measured PSD's, non-dimensionalized with the local variance, the local wind speed and an integral length scale, shows good agreement with Power spectral density function given by ESDU. Thanks to this the integral length scale of the turbulence can easily be derived by fitting the measured data on the ESDU function. The length scales of the 7D single wake data are about 0.75 times the length scale of the undisturbed wind. This value is close to the average wind speed ratio.

5.4.3 4D single wake

The shape of the measured non-dimensionalized PSD's also shows good agreement with the ESDU spectral density function. This seems independent of the lateral or vertical position in the wake.

A length scale ratio has been defined, i.e. the length scale derived from measured data in the wake divided by the length scale simultaneously derived from measured data in the undisturbed wind. The smallest length scale ratio (at the centre-line of the wake) is about 0.25.

6 Conclusions

6.1 General

The project Full-scale measurements in wind turbine arrays has resulted in a reliable data base, containing a large body of data on:
- the power performance of the wind farm;
- the properties of the wind in the wake of a single turbine and of two turbines in line at various distances. The data will be used for the validation of wake and wind farm models;
- power spectral densities of the turbulence in a wind turbine wake.

Further the projects Dynamic Loads in Wind Farms and the project Wake and wind farm modelling have been provided with raw data for further processing.

6.2 Wake effects on wind farm power output

The long term measurements on the power output of the wind farm has resulted in the following conclusions:
- the wind farm power output is 4% lower than the free-stream power output;
- the lowest efficiency is found at the second and third row of the wind farm. Further downstream the power output recovers gradually;
- the average wake effects are predicted well by the wind farm code FARMS.

6.3 Measured properties of wind turbine wakes

The data base detained in the wake measurement campaigns contains data on undisturbed wind conditions, wind turbine power, wind speed components, turbulence and shear stress data in the wake of a single turbine and in the wake of two wind turbines in a row.

The data base has been analysed with respect to the undisturbed wind conditions, i.e. with respect to wind speed and wind direction outside the wind farm. The upstream roughness length was derived from the turbulence intensity.

The properties of the wake of two turbines in line at 4D behind the second have been determined. No individual overlapping can be recognized, but the wake gives the picture of one merged wake.
The measured wake shape shows some asymmetry. This is probably caused by the presence of lightning rod on top of the undisturbed wind measuring mast.
The u-component of the turbulence intensity shows peaks at the maximum wind speed gradient. The other components lack such a peaked shape and have a much more smooth course. This also holds for the turbulent kinetic energy.
The shear stresses have been measured successfully. The course of the individual shear stresses can be explained qualitatively by making some simple assumptions about the wind speed gradient in the wake. Further the shape is very similar to the one measured previously in the wind tunnel.

The wake deficit of a single wind turbine has been determined at various measuring positions. At X = 2.5 D the wake profile deviates markedly from a Gaussian shape, at larger distances this deviation disappears.
At X = 2.5 D the turbulence intensity shows peaks at the maximum wind speed gradient. These peaks disappear for positions further downstream the turbine (X = 5.5 D and X = 8 D).

6.4 Power spectral density in the wake of a wind turbine

Power spectral densities have been determined in the wake of a single wind turbine at a distance of 4 rotor diameters and at a distance of 7 rotor diameters. These spectra have been compared with the PSD of the undisturbed wind.

The shape of the measured PSD's, non-dimensionalized with the local variance, the local wind speed and an integral length scale, shows good agreement with Power Spectral Density functions given by ESDU.

At a distance of 7 rotor diameters behind the wind turbine there is no significant distinction between the PSD of the undisturbed wind and the PSD in the wake.

7 References

[1] Beljaars, A.C.M.;
The measurements of gustiness at routine wind stations - A review;
WMO instruments and observing methods, report no. 31, Genève, 1987.

[2] Bendat, J.S., A.G. Piersol;
Random data; Analysis and Measurement procedures; 2nd edition;
Wiley, 1986.

[3] Bulder, B.H., J.G. Schepers;
Calculation data base of the WPS-30 wind turbine;
ECN report ECN-CX--91-053, September 1991.

[4] Busch, Christensen, Kristensen, Lading and Larsen;
Meteorological Field Instrumentation. Wind speed and direction by means of cups, vanes, propellers and lasers;
RISØ-R-400, January 1979.

[5] Cleijne, J.W.;
Local wind speed distribution around the SEP experimental wind farm (in Dutch);
TNO report 91-421; January 1992.

[6] Cleijne, J.W.;
Results of Sexbierum Wind Farm - double wake measurements;
TNO Environmental and Energy Research, 92-388, Apeldoorn, November 1992.

[7] Cleijne, J.W.;
Results of Sexbierum Wind Farm; single wake measurements.
TNO Environmental and Energy Research, 93-082, Apeldoorn, March 1993.

[8] Crespo, A.;
2nd progress report JOUR0087 'Wake and wind farm modelling';
May, 1992.

[9] ESDU;
Characteristics of atmospheric turbulence near the ground. Part III: variations in space and time for strong winds (neutral atmosphere);
Engineering Sciences Data Item 75001, July 1975.

[10] ESDU;
Strong winds in the atmospheric boundary layer. Part 1: mean-hourly wind speeds;
Engineering Sciences Data Item 82026, September 1982.

[11] ESDU;
Strong winds in the atmospheric boundary layer. Part 2: discrete gust speeds;
Engineering Sciences Data Item 83045, November 1983.

[12] ESDU;
Characteristics of atmospheric turbulence near the ground. Part II: single point data for strong winds (neutral atmosphere);
Engineering Sciences Data Item 85020, October 1985.

[13] Kamphuis, I.G., R.P.M. Schoenmaker, E. Bink;
Data-acquisitie/Verwerkingssysyteem SEP-proefwindcentrale;
Gebruikershandleiding;
ENR rapport 237, mei 1989.

[14] Kreyszig, E.;
Advanced Engineering Mathematics;
Wiley, 1988.

[15] Panofsky, H.A., J.A. Dutton;
Atmosperic Turbulence, models and methods for engineering applications;
Wiley, 1984.

[16] Smith, D.;
An experimental and theoretical investigation of wind turbine wakes in arrays and complex terrain;
Ph.D. Thesis, NP-TEC, 1991.

[17] Taylor, G.J.;
Full-Scale Measurements in Wind Turbine Arrays JOUR-0064;
Kick-off document, 1990.

[18] Toussaint, P., H.K. Hutting, J.W. Cleijne, M. Mortier;
Results from operation and research of the experimental wind farm of the Dutch Electricity Generating Board;
Proceedings EWEA special topic conference '92, Herning, 1992.

[19] Verheij, F.J.;
Power Spectra and Coherence Functions measured in the Dutch experimental wind farm;
TNO-report, to be published in 1993.

[20] Wieringa, J. and Rijkoort, P.J.;
Wind Climate of The Netherlands (in Dutch);
Staatsuitgeverij, Den Haag, 1983.

8 Authentication

Name and address of the principal
Commission of the European Community
contract JOUR 0064

Names and functions of the cooperators
Ir. J.W. Cleijne - TNO Environmental and Energy Research
Ir. H.K. Hutting - NV Kema

Names of establishments to which part of the research was put out to contract

Date upon which, or period in which, the research took place
August 1991 - April 1993

Signature

Ir. J.W. Cleijne
project manager

Approved by

Ir. N.J. Duijm
sector manager wind engineering

Annex A1 Specification of the holec WPS-30/3 wind turbine

Type:		HAWT
Rotor:		upwind
Number of blades:		3
Blade material:		steel
Rotor diameter:		30.1 m
Blade root radius:		1.14 m[1)]
Blade profiles:		NACA 230xxx series
Mass of one blade:		1800 kg
Mass of blade foot:		1360 kg
Mass of rotor (inc. hub):		15400 kg
First flap-wise Eigen-frequency:		3.35 Hz
Rotor rotation direction:		clockwise (looking downwind)
Tilt angle:		5.5°
Cone angle:		0.0°
Tower material:		steel
Tower diameter	-base:	3.2 m
	- top:	1.32 m
Tower height:		35 m
Distance rotor-tower:		1.67 m (at hub height)
Rated Power:		310 kW
Rated wind speed:		14 m/s
Cut-in wind speed:		5 m/s
Cut-out wind speed:		20 m/s
Generator:		synchronous with DC link
Control:		variable speed/ variable pitch

1) The blade root is defined to be the position of the outer bearing of the blade the blade lay-out.

Annex A2 Specification of the extra instrumentation on turbine 36

Channels

Blades and hub
8 locations for strain measurements on each blade
4 locations for strain measurements on the hub
6 locations for strain measurements on the joint between hub and blades

Rest of turbine
torque on the main shaft
torque on the fast shaft
bending moments in N-S and E-W direction's 6 m below the tower top
bending moments in N-S and E-W direction's 4 m above the tower base
pitch angle
blade position
nacelle direction
Yaw moment

Electrical and control signals
field voltage of the generator
field current of the generator
voltage of all 3 phases of the generator
current of 3 phases of the generator
frequency of the generator
set point field current
set point DC current
set point pitch angle
DC Voltage
DC current turbine
DC current converter
voltage of all phases of the 10 kV grid connection

All above signals are sampled at a 32 Hz rate

Annex A3 Figuren Power output

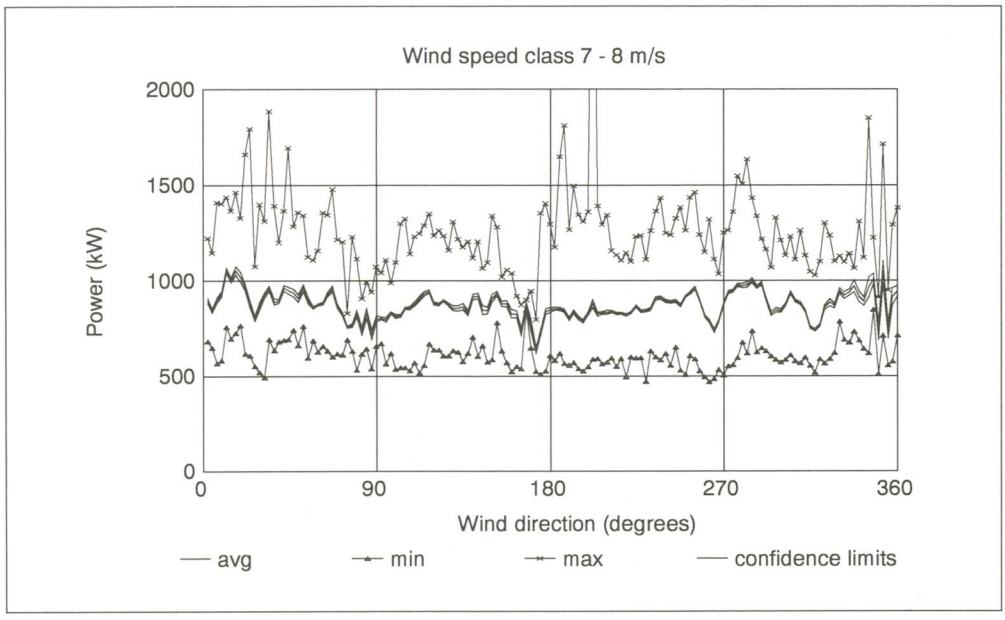

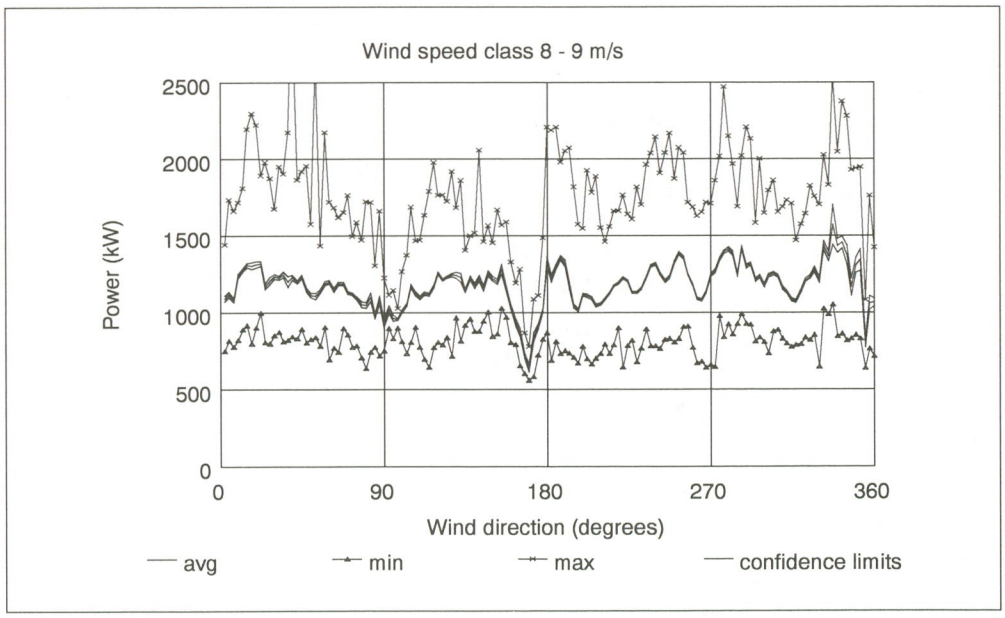

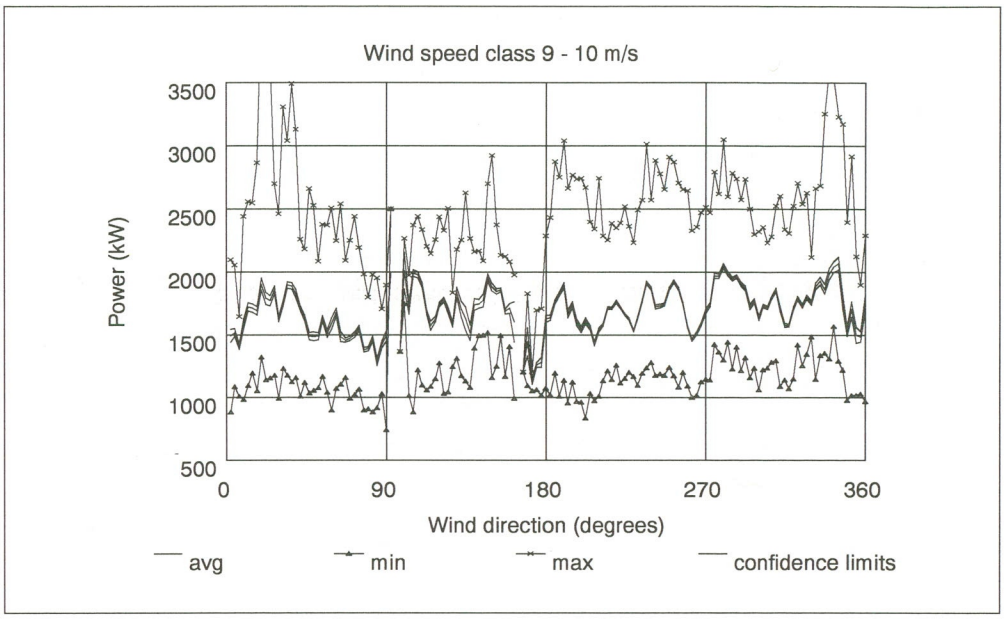
Wind speed class 9 - 10 m/s
Power (kW)
3500
3000
2500
2000
1500
1000
500
0
90
180
270
360
Wind direction (degrees)
avg
min
max
confidence limits

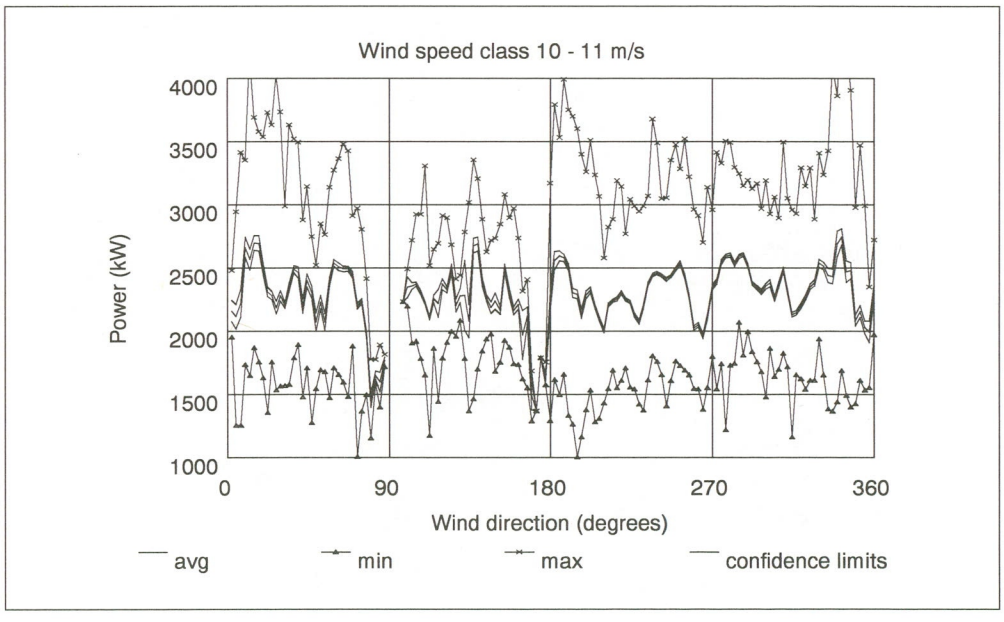
Wind speed class 10 - 11 m/s
Power (kW)
4000
3500
3000
2500
2000
1500
1000
0
90
180
270
360
Wind direction (degrees)
avg
min
max
confidence limits

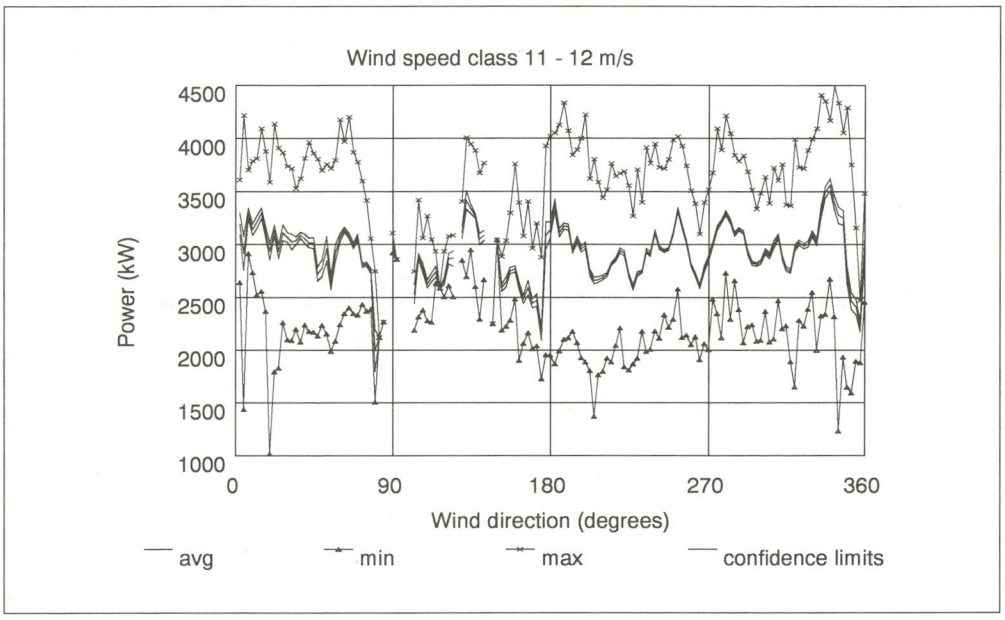
Wind speed class 11 - 12 m/s
Power (kW)
4500
4000
3500
3000
2500
2000
1500
1000
0
90
180
270
360
Wind direction (degrees)
avg
min
max
confidence limits

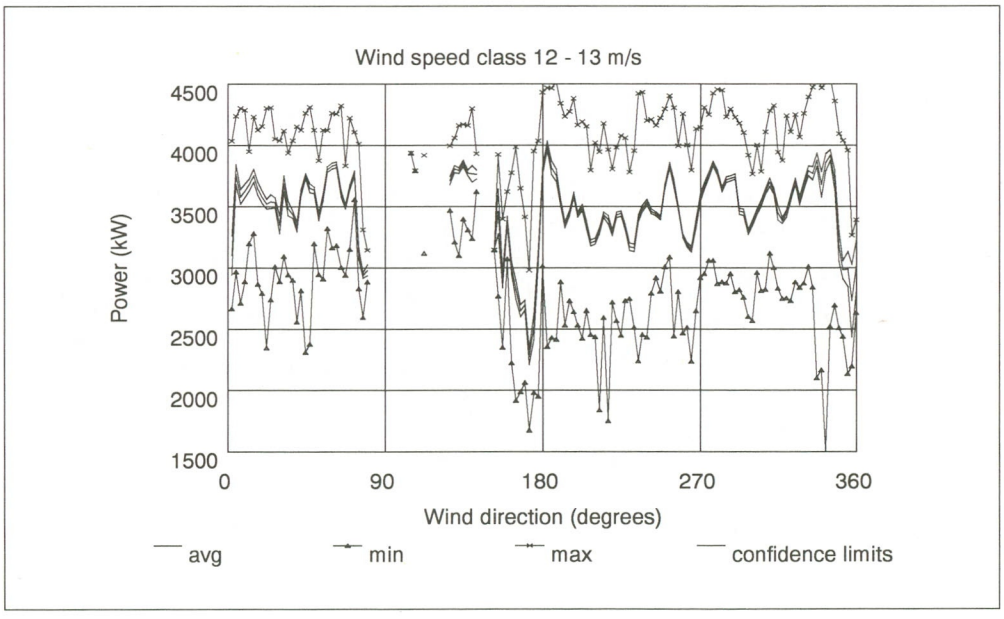
Wind speed class 12 - 13 m/s
Power (kW)
4500
4000
3500
3000
2500
2000
1500
0
90
180
270
360
Wind direction (degrees)
avg
min
max
confidence limits

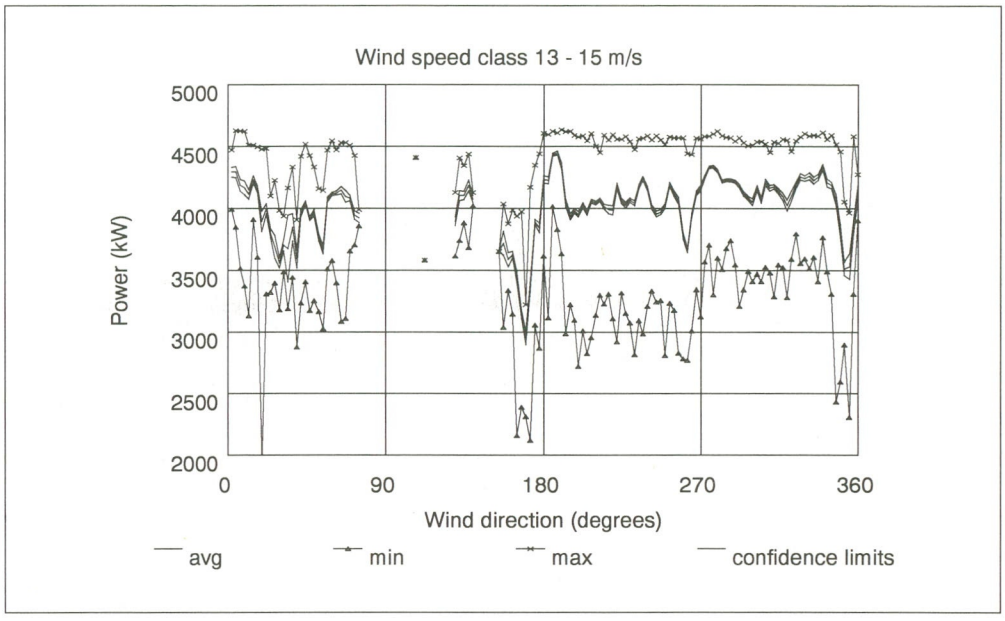
Wind speed class 13 - 15 m/s
Power (kW)
5000
4500
4000
3500
3000
2500
2000
0
90
180
270
360
Wind direction (degrees)
avg
min
max
confidence limits

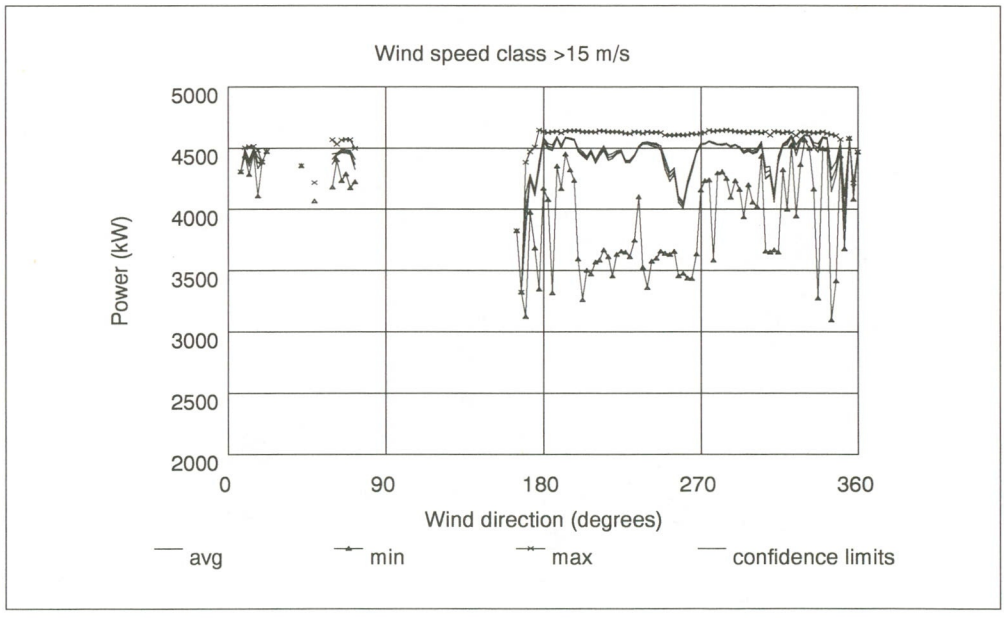
Wind speed class >15 m/s
Power (kW)
5000
4500
4000
3500
3000
2500
2000
0
90
180
270
360
Wind direction (degrees)
avg
min
max
confidence limits